Novel Octaheme Cytochrome *c* Tetrathionate Reductase (OTR) from *Shewanella oneidensis* MR-1

Fei WU

Thesis for the degree of Doctor of Philosophy

The University of Edinburgh

2010

DECLARATION

I declare that this thesis was composed by myself and the work presented in this thesis is my original work, except where specific reference is made to others.

Fei WU
20 July 2010

DEDICATION

For my Mom and Dad

Acknowledgements

I would like to thank my supervisors Prof. Graeme Reid and Prof. Steve Chapman for their great guidance and supervision in this course. Special gratefulness goes to Dr Chris Mowat and Dr Simon Daff for their helpful advices and discussion. Thanks are also to all lab members of the group in Darwin815 and N2.6 for their support over the last three years.

I am very grateful to Dr David Clarke for helping with the ESI mass spectroscopy experiment, to Dr Andrew Cronshaw for support in MALDI mass spectroscopy, and to Dr Paul Murray for suggestions in electrochemistry.

Many thanks go to the Darwin Trust Edinburgh for providing the financial support.

Abstract

Octa-heme cytochrome *c* tetrathionate reductase (OTR) from *Shewanella oneidensis* MR-1 is a periplasmic protein and shows several extraordinary structural features around its active-site heme. OTR has been found able to catalyse the *in vitro* reduction of tetrathionate, nitrite, hydroxylamine and hydrogen peroxide. However the physiological function of this novel protein remains unknown. The subject of this thesis is the *in vitro* catalytic mechanism and the *in vivo* function of OTR.

As OTR displays great similarity with bacterial penta-heme cytochrome *c* nitrite reductase (NrfA) in several aspects, it has been proposed that OTR might be physiologically involved in the metabolism of nitrite or other nitrogenous compounds. However kinetics assays and phenotypes studies carried out in this project suggest this is not the case. *In vitro* kinetic assays of the reduction of nitrite and hydroxylamine catalysed by OTR showed no significant difference in enzyme activities among the wild-type OTR and its mutant forms which have one active site residue replaced by alanine, namely OTR K153A, C64A, N61A and D150A. And the nitrite reductase activity of OTR ($k_{cat}/K_m = 1.0\times10^5$ $M^{-1}\bullet s^{-1}$) are much lower than that of NrfA ($k_{cat}/K_m = \sim10^8$ $M^{-1}\bullet s^{-1}$). These results indicate that OTR is not specifically adapted to reduce nitrite and it cannot compete for nitrite against NrfA *in vivo*. No phenotype difference was identified between the wild-type and the Δ*otr* strain of *Shewanella oneidensis* MR-1 when nitrite or nitrate served as the sole electron acceptor. OTR appears not to be involved in the respiration or detoxification of nitrite, which is consistent with previous transcriptional and phenotype reports that involve OTR or its homologues.

The *in vitro* tetrathionate reduction activity of OTR was unable to be reproduced in this project for unknown reasons. Although transcriptomic data from the literature suggest that OTR may be related to the metabolism of sulphur-containing compounds, kinetic and phenotype studies reveal that OTR does not directly participate in the respiration of thiosulfate, sulfite, tetrathionate, polysulfide or elemental sulphur.

Cysteine 64 is a highly-conserved amino acid residue of OTR close to the active site and its side-chain sulphur atom is covalently bonded by either an oxygen or a sulphur atom as observed in the crystal structure. Such a modification is potentially important to the function of OTR. ESI mass spectroscopy results show that in native OTR the modified form is around 48 Da heavier than the unmodified form, and the MALDI-TOF peptide mass spectra show that the modified form could be converted into the unmodified form by reducing agent DTT. These results suggest that the modification could be a cysteine persulfide attaching an extra oxygen atom in the form of water or hydroxide anion.

Abbreviations

Chemicals:

ACN	Acetonitrile
ADP	Adenosine diphosphate
ATP	Adenosine triphosphate
AQDS	Anthraquinone-2,6-disulphonate
CHCA	α-cyano-4-hydroxycinnamic acid
dH_2O	Distilled water
DMSO	Dimethyl sulfoxide
DTT	Dithiothreitol
EDTA	Ethylene diamine tetra-acetic acid
FAD	Flavin adenine dinucleotide
FMN	Flavin mononuclotide
HFO	Hydrous ferric oxide
HTP	Hydroxyapatite
IAA	Iodoacetamide
IPTG	Isopropyl β-D-1-thiogalactopyranoside
$MV^{+}\cdot$	Reduced methyl viologen cation radical
NaAc	Sodium acetate
NADH	Nicotinamide adenine dinucleotide
NADPH	Nicotinamide adenine dinucleotide phosphate
NH_4Ac	Ammonium acetate
PEG-4000	Polyethylene Glycol 4000
PMSF	Phenylmethylsulfonyl fluoride
SDS-PAGE	Sodium dodecyl sulfate polyacrylamide gel electrophoresis
TFA	Trifluoroacetic acid
TMBZ	3,3',5,5'-Tetramethyl benzidine
Tris	Tris(hydroxymethyl)aminomethane

Proteins:

Fcc_3	Flavocytochrome c_3 (fumarate reductase)
OTR	Octaheme cytochrome *c* tetrathionate reductase
N61A	OTR Asn61Ala mutant form
K153A	OTR Lys153Ala mutant form
D150A	OTR Asp150Ala mutant form
C64A	OTR Cys64Ala mutant form
K56A	OTR Lys56Ala mutant form
NrfA	Penta-heme cytochrome *c* nitrite reductase
HAO	Hydroxylamine oxidoreductase

Others:

Ccm system	Cytochrome *c* maturation system
E'°	Standard mid-point redox potential at pH=7.0
ESI	Electron spray ionization
FT-ICR MS	Fourier transform ion cyclotron resonance mass spectrometry
MALDI	Matrix-assisted laser desorption/ionization
PMF	Proton motive force
TCA cycle	Tricarboxylic acid cycle (Krebs cycle)
TEA	Terminal electron acceptor
TOF	Time-of-flight
OD	Optical density

Contents

List of Figures

List of Tables

Chapter 1 – Introduction

1.1 Microbial energy transduction and dedicated electron transfer pathways

Microorganisms acquire energy either from light or from the oxidation of various chemicals to support their self-maintenance and reproduction. The energy from these sources is transformed by the microbial cells into chemical energy, generally conserved in the energy currency ATP. Although some less efficient ATP-yielding processes such as substrate-level phosphorylation also exist in microbial metabolism, more efficient energy acquisition through respiration or photosynthesis is essential for microbes to quickly adapt to harsh or ever-changing environments and almost always involves fast cellular electron transfer in dedicated pathways. During the stepwise transfer of electrons from reductants with relatively low redox-potential to oxidants with higher redox potential, electric potential energy is released and partly used by the cell to produce and maintain a trans-membrane proton gradient, which provides the proton motive force (PMF) to drive the enzymatic synthesis of ATP and some other endergonic processes in living microorganisms.

1.1.1 Electron transfer in the aerobic respiration of eukaryotes

In chemotrophic microorganisms, electrons are transferred either between endogenous organic compounds in fermentation, or from organic or inorganic electron donors to exogenous electron acceptors in respiration. Fermentation generally implements no net oxidation of nutrients and thus provides a relatively small amount of ATP only from substrate-level phosphorylation. Therefore for most chemotrophic microbes respiration is the major way for the cell to obtain sufficient energy, and the proton motive force is normally produced while the electrons move along the respiratory electron transfer chain. The respiration system in microorganisms basically features three parts: the electron donor end which has a low redox-potential, the terminal electron acceptor (TEA) end which has a relatively high redox-potential, and the electron transfer chain that connects the two ends and comprises a series of

components to carry out the stepwise electron transportation. Eukaryotes and prokaryotes differ a lot in the composition and organisation of their electron transfer chain.

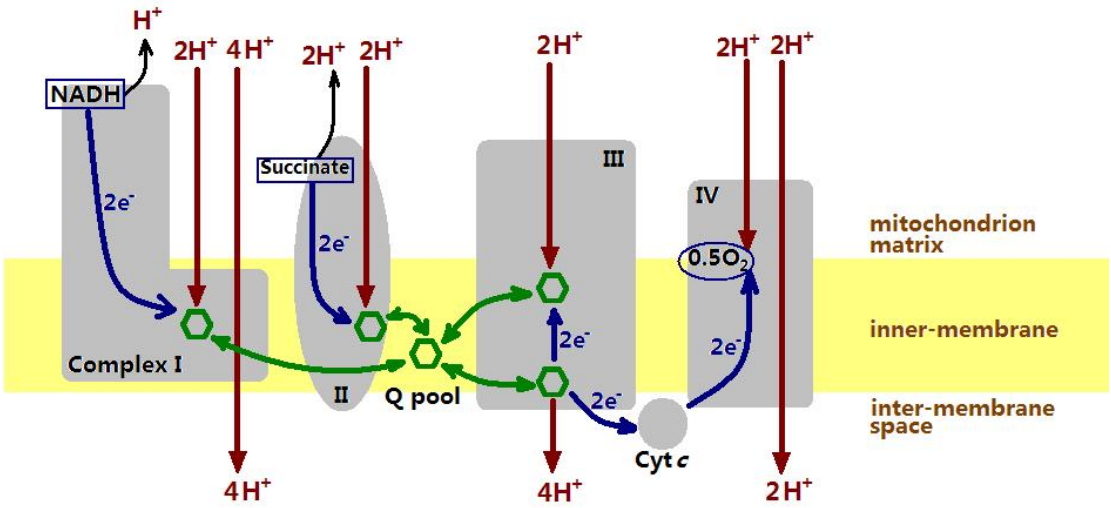

Figure 1-1. The classic model for mitochondrial respiratory electron transfer chain. The stepwise electron transfer from NADH and succinate to O_2 and the proton pumping processes are depicted in the coloured arrows. The grey blocks are Complex I to IV and cytochrome *c* as labelled. Green hexagons represent the various forms of ubiquinone (Q). The prosthetic groups in the protein complexes are omitted for clarity. The Complex I and III, and sometimes IV, are actually integrated together as one functional unit *in vivo* (see text for details). The picture is adapted from Moser *et al.*, 2006a.

In eukaryotes the electron transfer chain is elaborately built at the inner membrane of mitochondria and its composition has little variation between different eukaryote species. As shown in Figure 1-1, the general electron carriers in the chain are, in an ascending order of their redox-potentials, (i) Complex I which receives electrons from matrix NADH, (ii) Complex II which receives electrons from matrix succinate, (iii) the ubiquinones (Q) which receive electrons from Complex I and II respectively and serve as a large electron pool in the lipid bilayer in the reduced form ubiquinol (QH_2),

(iv) Complex III, i.e. the cytochrome bc_1 complex which receives electrons from QH_2, (v) cytochrome *c* which is water-soluble in the inter-membrane space and receives electrons from Complex III, and (vi) the complex IV which passes electrons from cytochrome *c* to O_2. The complex I to IV are all membrane-embedded protein complexes and are connected by freely-diffusing small molecules of Q/QH_2 and cytochrome *c*.

From NADH/succinate to O_2 the electrons are transferred in basically three mechanisms: (1) enzyme-catalysed redox process which extracts/feeds electrons from/to substrates that are bound to the enzyme active sites, as happened in the oxidation of NADH, succinate and QH_2 and the reduction of Q and O_2 (see Figure 1-1). (2) random diffusion in the solvent, as discrete electron-carrying complexes, Q/QH_2 and cytochrome *c* diffuse randomly in the lipid bilayer or inter-membrane space until the effective collision with each other at the binding sites (Hackenbrock *et al.*, 1986). In this mechanism the small Q/QH_2 and cytochrome *c* molecules exist in a vast number and make up electron pools to mediate the electron transfer between the large complexes they connect. However this classic model has recently been challenged by the findings that the respiratory membrane-embedded complexes in mitochondria physiologically form distinct supercomplexes, i.e. several complexes associate with each other and function as one integral entity which is often seen as Complex $I_1III_2IV_x$ (x=0, 1 or 2) (Vonck and Schäfer, 2009). As in mitochondria inner membrane Complex I and Complex III are usually associated to each other *in vivo* and the Q binding sites in the supercomplex are found to be facing each other, it is strongly suggested that Q is specifically channelled through the supercomplex I_1III_2 rather than diffuses freely between Complex I and III (Vonck and Schäfer, 2009). A similar mechanism may also apply to the cytochrome *c* movement in some supercomplexes, e.g. supercomplex III_2IV_1/III_2IV_2 discovered in yeast and $I_1III_2IV_1$ from bovine heart mitochondria (Vonck and Schäfer, 2009), which to some extent favours the 3-dimensional motion model of cytochrome *c* (Hackenbrock *et al.*, 1986; Gupte and Hackenbrock, 1988ab) over the theory of its 2-dimensional lateral movement on the membrane surface (Spaar *et al.*, 2009). The classic diffusion model of Q-pool still remains valid for the electron transfer between Complex II and Complex III as no supercomplex II_xIII_y has been identified (Vonck and Schäfer, 2009) and metabolic flux control results also support this conclusion (Lenaz and Genova,

2009). In addition, Q-pool is responsible for the maintenance of the binding equilibrium between the free Q and the supercomplex-bound Q, and responsible for mediating the electron transfer between Complex III and other minor respiratory dehydrogenases (Lenaz and Genova, 2009). (3) electron tunnelling through the protein media between redox centres which are featured by each complex. Complex I to IV have various redox centres including heme, Fe-S, FAD, FMN and Cu attached to their protein subunits, and the edge-to-edge distances between the electron-delivering redox centres within each complex are well designed below or close to the 14 Å limit to carry out efficient electron transfers which are faster than the turnover of the catalytic reactions in the chain (Page *et al.*, 1999; Moser *et al.*, 2006a).

The PMF generating sites which pump protons from the matrix face to the inter-membrane face of the mitochondrial inner membrane are Complex I, III and IV (see Figure 1-1). When two electrons are transferred from one molecule of NADH to half a molecule of O_2, there is a net 10 protons removed to the outside of the membrane. Although the framework of electron transfer chain in eukaryote mitochondria is strictly constructed, it ensures high efficiency in ATP generation. The transfer of 2 mole electrons from NADH to O_2 can release a total amount of energy of about 220 kJ and more than 200 kJ of this could be conserved in the trans-membrane proton gradient, which then drives the enzymatic synthesis of about 3 moles of ATP.

The final electron acceptor is always oxygen, while the NADH initialling the chain is generated from the oxidation of many kinds of organic compounds, mainly during glycolysis and the TCA cycle. The electron donor starting the chain can also be succinate which feeds electrons to complex II, or move extensively fatty acyl-CoA, $FADH_2$ and glycerol 3-phosphate which pass electrons to the membrane Q-pool through various dehydrogenases located in matrix or inter-membrane space. In a broader sense the electron transfer chain in eukaryotes could be branched and extended to a large amount of starting compounds which are funnelled into a few common reducing agents like NADH for further energetic metabolisms.

1.1.2 Electron transfer network of the respiration system in prokaryotes

In prokaryotes the electron donors and terminal electron acceptors utilised for respiration can be extended to a remarkable range of combinations (see Table 1-1) which not only expands the terminal electron acceptor from O_2 to many other organic/inorganic substances but also includes many inorganic electron donors other than organic compounds. Some individual bacterial species alone are able to respire on quite a large range of donors/acceptors in response to different environmental conditions and show a great diversity of respiration capability, e.g. *Paracoccus dinitrificans*, *Shewanella oneidensis* MR-1 and *Desulfovibrio vulgaris* Hildenborough which have been the research targets of many scientists as model organisms for studying the mechanism of prokaryote respiration network.

The detailed topology and mechanism of some respiratory electron transfer pathways in prokaryotes have been well documented but others are still yet to be clarified. Figure 1-2 shows several well-studied respiratory electron transfer pathways in Gram-negative bacterium *Paracoccus dinitrificans*. As exemplified in Figure 1-2b, the electron transfer chain in prokaryotes usually has a more branched and more complicated organisation than that in eukaryotes. Some part of the chain is built in or onto the plasma membrane similar to its counterpart in eukaryote electron transfer chain, e.g. the aerobic electron transfer pathway in *P. dinitrificans* (see Figure 1-2a), and others are soluble enzymes or electron carriers located in the periplasmic space of the cell, e.g. in the anaerobic denitrification pathway in *P. dinitrificans* (see Figure 1-2a). In general the respiratory electron transfer chains in prokaryotes are more like an electron transfer network, which encompasses many individual electron transfer pathways and each connects a pair of electron donor/acceptor. However most of these pathways in the network are not constitutively active and their components are only expressed under certain conditions in response to particular nutrient availability, in order to avoid unnecessary energy loss. Such a regulation mechanism gives the complex respiration system of prokaryotes great flexibility, which helps the cells to survive harsh environments with different but limited energy sources.

Table 1-1. Example Electron Donors and Acceptors Used in Prokaryote Respiration.

Electron acceptor	Example microbes	Electron donor	Example microbes
O_2	All aerobic prokaryotes	H_2	*Alcaligenes*, *Hydrogenophaga*, *Pseudomonas*
NO_3^-	Enteric bacteria, *Pseudomonas, Bacillus, Paracoccus*	NH_4^+	Nitrifying bacteria e.g. *Nitrosomonas*, *Nitrosospira*
NO_2^-	*Shewanella, E. coli*	NO_2^-	*Nitrobacter*, *Nitrococcus*
SO_4^{2-}	*Desulfovibrio*	$H_2S/HS^-/S^{2-}$	*Thiobacillus denitrificans*,
$S_2O_3^{2-}$	*Shewanella, Desulfovibrio*	S^0	*Thiobacillus*
SO_3^{2-}		$S_2O_3^{2-}$	
$S_nO_6^{2-}$ (n>=4)	*Salmonella enterica*	SO_3^{2-}	
S_n^{2-} (n>=2)		Fe^{2+}	*Thiobacillus ferrooxidans*,
S^0		CH_4	*Methylococcus*
R-C-SO_3^{2-}	*Desulfovibrio desulfuricans*	CO	Carboxydotrophic bacteria
Fe^{3+}	*Pseudomonas, Bacillus, Geobacter, Shewanella*	CH_3OH CH_3NH_2	*Methylobacterium*
$HAsO_4^{2-}$	*Bacillus, Desulfotomaculum, Sulfurospirillum*	HPO_3^{2-}	Phosphite bacteria
SeO_4^{2-}	*Aeromonas, Bacillus, Thauera*		
CO_2	Methanogens*		
Fumarate	*Shewanella oneidensis* MR-1		
DMSO			
TMAO			
MnO_2			
Glycine			
Phenol-Cl	*Anaeromyxobacter dehalogenans*		

Notes:
1. The list does not cover all electron donor/acceptors found in prokaryotes.
2. Archaea are marked with "*".
3. DMSO - dimethyl sulfoxide.
4. TMAO - Trimethylamine N-oxide.

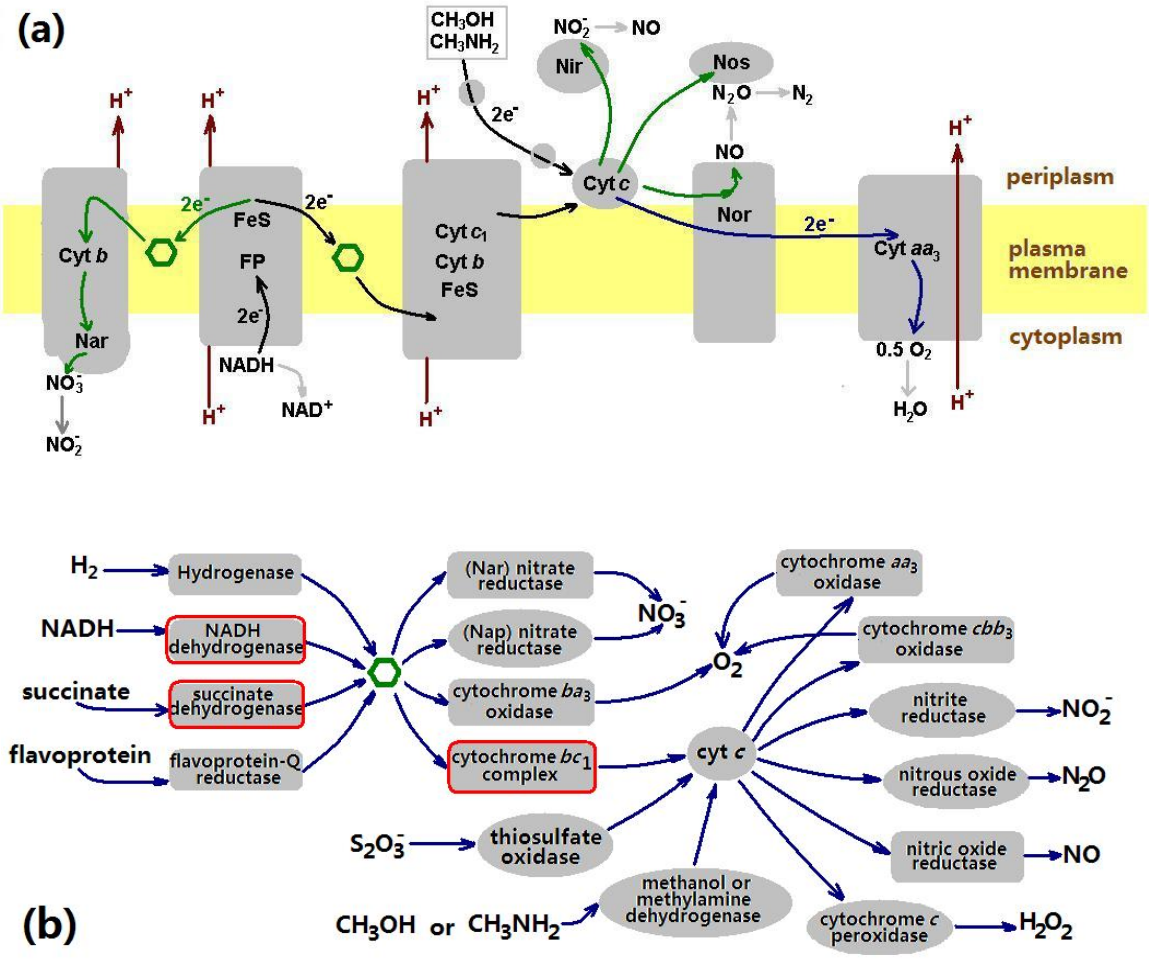

Figure 1-2. The complexity and diversity of the respiratory electron transfer chains in *Paracoccus denitrificans*. Gray blocks represent proteins or protein complexes carrying out electron transfers, among which the rectangular shaped are membrane-embedded and the ovals are soluble in the periplasm. Green hexagons represent membrane quinones (Q). **(a)** The aerobic respiratory electron transfer pathway which passes electrons from NADH, methanol or methylamine to O_2 and is presented by black and blue arrows, and the anaerobic denitrification pathway which passes the electrons to nitrate, nitrite, nitric oxide, and nitrous oxide via different enzymes respectively, presented by black and green arrows. Proton pumping sites are labelled with red arrows which however do not indicate the exact amount of protons. Abbreviations for enzymes: nitrate reductase (Nar), cytochrome cd_1 nitrite reductase (Nir), nitric oxide reductase (Nor) and nitrous oxide reductase (Nos). **(b)** The overall electron transfer network connecting various electron donors and acceptors (adapted from Ferguson 2001), but not 100% complete. Grey blocks within red boundary here are constitutive proteins while the rest are only expressed due to certain conditions. Blue arrows indicate the electron flows.

Despite the complexity of the prokaryotes electron transfer network, the numerous pathways share some common part in their composition, such as the membrane quinone pool and periplasmic *c*-type cytochromes. The membrane quinone serves as a universal electron transferring agent diffusing in the hydrophobic membrane lipid phase to shuttle electrons between its electron donor and acceptor, similar to the role of ubiquinol in eukaryote mitochondria electron transfer chain. The actual form of quinones varies between different bacterial species, featuring different mid-point redox potential of the Q/QH_2 pair. Water-soluble *c*-type cytochromes mediate many redox reactions not only on the outer surface of plasma membrane but also in the periplasmic space (Figure 1-2ab).

However complex the electron transfer network is in prokaryotes, it produces a PMF across the plasma membrane to drive the enzymatic synthesis of ATP. The ATP yield per electron transferred in prokaryotes is almost certainly less than that during the electron transfer from NADH to O_2 in mitochondria, but in general it is still greater than the yield of fermentation and is sufficient for prokaryote cells to survive the conditions with very limited nutrients. Sometimes in order to obtain a net amount of energy some ATP must be consumed first to activate the respiration process because no reducing agent in the cell is capable of directly reducing the available terminal electron acceptor. For example in the respiration of sulphate reducing bacteria like *Desulfovibrio* species, sulphate as the terminal electron acceptor is first transformed into adenosine-phosphosulphate (APS) at the cost of ATP, resulting in an intermediate which is much easier to be reduced into sulphite by NADH ($E'^{o}_{\text{sulphate/sulphite}}$ = -0.52 V, $E'^{o}_{\text{APS/sulphite}}$ = -0.06 V, $E'^{o}_{\text{NAD}^+/\text{NADH}}$ = -0.32 V) (Muyzer and Stams, 2008).

Most strict and facultative anaerobic bacteria species are capable of utilising many electron donor/acceptor pairs for respiration. When mixtures of these electron donors/acceptors are available in the environment, these bacteria cells do have a preference to use them. It is generally accepted that the electron donor/acceptor pair which supports the best growth of a particular bacterium species when they serves as the only electron donor/acceptor is given the priority by the bacterium for respiration. For example the facultative aerobe *E. coli* always chooses oxygen as the only terminal electron acceptor and shuts off other respiratory pathways even if the corresponding oxidants like nitrate or fumarate are also available. If there is no O_2, *E. coli* prefers

nitrate to fumarate as the terminal electron acceptor. The preference of *E. coli* for different electron acceptors seems fairly self-explanatory because the transfer of electrons to O_2 releases the most free energy under physiological conditions, i.e. the pair O_2/H_2O has the most positive redox potential. In fact the domination of O_2 over other terminal electron acceptors in the respiration applies to nearly all facultative aerobic bacteria. However for some strict or almost strict anaerobic bacteria species the electron acceptor which potentially provides the most energy per molecule in respiration does not always give the cells best growth, e.g. for *Wolinella succinogenes* the most preferred terminal electron acceptor is polysulfide which provides the lowest molar energy in respiration but supports the best growth of the cells in comparison with nitrate, DMSO and fumarate (Unden and Bongaerts, 1997). Such a preference of *W. succinogenes* indicates a respiration system which has probably been well-adapted to a particular environment. Recently a report shows that although nitrate as the sole electron acceptor gives the best growth to a *Desulfovibrio desulfuricans* strain, sulphate is still the preferred terminal electron acceptor for this bacterium even if nitrate is also available at the same concentration with sulphate (Marietou *et al.*, 2009). This finding reveals the limitation of the bacterial regulation system which may still have space to optimise.

Electron transfer chain in prokaryotes is not always used for PMF generation. Some lithotrophic bacteria carry out an electrochemically unfavourable electron transfer process to obtain reducing power like NADH for CO_2 reduction. For example, the nitrifying bacteria *Nitrobacter* species which use reduced nitrogenous compounds like nitrite as electron donor in the respiration, cannot exergonically deliver electrons from nitrite to NAD^+ to produce NADH because the standard mid-point redox potential of the nitrate/nitrite pair ($E'^o_{\text{nitrate/nitrite}}$ = 0.42 V) is much more positive than that of NAD^+/NADH at the physiological pH ($E'^o_{NAD^+/NADH}$ = -0.32 V), unlike eukaryotes which can make NADH or other reducing equivalents available from the break-down of various organic low-valence carbon compounds. Many sulphur-oxidising bacteria that obtain energy by oxidising various reduced sulphur compounds or elemental sulphur into sulphate also face the same problem ($E'^o_{\text{sulphate/H2S}}$ = -0.11 V, $E'^o_{\text{sulphate/S(0)}}$ = -0.05 V, $E'^o_{\text{sulphate/thiosulphate}}$ = -0.12 V). Therefore, a reversed electron flow is adopted by nitrifying bacteria and sulphur-oxidising bacteria to generate NADH, and

such an endergonic process is driven by the PMF which is produced during normal respiratory electron transfer (see Figure 1-3).

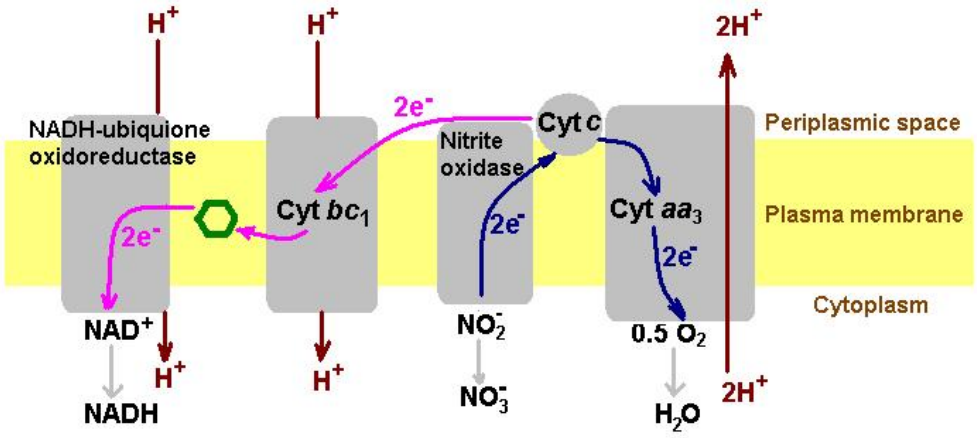

Figure 1-3. Electron transfer pathways in nitrifying bacteria genus *Nitrobacter*. Blue arrows show the pathway of respiratory electron transfer from nitrite to oxygen, which generates PMF as the right-hand red arrow shows. Pink arrows demonstrate the uphill electron flow from nitrite to NAD^+ with NADH as the product, which is driven by the PMF.

Another important function of some electron transfer components is to scavenge toxic substance, e.g. the periplasmic penta-heme nitrite reductase (NrfA) in *Desulfovibrio vulgaris* Hildenborough is only used to detoxify nitrite rather than respire on it (Pereira *et al.*, 2000; Haveman *et al.*, 2004), and its homologue in *E. coli* can also detoxify NO as a supplement function to the nitrite respiration (Poock *et al.*, 2002). Furthermore, some bacteria could use part of its electron transfer network to dispose excess reducing power to maintain a redox balance in the cell. For example periplasmic nitrate reductase (Nap) in aerobically growing *Thiosphaera pantotropha* and *Paracoccus dinitrificans* does not directly contribute to the growth but is more expressed if a more reducing carbon source is used as the electron donor (Richardson and Ferguson, 1992; Sears *et al.*, 1997). Besides the Nap system *Paracoccus* strains could also employ many other pathways from the electron transfer chains to relieve themselves of excessive reductants, depending on the different environments

(Richardson, 2000). Such a mechanism adds to the great flexibility of bacterial respiration system which takes advantage of many of its very loosely coupled electron transfer pathways that eukaryotes generally do not have.

1.1.3 Electron transfer pathway in photosynthetic microorganisms

In phototrophic microbes, electron transfers are carried out in two types of pathways: (1) the cyclic electron transfer pathway, featured by all photosynthetic microbes including unicellular eukaryote algae and prokaryote phototrophs such as cyanobacteria, green and purple (non-)sulphur bacteria. In this pathway electrons are passed from the light-excited form of a special reaction-centre pigment, which has a very negative redox-potential, to the ground form of that pigment via a series of electron carriers in a cyclic chain (see Figure 1-4). PMF is generated during this cyclic electron transportation and drives the enzymatic synthesis of ATP, i.e. cyclic photophosphorylation. The composition of the cyclic chain varies between different microbes (see the legend of Figure 1-4 for more details). (2) The non-cyclic electron pathway. To compensate for the electron loss in a branch of the cyclic electron transfer pathway where some electrons are one-way delivered to $NAD(P)^+$ to form NAD(P)H, fresh electrons are injected into the cyclic chain from various exogenous electron donors (see Figure 1-4). The electron source could be water as in eukaryotic phototrophs and cyanobacteria, or other electron donors like H_2, H_2S, S^0, $S_2O_3^{2-}$, Fe(II) and organic compounds as in green and purple photosynthetic bacteria. In eukaryotes and cyanobacteria the electrons injection is driven by the light via another reaction-centre pigment which contributes to O_2 generation and enzymatic ATP synthesis (non-cyclic phosphorylation), while in green sulphur bacteria the non-cyclic pathway is only used to fill up the electrons donated to $NAD(P)^+$. Purple bacteria carry out a reversed electron flow along part of the cyclic chain to produce NAD(P)H driven by PMF. In eukaryotic algae and cyanobacteria the photosynthetic reaction centre is located in the chloroplast thylakoid membrane, whereas in green and sulphur bacteria the reaction centre is in the plasma membrane (Hauska *et al.*, 2001; Nogi *et al.*, 2000).

Some facultative photosynthetic bacteria, namely the purple non-sulfur bacteria *Rhodospirillaceae*, could also undergo aerobic respiration to obtain energy, especially

when O_2 is available and light is limited (Klamt *et al.*, 2008). Some other phototrophic bacteria have a functional reaction-centre bacteriochlorophyll (Bchl) but seem unable to grow anaerobically with light as the only energy source. These bacteria appear to be strict aerobes and can only carry out photosynthesis when grown under aerobic conditions (Yurkov and Beatty, 1998).

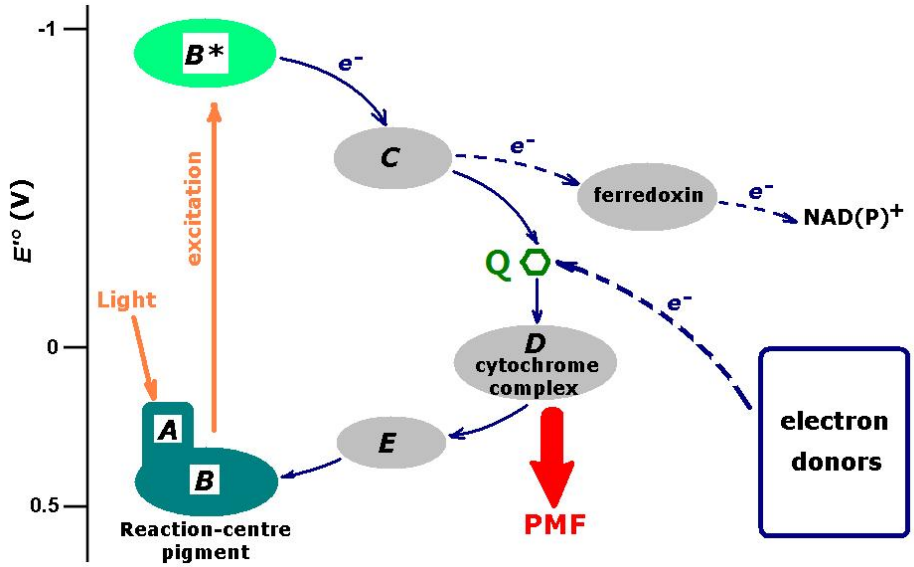

Figure 1-4. A simplified general scheme of electron transfer pathways in photosynthetic microorganisms. Only the identified major components in the pathways are shown in blocks and positioned approximately according to their redox potentials. Blue arrows outline the electron flow where the solid arrows are for cyclic pathway and the dotted for the non-cyclic pathway. The antenna pigments (*A*) harvest light and transfer the excitation to the reaction centre pigment (*B*) which is chlorophyll in eukaryotic algae and caynobacteria, or bacteriochlorophyll in green and purple bacteria. The excited pigment (*B**) then passes electrons to the next electron carrier (*C*) which could be an A_0-A_1 complex in algae, cyanobacteria and green sulphur bacteria, or bacteriopheophytin in purple bacteria. A_0-A_1 complex delivers part of the electrons to a ferredoxin complex which passes the electrons further to $NAD(P)^+$ to form NAD(P)H, whereas bacteriopheophytin only transfers electrons to membrane quinone (Q, green hexagon). The PMF is generated at the next carrier (*D*), which is the cytochrome b_6f complex in algae and cyanobactera, or the cytochrome bc_1 complex in green and purple bacteria. Electrons finally flow back to reaction-centre pigment to finish the cycle through a cytochrome *c* or a copper protein (*E*). The electrons donated to $NAD(P)^+$ are balanced by exogenous electrons from certain electron donors, most of which enter the quinone pool in the chain.

1.2 Cytochromes in bacterial respiratory electron transfer chains

Heme proteins that either carry out electron transport or catalyse redox processes in cell are generally referred to as cytochromes (Stevens *et al.*, 2004), which could be classified as *a*-, *b*-, *c*- , *d*- and *o*-types depending on the variation(s) on the protoporphyrin ring (Ferguson, 2001). Among all types of hemes only the *c*-type heme is covalently bonded to the protein polypeptide. As seen in section 1.1 cytochromes extensively exist in the electron transfer chains of microorganisms as either membrane proteins or soluble periplasmic proteins. They are vital for the functional run of microbial respiration and photosynthesis system, either as pure electron carriers to shuttle electrons or as enzymes to exchange electrons with the bound substrates. The purpose of nature to produce and employ so many types of cytochromes is yet to be found out.

1.2.1 Cytochromes as either enzymes or electron transfer proteins

Hemes in cytochromes could serve as part of the catalytic active sites of enzymes for oxidizing or reducing substrates. Active site hemes are often found as 5-coordinated in which the iron centre of the heme has an empty 6th coordination place—in fact always weakly binds a water or hydroxyl anion—to bind the substrate, such as the heme I of bacterial penta-heme nitrite reductase (NrfA) (Stach *et al.*, 2000) and the heme P460 of bacterial octa-heme hydroxylamine oxidoreductase (HAO) (Igarashi *et al.*, 1997). Sometimes the active site heme is 6th coordinated with a distal amino-acid ligand which could be replaced by a substrate molecule, for example the asparagine on SHP heme is replaced by oxygen (Li *et al.*, 2008). Once redox reactions proceed at the active site, electrons must exchange between the substrate and its electron donor/acceptor which is usually bound at the active site of another enzyme. When such an exchange can hardly happen directly due to the long distance between the two active sites, which is the most common case, the electrons are shuttled either by the

diffusion of specific electron carriers or by electron tunnelling via a series of closely-placed redox centres that outline a redox chain within a single protein or across a protein complex. About two thirds of cytochrome hemes are redox cofactors delivering electrons alongside an electron transfer chain, while the rest are enzyme active sites (Page *et al.*, 2003). In the bacterial anaerobic respiration network many enzymes and substrates are located in the periplasmic space; cytochromes and other redox cofactor-containing proteins act as both long electronic wires and transient electron stores to conduct the electron transfers between these enzymes, typically from hydrogenases to reductases via the quinone pool (see Figure 1-5 for example).

Under physiological conditions, two prerequisites are found to be generally necessary to achieve a sufficiently fast electron transfer rate (>1000 s^{-1}) between the two enzymatic active sites which are connected by heme chains: (1) the edge-to-edge distances between adjacent hemes in the chain are no more than 14 Å, and between the active site hemes and the bound substrates are less than 7 Å. (2) the redox potential difference between the two redox active sites favours a net downhill electron transfer although usually only slightly, while the hemes connecting them are not necessary to have ordered descending/ascending redox potentials along the chain. In fact endergonic electron tunnelling steps often take place during cellular electron transfers (Page *et al.*, 1999; Moser *et al.*, 2006b).

The redox potential of an active-site heme is an essential attribute to its catalytic activity, not only because it needs to have an adequate value to help activate the electron transfer at the active site but also because the value is often fine-tuned by natural selection to within a certain range, allowing reversed reactions to be catalysed as well (Moser *et al.*, 2006b). Mutation of the proximal lysine ligand of the active-site heme of NrfA into a histidine, which should cause a decreased redox potential of the heme (Einsle *et al.*, 1999), results in the almost complete loss of nitrite reductase activity of NrfA (Eaves *et al.*, 1998; Pisa *et al.*, 2002). On the other hand, redox potentials of the electron-delivering hemes between the active sites do not seriously affect the overall electron transfer rate and the pattern of their values in a redox chain is often seen as alternating ups and downs (Page *et al.*, 1999; Mowat and Chapman, 2005), which maybe important for stepwise accumulation of electrons in a multiple electron transfer reaction (Moser *et al.*, 2006b).

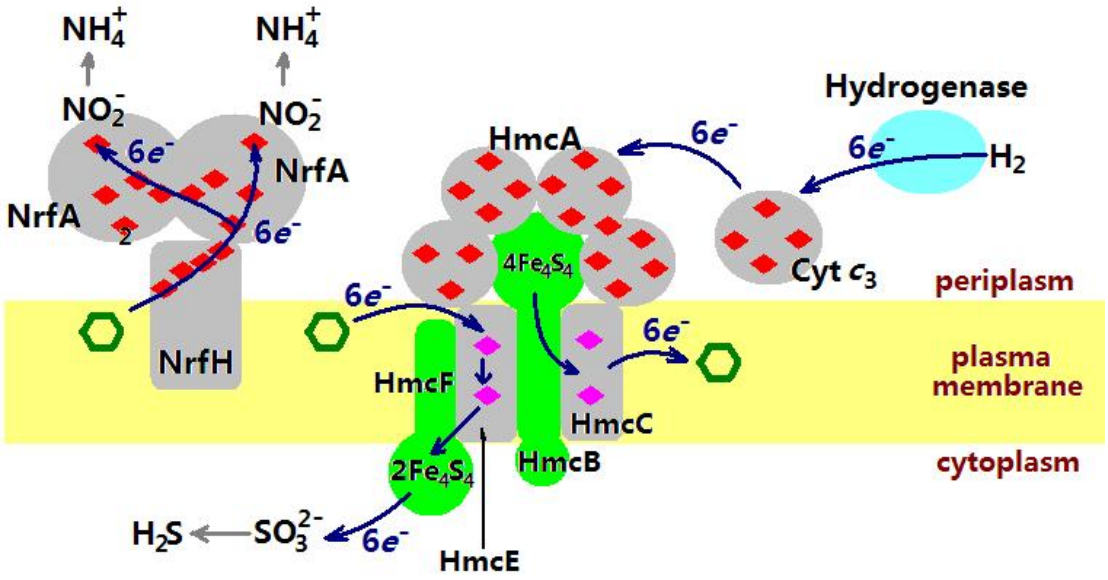

Figure 1-5. Model of the functions of several cytochromes in the electron transfer network of the sulphate reducing bacterium *Desulfovibrio vulgaris* Hildenborough. Grey blocks represent cytochromes where red rhombuses are *c*-type hemes and pink rhombuses are *b*-type. Green hexagon represents the quinone pool. Blue arrows outline the electron flows. $NrfA_2H$ on the left is the asymmetric nitrite reductase complex in which the two NrfA subunits feature the nitrite binding hemes and the NrfH subunit is the menaquinone dehydrogenase (Rodrigues *et al.*, 2006). Most of the hemes lying between the enzyme active sites in $NrfA_2H$ are on the electron transfer pathways. HmcA is the 16-heme high molecular weight cytochrome which in complex with HmcBC conducts the electron transfer between the membrane quinone pool and the soluble electron carrier tetra-heme cytochrome c_3 (Matias *et al.*, 2002; Guiral *et al.*, 2005; Richardson, 2000). Cytochrome c_3 appears to be a universal electron transferring agent in sulphate reducing bacteria bridging various oxidoreductases (Heidelberg *et al.*, 2004), and in this example it delivers electrons from periplasmic hydrogenase to HmcA.

In addition, a minority of hemes in microbial cytochromes are neither a part of an enzyme active site nor an electron transferring redox cofactor. For example the heme *b* in mitochondria inner-membrane Complex II is not on the pathway of electron flow, which may protect electrons from leaking to O_2 directly. Similarly the heme II of the external nitrite reductase subunit (NrfA) in the $NrfA_2H$ complex from *Desulfovibrio vulgaris* Hildenborough seems not to be necessary for the fast electron tunnelling from membrane quinone to the active site nitrite (see Figure 1-5) (Rodrigues *et al.*, 2006). As heme II has the most positive redox potential among the 5 hemes in NrfA (Mowat and Chapman, 2005), it may just act as a temporary electron store supporting the stepwise 2-electron transfers for the 6-electron reduction of nitrite.

1.2.2 *C*-type cytochromes, function and significance

Among the different types of widespread cytochromes, *c*-type cytochromes are a distinct group because of both their large existence in the bacteria periplasm and the covalent attachment of their hemes to the protein polypeptide. *C*-type hemes are covalently ligated to the side chain of cysteine residues in the protein backbone via two thioether bonds (see Figure 1-6). This feature reveals a general CXXCH motif in the protein sequence as a standard (but not sufficient) signature of a cytochrome *c*, although it may vary to CX_nCH (n=3, 4 or 15), A/FX_2CH or CXXCK in some cases (Stevens *et al.*, 2004; Ferguson *et al.*, 2008).

The *in vivo* formation of heme *c* architecture needs dedicated heme-attaching enzymes in microorganisms, typically the bacterial Ccm (cytochrome *c* maturation) systems (Stevens *et al.*, 2004; Ferguson *et al.*, 2008) plus some other mechanisms (Eaves *et al.*, 1998; Pisa *et al.*, 2002). Strict or facultative anaerobic bacteria produce a wealth of *c*-type cytochromes to carry out various respiratory redox processes when oxygen is limited or completely unavailable, and many of these cytochromes are multi-heme proteins especially in bacteria involved in either the nitrogen or the sulphur cycle (see Table 1-2).

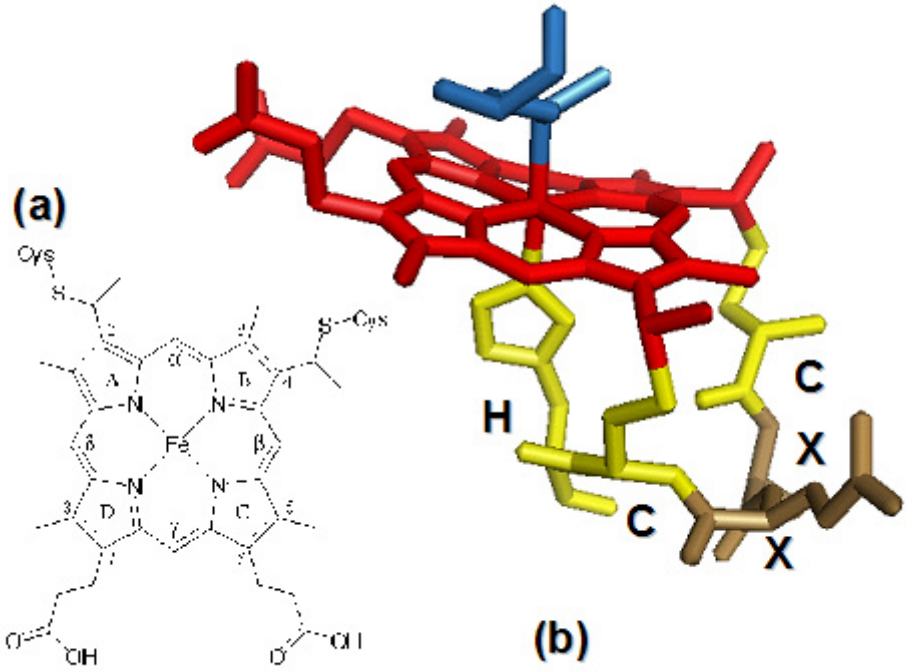

Figure 1-6. *C*-type heme in cytochromes. **(a)** Formula structure of heme *c*. **(b)** 3D structure showing typical heme *c* architecture and the CXXCH motif in horse heart cytochrome *c*. Heme (red) is thioether-bonded to the side chains of two cysteines (yellow) in the CXXCH motif where the histidine residue (yellow) ligates the heme iron at the 5th coordination position. A distal methionine (blue) occupies the 6th coordination site.

Table 1-2. Number of *c*-type cytochromes in several bacteria species based on the genome analysis.

Bacteria species	**Number of *c*-type cytochromes**	**Number of multi-heme cytochromes *c* (heme ≥ 2)**	**Maximum number of hemes per polypeptide**	**Reference**
Geobacter sulfurreducens	111	73	27	Mowat and Chapman, 2005
Shewanella oneidensis MR-1	42	32	10	Meyer *et al.*, 2004
Nitrosomonas europaea	≥ 27	≥ 13	8	Chain *et al.*, 2003
Desulfovibrio vulgaris Hildenborough	≥ 18	≥ 15	16	Heidelberg *et al.*, 2004
Wolinella succinogenes	≥ 13	≥ 10	7	Baar *et al.*, 2003

Apparently microorganisms, especially the bacteria respiring on nitrogen and sulphur containing compounds, invest significant amounts of energy and materials to build different mono- or multi-heme *c*-type cytochromes. A question is therefore raised about what is the purpose or advantage of such a huge investment made by microbes. The first speculation coming to mind is that the covalent thioether bonds prevent heme dissociation from the polypeptide and thus the integrity and stability of cytochrome *c* are securely maintained, which was backed up by the report that turning a cytochrome *c* into cytochrome *b* by mutating the CXXCH motif to AXXAH results in significantly decreased stability of the protein (Tomlinson and Ferguson, 2000) and vice versa (Arnesano *et al.*, 2000). However this theory is challenged by the fact that various functioning *b*-type and *d*-type cytochromes do naturally exist in the periplasmic space without suffering from heme loss or unfolding (Allen *et al.*, 2003), although it could be possible that microbes may spend more energy in maintaining the integrity of these cytochromes under physiological conditions. Microbes may use the thioether modification to adjust the redox potential of a heme in certain protein, but it has been shown that turning a heme *c* to heme *b* only causes a 75 mV decrease in the redox potential (Tomlinson and Ferguson, 2000), which is not remarkable compared to the hundreds of millivolts variation in redox potential due to the different heme environments and its axial ligands (Paoli *et al.*, 2002).

Recently it has been generally accepted that the introduction of heme *c* to a protein is vital to achieve closely packed multiple hemes (>4) in a single polypeptide chain (Allen *et al.*, 2003), as observed in many *c*-type cytochromes such as NrfA, NrfH, HAO, HmcA, cytochrome c_3 and more indicated in Table 1-2. As mentioned previously, these multi-heme clusters in cytochromes *c* build up an electron transfer wire with the edge-to-edge distances between adjacent hemes less than 14 Å to carry out fast electron tunnelling between remotely positioned enzyme active sites in the periplasm of bacterial cells. Such a design confines the hemes into a fixed arrangement, which has a dimension number much less than 3 as the freely diffusing mono-heme cytochromes would have, and therefore dramatically increases the efficiency of electron transfer. However, as there are still many mono-heme cytochromes *c* existing in the periplasm, whether the enhanced electron transfer rate is the major profit of the investment put into cytochrome *c* formation needs further studies to answer. Interestingly the patterns of the heme arrangements appear to be

well conserved among multi-heme cytochromes *c* despite the fact that these cytochromes have little homology in amino acid sequences or similarity in tertiary structures. Examples of superposable heme clusters in multi-heme cytochromes can be seen among NrfA, HAO and cytochrome c_{554} (Mowat and Chapman, 2005), and among HmcA, 9HcA (nine heme cytochrome *c*) and typeII cytochrome c_3 (Matias *et al.*, 2002). The conserved heme *c* clusters may be used as building blocks to assemble various electron transfer pathways for the microbes to effectively compete for the limited energy sources in the environments.

1.3 *Shewanella* species

Shewanella species have drawn great scientific research and industrial interests thanks to their remarkable respiratory versatility in reducing a broad range of electron acceptors from strong oxidant like O_2 to weak oxidant like elemental sulphur, from the dissolved substances to the solid minerals, and from inorganic to organic compounds. Such a distinct feature not only makes Shewanellae a model system for laboratories to explore the mechanism of their robust respiration network, but also forwards their special abilities to potential applications in bioremediation and microbial fuel cells.

1.3.1 The genus *Shewanella*

Shewanellae are Gram-negative facultative anaerobic bacteria belonging to the γ-Proteobacteria, consisting of more than 40 species. The cells of Shewanellae are rod-shaped with a length of 2-3 μm and a diameter of 0.4-0.7 μm (Hau and Gralnick, 2007). Since 1931 *Shewanella* species have been isolated from various environments such as freshwater lake sediments, spoiled butter surface, seawater, marine sediments, marine sponge, crude oil, deep-sea oil pipelines, human clinical samples and various hosts like squid, algae, oyster and fish (Pickard *et al.*, 1993; Khashe and Janda, 1998;

Hau and Gralnick, 2007). These environments contains some generally harsh conditions like low temperature (< 4 °C), low oxygen, limited nutrient type, high salinity and sometimes high toxicity, which reflects the robustness of metabolic capability of *Shewanella* species. This capability, although the inside mechanism is only partially known, has made Shewanellae promising to be employed in applicable biotechnologies like bioremediation and power generation.

Environment contamination has been a serious threat to human life and potentially the whole biosphere. Microorganisms like Shewanellae capable of reducing toxic contaminants have shown great potential in bioremediation as economic environment cleaners. Nuclear pollutants like U(VI), ^{60}Co(III) and ^{99}Tc(VII) and heavy metal ions like Cr(IV) and Cr(III) that are soluble and could spread easily with groundwater can be reduced by some *Shewanella* species into insoluble forms and thus precipitate (Hau and Gralnick, 2007). This mechanism however could also cause problems if Hg(II) and As(V) are present, because their reduced forms Hg(0) and As(III) produced by Shewanellae are toxic and even easier to spread (Hau and Gralnick, 2007). Many toxic halogenated organic compounds like carbon tetrachloride (CCl_4) could also be efficiently dehalogenated, i.e. reduced by Shewanellae. However the side products like chloroform ($CHCl_3$) are still equally toxic and need further treatment. Some *Shewanella* species have been found able to help degrade explosive contaminant RDX (cyclotrimethylene trinitramine) but little is known about the mechanism (Hau and Gralnick, 2007). *Shewanella* species could also produce and release a large amount of toxic H_2S if grown anaerobically in sulphur-rich environments (Perry *et al.*, 1993; Moser and Nealson, 1996). Therefore a practical bioremediation strategy using Shewanellae for a particular contaminated site should be carefully designed to minimise secondary pollution before going into large scale application.

Shewanella strains have been shown able to reduce solid metal oxides through direct contact of the outer membrane of the cells with the surface of minerals such as hematite (Fe_2O_3), pyrolusite (MnO_2), goethite (FeO(OH)), and birnessite ($Na_{0.3}Ca_{0.1}K_{0.1}Mn^{4+}Mn^{3+}O_4 \bullet 1.5(H_2O)$) (Ruebush *et al.*, 2006). This feature has been exploited in designing biofuel cells, in which a solid electrode acts as the terminal electron acceptor for *Shewanella* cells and electron sources are various organic compounds that could be found in waste (Hau and Gralnick, 2007). The mechanism

of electron transfer to solid surface is not fully understood but the outer membrane *c*-type cytochromes of *Shewanella* play crucial roles (Xiong *et al.*, 2006).

1.3.2 *Shewanella oneidensis* MR-1

As biotechnological applications of Shewanellae are still limited by the unknown mechanisms of many metabolic processes carried out in *Shewanella* species, studies of the electron transfer network of Shewanellae have been necessarily continuing. *Shewanella oneidensis* MR-1, formally known as *Shewanella putrefaciens* MR-1, *Shewanella* sp. MR-1 or *Alteromonas putrefaciens* MR-1, is the most extensively studied species in *Shewanella* genus. *S. oneidensis* MR-1 appears to be a psychrotroph (Tadokoro *et al.*, 2007) due to its ability to grow at as low as 3 °C (Abboud *et al.*, 2005), although the optimal growth temperature of this species is 30 °C. *S. oneidensis* MR-1 was originally isolated from Lake Oneida, New York, the U.S.A. (Myers and Nealson, 1988), the full genome sequence of this species was published in 2002 (Heidelberg *et al.*, 2002) and many transcriptome studies followed thereafter.

Until now *S. oneidensis* MR-1 has been found able to reduce an astonishing range of substances which are listed in Table 1-3 and seem still extendable. Reduction of most of these substances by *S. oneidensis* MR-1 is for energy purpose coupled with the oxidation of various low-valence carbon sources or H_2. It appears that *S. oneidensis* MR-1 can only obtain energy from respiration, as fermentation has not been observed in its strains so far (Venkateswaran *et al.*, 1999) despite the presence of many fermentation enzyme genes in its genome (Serres and Riley, 2006).

The remarkable capability of the respiration system shown by *S. oneidensis* MR-1 reveals a uniquely flexible and robust electron transfer network processed by the cells of this species. Figure 1-7 shows part of the network with the well-studied pathways responsible for the reduction of many electron acceptors located either outside of the cell or in the periplasmic space. This network features a large periplasmic profile consisting of many enzymes and electron transferring proteins, mainly *c*-type cytochromes which are crucial to the respiratory versatility of MR-1 (Fredrickson *et al.*, 2008). From the genome sequence of *S. oneidensis* MR-1 42 *c*-type cytochromes

in total have been identified mainly based on the occurrence of the CXXCH fingerprint in the open reading frames (Meyer *et al.*, 2004). Among these cytochromes some have been well studied such as the outer membrane cytochromes OmcA and MtrC, the fumarate reductase flavocytochrome c_3 (Fcc_3), and the tetra-heme cytochrome *c* (CymA) (see Figure 1-7). CymA is anchored on the periplasmic side of the plasma membrane and has been shown to be a key electron transferring agent connecting various periplasmic reductases or reductase complexes with the membrane quinone pool (Schwalb *et al.*, 2003). However there are still many *c*-type cytochromes encoded in the genome of *S. oneidensis* MR-1 that need further investigation, especially those with unknown functions.

Table 1-3. List of substances identified so far that can be bio-reduced by *Shewanella oneidensis* MR-1.

Electron acceptor	Reduced product	Support growth	Reference
O_2	H_2O	Yes	Myers and Nealson, 1988
Fe(III)	Fe(II)	Yes	
Mn(IV)	Mn^{2+}	Yes	
NO_3^-, NO_2^-	NH_4^+	Yes	
$S_2O_3^{2-}$, SO_3^{2-}	H_2S	Yes	
$S_4O_6^{2-}$	H_2S	Yes	
Glycine		Yes	
Fumarate	Succinate	Yes	
TMAO	TMA	Yes	
S(0)	H_2S	Yes	Moser and Nealson, 1995
DMSO	DMS	Yes	Gralnick *et al.*, 2006
AQDS		Yes	Beliaev *et al.*, 2005
Co(III)	Co(II)	Yes	Liu *et al.*, 2002
Tc(VII)	Tc(IV)	Yes	
Cr(VI)	Cr(III)	Yes	
Mn(III)	Mn^{2+}	Yes	Payne and Dichristina, 2006
U(VI)	U(IV)	Yes	
Pd(II)	Pd(0)	Yes	De Windt *et al.*, 2005
V(V)	V(IV)	Yes	Carpentier *et al.*, 2005
Hg(II)	Hg(0)	No	Wiatrowski *et al.*, 2006
Se(IV)	Se(0)	No	Klonowska *et al.*, 2005
Te(IV)	Te(0)	No	

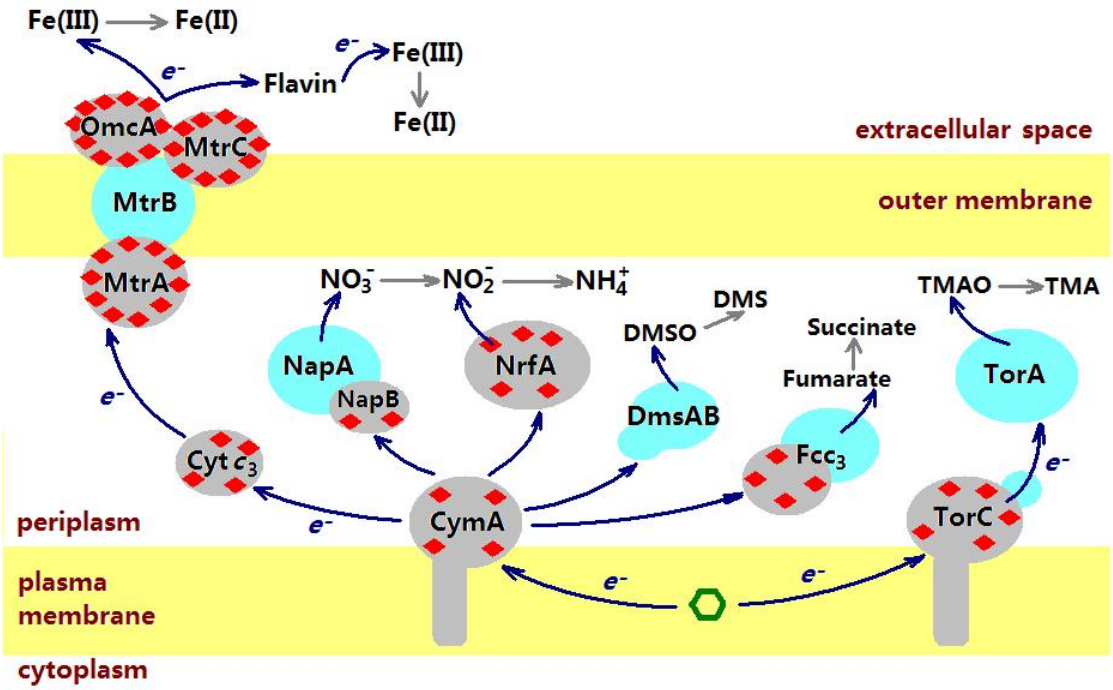

Figure 1-7. Model of several anaerobic respiratory electron transfer pathways in *Shewanella oneidensis* MR-1. Grey blocks represent cytochromes with red rhombuses as hemes and cyan blocks are none-heme proteins. Green hexagon represents the membrane quinone pool. Blue arrows outline the electron flows (Schwalb *et al.*, 2003; Fredrickson *et al.*, 2008).

1.4 The Octaheme Tetrathionate Reductase (OTR) from *Shewanella oneidensis* MR-1

A soluble *c*-type cytochrome from *Shewanella oneidensis* MR-1, encoded by gene SO4144 featuring 442 amino acid residues and 8 CXXCH motifs (Heidelberg *et al.*, 2002), has been over-expressed by our group and has a molecular weight of ~54 kDa. Before knowing any physiological function of this protein, its crystal structure was solved and showed that it is an octa-heme cytochrome *c* with several novel structural features (Mowat *et al.*, 2004). Its name octaheme tetrathionate reductase (OTR) came

after the finding that this protein was able to catalyse the reduction of tetrathionate *in vitro* (Mowat *et al.*, 2004). Sequence analysis identifies an N-terminal signal peptide in OTR precursor (see OTR sequence in Appendices-1.1), indicating that OTR is a periplasmic cytochrome and most possibly part of a respiratory electron transfer pathway of *S. oneidensis* MR-1. OTR homologues have been identified in many bacterial genomes, and most of these species belong to the group of sulphur oxidising or sulphate reducing anaerobes, such as *Geobacter*, *Anaeromyxobacter*, *Desulfovibrio* and *Chlorobium*. However, none of these homologues has its function identified, and none of the numerous transcriptional studies reveals a possible function that OTR may fulfil.

1.4.1 The overall structure of OTR

Figure 1-8 shows the overall structure of OTR which clearly contains an α-helical domain attaching the 8 *c*-type hemes and a β-sheet domain covering the space above heme II. Heme II is 5-coordinated and binds an exogenous thiocyanide anion (SCN^-) at its 6^{th} coordination position, indicating that OTR is an enzyme and heme II is the active site. The surface view of the structure shows that the distal cavity of heme II is accessible for small molecules diffusing in the solvent. Five hemes (I, III and VI-VIII) are exposed to the solvent and connected to heme II via heme IV and V. These surface hemes may cover the contacting interface of OTR and its cellular redox partner. The edge-to-edge distances between adjacent hemes are all less than 4 Å, much shorter than the general 14 Å limit (Page *et al.*, 1999). Such an intensively packed heme cluster ensures very fast electron tunnelling ($>10^3$ s^{-1}) even if there are energy barriers as much as 14 kcal/mol between the adjacent hemes in the electron transfer chain (Moser *et al.*, 2006b).

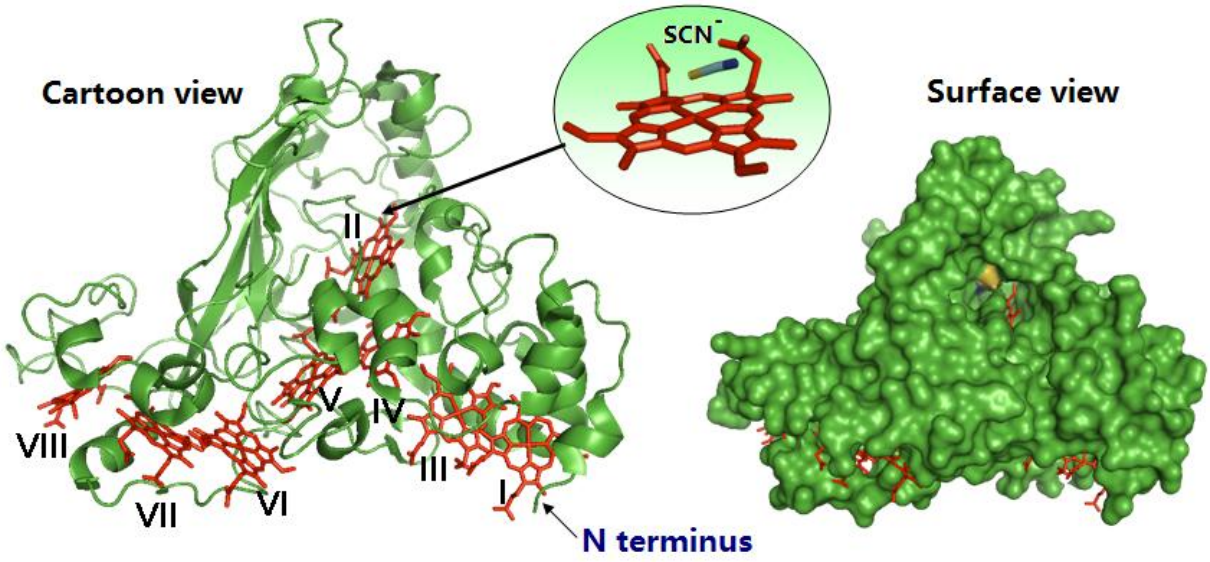

Figure 1-8. 3D structure of the octaheme tetrathionate reductase (OTR) from *Shewanella oneidensis* MR-1 (PDB code: 1SP3). N terminus and all 8 *c*-type hemes (red) of this protein are labelled in the cartoon view (left). The zoomed blow-up shows a SCN^- anion bound to the iron of heme II. The surface view (right) is positioned at the same viewing angle as the cartoon view.

1.4.2 The novel heme ligation of heme II in OTR

The axial ligands of heme *c* vary among different cytochromes but in general the proximal ligand is always the last amino acid residue in the CXXCH or CXXCK motif, i.e. a histidine or lysine (see Figure 1-6). However in OTR the iron of heme II is proximally ligated by a lysine residue (Lys56) which in the amino acid sequence is distant from the $C_{74}X_{75}X_{76}C_{77}H_{78}$ motif that attaches heme II (see Figure 1-9a). The His78 in the CXXCH motif swings away from the 5th coordination position of heme II. This novel heme ligation had been a unique exception until another similar case was found in NrfH a few years later, in which the 5-coordinated heme I is proximally ligated by a methionine (Met49) two residues downstream from the $C_{43}X_{44}X_{45}C_{46}H_{47}$ motif that attaches this heme (see Figure 1-9b) (Rodrigues *et al.*, 2006). More interestingly, these unusual proximal amino acids, including the lysine from a CXXCK motif in NrfA (Einsle *et al.*, 1999), are all highly conserved among homologues. The conservation of the novel ligation suggests that it is necessary for a

certain function. One possible purpose for such a kind of design is to alter the redox potential of the heme so that it could properly activate the electron transfer from/to the bound substrate.

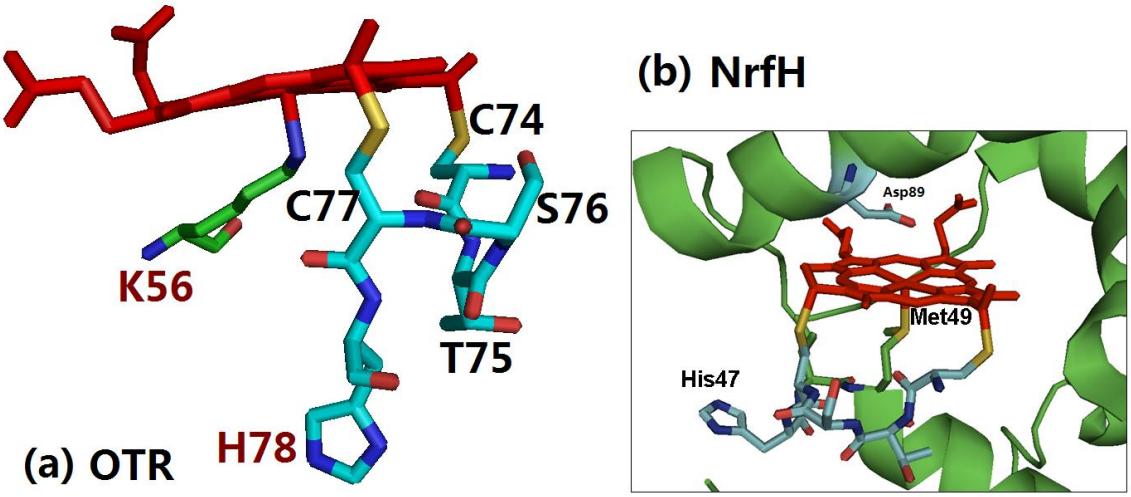

Figure 1-9. The novel heme proximal ligation in (a) Heme II of OTR and (b) Heme I of HrfH. In both cases the histidine from the CXXCH is located away from the 5th coordination position of the heme which is occupied by an amino acid residue outside the heme-attaching motif.

1.4.3 The potentially functional groups in the distal pocket of heme II

As OTR appears to be an enzyme and heme II is the active site binding exogenous molecules, the amino acids in the distal pocket of heme II may play important roles by interacting with the bound substrate, especially those that are highly conserved. Figure 1-10 shows these active site residues including Lysine 153, Asparagine 61 and Cysteine 64. The whole heme distal cavity is covered by two loops, each of which links two α-helices. Aspartate 150 may be also close to the heme centre but cannot be seen in the structure because no electron density was observed for the 6 amino acid residues from Gly147 to Val152. Among the missing 6 residues $G_{147}G_{148}G_{149}$ is a highly conserved segment suggesting that the missing part in the structure is a fairly flexible region which could swing around the GGG hinge and may help fit the substrate.

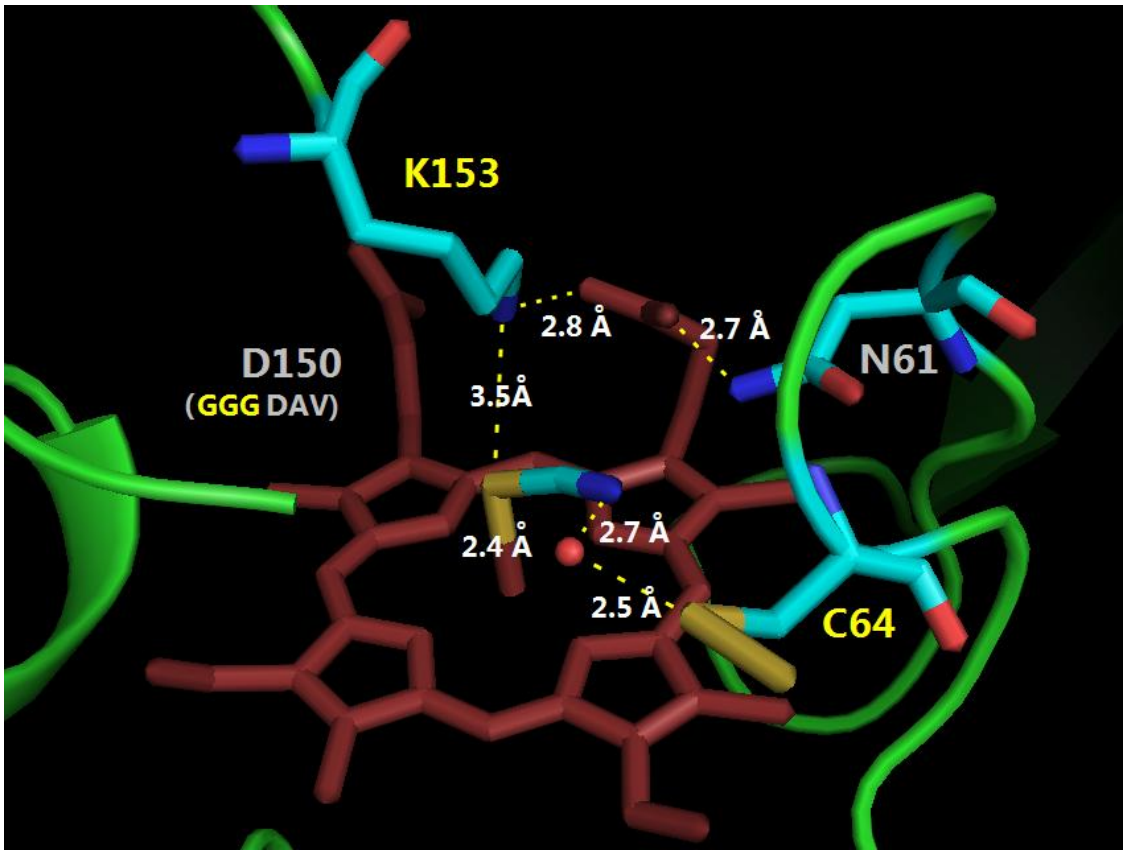

Figure 1-10. Close view of the distal pocket of Heme II in OTR structure. The structure of six amino acid residues (G147-V152) is not available. Conserved amino acids are labelled in bright yellow. Heme II is in dark red. Coloured atoms in the amino acid site chains are: blue (nitrogen), red (oxygen), cyan (carbon) and dark yellow (sulphur). The γ-sulphur of Cysteine 64 is modified with an unidentified atom which is shown as sulphur here (Mowat, unpublished data).

In the structure of OTR a SCN^- anion is bound to the heme iron with its sulphur atom bonded to Fe at a distance of 2.4 Å. The sulphur is also hydrogen-bonded to the terminal nitrogen atom of Lys153 side chain with a N-S distance of 3.5 Å. Lys153 is highly conserved among OTR homologues and probably interacts with the substrate with its side-chain amine group. The nitrogen atom of the SCN^- is hydrogen-bonded to an ambient water molecule (Wat470) with a N-O distance of 2.7 Å. This water also hydrogen-bonds the side-chain sulphur of Cys64 with a O-S distance of 2.5 Å. These two hydrogen bonds link the SCN^- with Cys64, suggesting that Cys64, also a highly conserved residue, may interact with the substrate through Wat470. More intriguingly,

Cys64 is modified on its sulphur on the other side with an unidentified atom (see Figure 1-10), which could be either a sulphur or an oxygen (Mowat *et al.*, 2004). A functional Cys-SSH group in catalytic active sites was previously reported in sulphurtransferase (Bordo *et al.*, 2000) and thiosulfate oxidase (Bamford *et al.*, 2002b). Stable cysteine sulfenic acid (Cys-SOH) plays various roles in the active sites of many enzymes such as NADH peroxidase and NADH oxidase, nitrile hydratase, and the AhpC peroxiredoxins (Claiborne *et al.*, 1999; Claiborne *et al.*, 2001). Therefore identifying the modification on Cys64 in OTR could be vital for clarifying the function and catalytic mechanism of this enzyme.

In either the SCN-bound or the SCN-absent crystal structure of OTR, Asn61 does not have any bond with heme iron or SCN^- (Mowat *et al.*, 2004; Mowat, unpublished data). Considering the 5.6 Å distance from the δ-Nitrogen of Asn61 to the heme iron and the low amino acid conservation at this position, Asn61 may help to stabilise the heme moiety by hydrogen-bonding one of the oxygen atom in the heme carboxyl group (see Figure 1-10). A similar role may be shared by Lys153 due to a hydrogen bond between its terminal amine and the other oxygen in the carboxyl group. Asp150, although not seen in the structure and not highly conserved, may be located close to heme iron after the mobile region GGGDAV fits the substrate and may serve as a proton donor in the reaction.

1.4.4 *In vitro* catalytic activities of OTR suggesting its possible *in vivo* function

After being over-expressed and purified, OTR was assayed *in vitro* for its activities and was found to be able to catalyse the reduction of tetrathionate and the reversed oxidation of thiosulfate, the reduction of trithionate, nitrite, hydroxylamine and peroxide (Rothery, 2004; Atkinson *et al.*, 2007; Atkinson, 2009). The reactions and key catalytic parameters are listed in Table 1-4.

The reduction of tetrathionate and trithionate implies some connection with the Cys64 and possibly with its modification. The previously reported tetrathionate reductases are molybdoenzymes from *Salmonella* species, featuring a MGD (molybdopterin guanine dinucleotide) cofactor. A highly conserved cysteine was predicted to be

bound to the molybdenum in the MGD cofactor (Hensel *et al.*, 1999) and is critical for the enzyme activity (Hinsley and Berks, 2002). *S. oneidensis* MR-1 is known to be able to grow on tetrathionate as the terminal electron acceptor (Myers and Nealson, 1988) but the enzyme responsible for tetrathionate respiration has not been identified. Therefore OTR could be the respiratory tetrathionate reductases of *S. oneidensis* MR-1 involved in the sulphur compounds metabolism pathway.

Table 1-4. Reactions catalysed by OTR *in vitro* and kinetic parameters. Numbers were obtained at pH=7, Ionic strength=0.1M and room temperature (Rothery, 2004; Atkinson, 2009).

Reactions	K_m (μM)	k_{cat} (s^{-1})	k_{cat}/K_m ($M^{-1}•s^{-1}$)
$S_4O_6^{2-} + 2e^- \rightarrow 2S_2O_3^{2-}$	70 ± 9	19.9 ± 0.6	2.9×10^5
$2S_2O_3^{2-} \rightarrow S_4O_6^{2-} + 2e^-$	7100 ± 2500	16.8 ± 0.9	2.4×10^3
$S_3O_6^{2-} + 2e^- \rightarrow S_2O_3^{2-} + SO_3^{2-}$	357 ± 40	1.9 ± 0.5	5.3×10^4
$NO_2^- + 8H^+ + 6e^- \rightarrow NH_4^+ + 2H_2O$	5.2 ± 1.0	2.8 ± 0.4	5.3×10^5
$NH_2OH + 3H^+ + 2e^- \rightarrow NH_4^+ + H_2O$	2200 ± 400	849 ± 7	3.9×10^5
$H_2O_2 + 2H^+ + 2e- \rightarrow 2H_2O$	15800 ± 500	17.5 ± 0.6	1.1×10^3

The reduction of nitrite and hydroxylamine into ammonium ions is similar to the bacteria penta-heme nitrite reductase (NrfA) which catalyses the same reactions. In fact there are a few other attributes of OTR found to be similar with those of NrfA. The active site hemes in OTR and NrfA are both 5-coordinated and proximally ligated by a lysine residue, and the distances between the lysine side-chain nitrogen and heme iron are nearly the same (~2.1 Å). Furthermore, the spatial arrangements of the heme cluster in OTR and NrfA are superposable and show great similarity to each other including the active site heme (see Figure 1-11). As introduced in section 1.2.2, bacteria multi-heme cytochromes *c* seem to have conserved heme clusters although they may genetically heterogeneous to each other. This conservation can also be found by comparing the heme arrangements between OTR and HAO and all the 7 non-active-site hemes of both enzymes are almost in the same configuration (see Figure 1-11). In addition, the active site heme in all these three enzymes is linked to

two heme chains which could potentially facilitate the stepwise 2-electron transfers in a multi-electron redox reaction (Moser *et al.*, 2006b). As NrfA and HAO are both important enzymes involved the bacterial nitrogen cycle, it has been hypothesized that OTR may function as an enzyme catalysing the oxidoreduction of nitrogenous compounds *in vivo* inspired by its similarities with NrfA and HAO (Atkinson *et al.*, 2007).

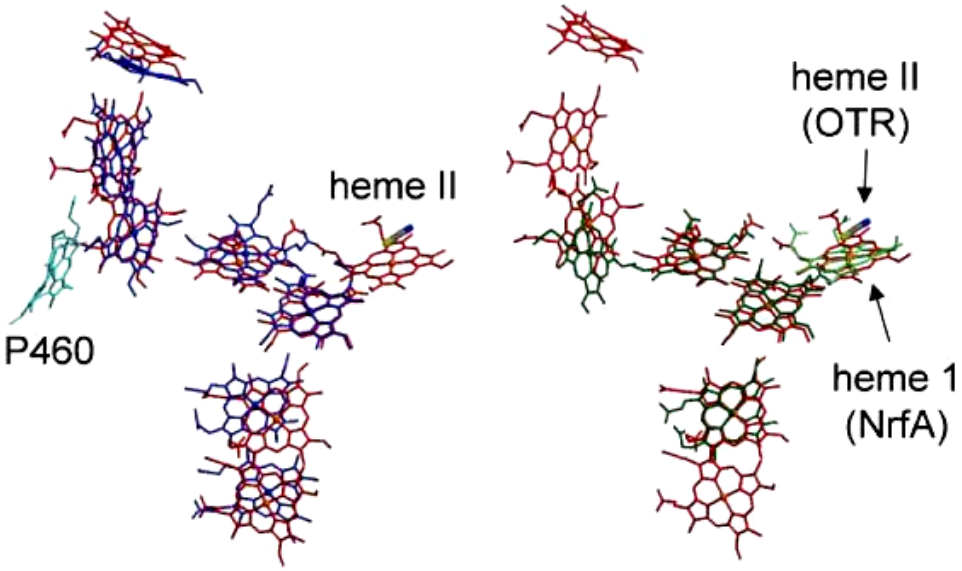

Figure 1-11. Superposition of heme arrangement in OTR (red) with hemes in HAO (blue, left panel) and in NrfA (green, right panel). HAO (hydroxylamine oxidoreductase) is an octaheme cytochrome *c* containing an active 5-coordinated heme P460 (cyan, left panel). NrfA is the cytochrome *c* pentaheme nitrite reductase. (Figure copied from Mowat and Chapman, 2005).

1.4.5 Microbial species containing OTR homologues

Besides *S. oneidensis* MR-1, genome analysis through *SIB BLAST Network Service* (http://www.expasy.ch/tools/blast/) has identified 56 bacteria and archaea strains whose genomes have at least one *otr*-homolog gene. 38 species from them have

complete typical gene clusters containing *otr* in the genome. In general OTR gene is present in three types of clusters (see Figure 1-12a).

The first type of these clusters (named Cluster I) has a conserved gene segment encoding a small mono-heme cytochrome *c* (M), a large none-heme protein (N) and OTR in the transcribing reading direction. Both M and N are periplasmic proteins and have unknown functions. This cluster exists in several *Shewanella* species including MR-1. Cluster II encodes a large none-heme protein homologous to N in Cluster I, a small none-heme protein (U) and OTR. None-heme periplasmic protein U has the similar size but poor sequence homology with the mono-heme protein M in Cluster I. Interestingly both U and M have a conserved cysteine residue near their C-terminus, suggesting they may have the similar function. In addition the large none-heme protein N in both clusters also has a conserved cysteine residue in the sequence. Cluster II is found in several *Geobacter* and *Anaeromyxobacter* species. Cluster III is quite different from the above two clusters, which encodes a trans-membrane cytochrome *b* and OTR with a trans-membrane helix tail at the C-terminus. Cytochrome *b* encoded in this cluster is a typical di-heme electron transferring and quinone reducing protein, which is homologous to the cytochrome *b* subunit of the thiosulfate reductase complex from *Salmonella* species, to the cytochrome *b* subunit of the putative Ni-dependent hydrogenase complex in *E. coli* strains, and to the γ-subunit of formate dehydrogenase-N in *E. coli* (Berks *et al.*, 1995; Jormakka *et al.*, 2002). It could be postulated that OTR expressed from this cluster is anchored onto the plasma membrane with its trans-membrane tail associated with the di-heme cytochrome *b*, and is exposed in the periplasmic space with the rest of the protein (see Figure 1-12b). Cluster III is distributed among various bacteria species from genus *Rhodoferax*, *Magnetococcus*, *Marinobacter*, *Desulfatibacillum*, *Desulfovibrio*, *Desulfococcus*, *Syntrophobacter*, *Prosthecochloris*, *Chloroherpeton*, *Halorhodospira* and *Chlorobium*. Cluster III in *Rhodoferax ferrireducens* is followed by two downstream genes encoding two proteins homologous to N and U in Cluster II respectively (see Figure 1-12a), suggesting the function of U and N in association with OTR may have been replaced by some other proteins in most species containing Cluster III.

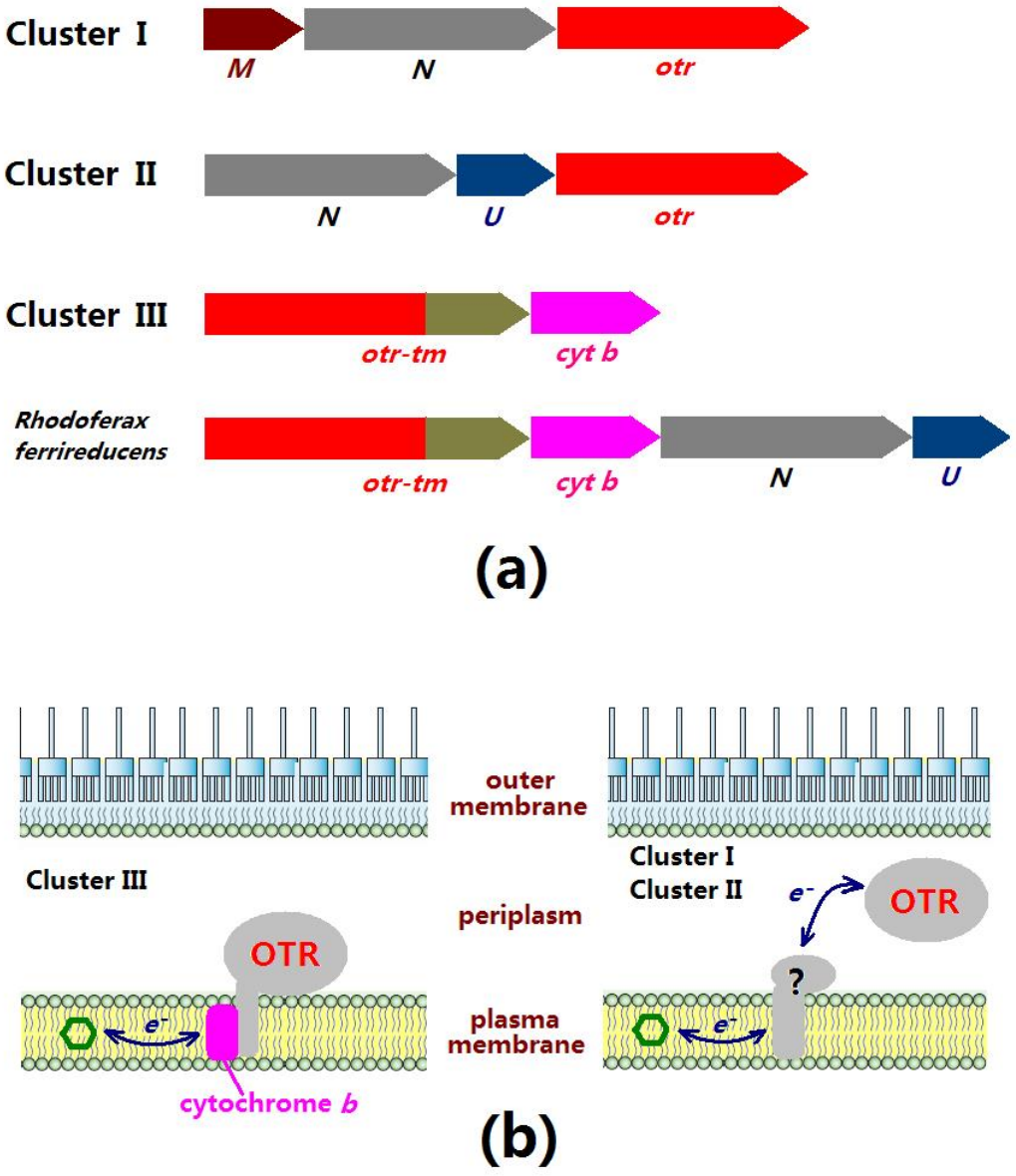

Figure 1-12. The OTR family. (a) Typical clusters encoding OTR and potentially associated functional proteins. Genes with the same colour are homologous to each other. Abbreviations: (M) small mono-heme cytochrome *c*, (N) large none-heme protein, (U) small none-heme protein, (Cyt *b*) di-heme cytochrome *b*, and (OTR-tm) OTR with trans-membrane tail (see text for details). **(b)** Hypothesized models of the location and electron transfer mechanism of OTR expressed from different clusters.

1.5 Aims of this thesis

Because the function and catalytic mechanism of OTR still remains unknown, further investigations to this novel enzyme were carried out in this project. First question is about the nature of substrate binding and catalysis. As some *in vitro* substrates have been identified for OTR, whether and how the active side amino acid residues are involved in the catalysis of these reactions need to be clarified. This question could be addressed by investigating the *in vitro* catalytic activities of various mutant forms of OTR, in which one of these residues is replaced by an alanine which generally does not participate in redox catalysis. If one or more mutations at the active site residues cause a dramatic decrease to the *in vitro* enzyme activity for some substrate, it will be a sign that the corresponding residue effectively interacts with the substrate and is vital for the physiological function of the enzyme. And therefore the substrate could be (or be very similar to) the *in vivo* substrate of OTR. Based on the results of the *in vitro* assays, phenotype studies could be carried out to help identify the physiological role of OTR. Furthermore, identification of the modification on the Cysteine64 will definitely be a clue to find out the function of OTR, which could be carried out using mass spectra and crystallography technology.

The objectives for this thesis are:

1. To describe the *in vitro* catalytic activities of the wild-type OTR and its mutant forms including N61A, K153A, D150A, C64A and K56A in both steady-state and pre-steady-state for the known substrates.
2. To present the studies exploring the physiological function of OTR by comparing the phenotypes of wild-type *S. oneidensis* MR-1 and its OTR knock-out strain under various conditions with single terminal electron acceptors or toxic additives.
3. To identify the modification of Cysteine64 by studying the mass spectra of intact proteins and digested peptides for both wild-type OTR and the C64A mutant. The difference in mass and in their reactions to modifying treatments could help tell the nature of this modification.

Chapter 2 – Materials and Methods

2.1 Bacteria strains and plasmids

Bacteria strains used in this work were *Shewanella oneidensis* MR-1 wild-type strain, *Shewanella oneidensis* MR-1 Δ*otr* strain (OTR-knockout) and *Shewanella frigidimarina* EG301 strain (a Fcc_3-knockout strain, Gordon *et al.*, 1998). All three trains are naturally Rifampicin and Kanamycin resistant.

All vectors used in this project for protein over-expression were lab-stocks made by Dr Caroline. S. Miles (School of Physics & Astronomy, University of Edinburgh). Genes encoding the proteins of interest, including wild-type OTR and its mutant forms N61A, K153A, C64A, D150A and K56A, were incorporated into the plasmid pMMB503EH which features a Streptomycin resistance gene and an IPTG inducible site (Michel *et al.*, 1995). These vectors were transformed from the *E. coli* SM10 lab-stock into *Shewanella frigidimarina* EG301 strain via bacterial conjugation (see Table 2-1 and Section 2.3.1 for details).

Table 2-1 Bacteria strains and plasmids used in this work.

Bacteria stains	Growth Purpose	Description	Source
Shewanella oneidensis MR-1	Phenotype studies	wild-type strain	Lab stock
Shewanella oneidensis MR-1 *Δotr*		OTR knock-out strain	Lab stock
Shewanella frigidimarina EG301 carrying pMMB503EH-*otr*	Protein expression	Fcc_3 knock-out strain + plasmid	Lab stock
Shewanella frigidimarina EG301 carrying pMMB503EH-*n61a*			This work
Shewanella frigidimarina EG301 carrying pMMB503EH-*k153a*			This work
Shewanella frigidimarina EG301 carrying pMMB503EH-*c64a*			This work
Shewanella frigidimarina EG301 carrying pMMB503EH-*d150a*			This work
Shewanella frigidimarina EG301 carrying pMMB503EH-*k56a*			This work
Shewanella frigidimarina EG301	Bacterial conjugation	Fcc_3 knock-out strain	Lab stock

2.2 Media and antibiotics

Luria-Bertani media (LB) and Minimal media, as either liquid solution or solid agar plate, were used to grow bacteria cells in this work with appropriate amount of antibiotics (see Table 2-2). The LB media were provided by the Media Room in the Darwin Building, the University of Edinburgh. The liquid minimal media was made up with 10 ml Trace elements stock (see Table 2-3), 390 ml Minimal media base (see Table 2-3), 0.4 ml Rifampicin stock (see Table 2-2), the electron donor (40 mM lactate) and certain electron acceptor.

Table 2-2 Antibiotics used in this work.

Antibiotics	Stock solvent	Stock concentration	Working concentration in media
Kanamycin	dH_2O	50 mg/ml	50 μg/ml
Rifampicin	methanol	10 mg/ml	10 μg/ml
Streptomycin	dH_2O	50 mg/ml	25 μg/ml

Table 2-3 The recipe of liquid minimal media used in this work.

Trace elements stock (40x) (500 ml, pH 7.4)		
Chemical	**MW (Da)**	**Amount**
EDTA	372.24	500 mg
H_3BO_3	61.83	70 mg
$Na_2WO_4 \cdot 7H_2O$	419.9	1.6 mg
$FeSO_4 \cdot 7H_2O$	278.0	30 mg
$CoSO_4 \cdot 7H_2O$	281.12	28 mg
$NiCl_2 \cdot 6H_2O$	237.7	25 mg
$Na_2MoO_4 \cdot 2H_2O$	241.9	20 mg
Na_2SeO_4	172.94	5 mg
$ZnSO_4 \cdot 7H_2O$	287.54	10 mg
$CuSO_4$ (4% aq)		16 mg
$MnSO_4 \cdot H_2O$	169.02	10 mg
Minimal Media Base (500 ml, pH 7.4)		
$(NH_4)_2SO_4$	132.1	0.92 g
K_2HPO_4	174.2	0.5 g
KH_2PO_4	136.1	0.34 g
$NaHCO_3$	84.01	0.084 g
$MgCl_2$	203.31	0.1 g
$CaCl_2$ †	147.0	0.015 g
NaCl	58.44	1.5 g
Amino acids ‡		10 mg each

Notes:

† $CaCl_2$ was made in a separate bottle of dH_2O (5 ml) first and added it into the large volume of MM Bases after autoclave and cooling-down.

‡ Amino acids used were L-Serine, L-Asparagine, and L-Glutamine.

2.3 Protein expression and purification

2.3.1 Bacterial conjugation

OTR were initially over-expressed in *Shewanella oneidensis* MR-1 *Δotr* strain but it was difficult to be separated from the fumarate reductase (Fcc_3) (see Appendices 2.1 & 2.2). Therefore all vectors encoding the proteins of interest which were originally

stored in the *E. coli* SM10 strain were transformed into *Shewanella frigidimarina* EG301 (a Fcc_3 knock-out strain) through bacterial conjugation.

E. coli SM10 cells carrying the plasmid of interest were grown overnight in 5 ml LB liquid media (with 50 μg/ml Kanamycin) at 30 °C, 170 rpm. The cells of *Shewanella frigidimarina* EG301 were grown under the same condition as *E. coli* SM10 except that the temperature was 23 °C. Then 1.5 ml of the overnight culture of each strain was added into an Eppendorf tube and centrifuged at 5,000 rpm for 3 min at room temperature. The cell pellets were suspended with 200 μl fresh LB (antibiotic-free). 5 μl cell suspension of *E. coli* SM10 and 45 μl cell suspension of *S. frigidimarina* EG301 were mixed together and spotted onto a small piece of sterile filter paper placed on the surface of an antibiotic-free LB-agar plate. After the plate was incubated for 24 hours at 23 °C, the filter paper was removed into an Eppendorf tube and washed with 1 ml fresh LB by vortexing to suspend the cells. The cells suspension was then centrifuged at 5,000 rpm for 3 min after removing the filter paper. The pellet was re-suspended with 200 μl fresh LB and the suspension was spread onto a LB-agar plate containing appropriate amounts of Rifampicin, Kanamycin and Streptomycin (see Table 2-2). This plate was incubated at 23 °C for a further 48 hours. Only the *S. frigidimarina* EG301 cells carrying the plasmids of interest could survive on the plate.

The successfully transformed *S. frigidimarina* EG301 cells were inoculated into liquid LB and grown to mid-exponential phase at 23 °C. 1 ml of the cell culture was mixed with 77 μl DMSO and stored at -80 °C for future use.

2.3.2 SDS-PAGE, heme-staining and coomassie-staining

NuPAGE® 4-12% Bis-Tris gels purchased from Invitrogen™ were used to identify the presence of OTR in various samples. The gel was run under the controlled conditions (voltage <150 V and current<90 mA) for 1 hour in 20-fold diluted NuPAGE MES SDS Running Buffer®.

Heme staining of the gel was carried out using a modified method from the previously described (Goodhew *et al.*, 1986). The NuPAGE® gel was first soaked in 100 ml solution-I (30 ml methanol, 70 ml 250 mM NaAc, pH=5.2) for 10 min, and then was moved into 50 ml solution-II (15 mg TMBZ, 15 ml methanol and 35 ml 250 mM NaAc, pH=5.2; TMBZ was prepared by dissolving the power in methanol and placed in the dark) in an opaque box to prevent the light. The box was incubated for 25 min at room temperature. 150 µl 30% (w/w) H_2O_2 solution was then added into the box which was further incubated in the dark for 3~5 min after gentle mixing. The stained bands were fixed by washing the gel with dH_2O before scanning.

Coomassie staining was implemented by soaking the gel in the staining solution (0.25% (w/w) coomassie brilliant blue G250, 45% (v/v) methanol, 45% (v/v) dH_2O and 10% (v/v) glacial acetic acid) for 1h~overnight. The gel was then destained with the destaining solution (staining solution without the dye).

2.3.3 Protein expression in *Shewanella frigidimarina* EG301

Shewanella frigidimarina EG301 strain carrying pMMB503EH encoding the target protein was inoculated into a 100 ml LB starter culture with defined amounts of Rifampicin, Kanamycin and Streptomycin (see Table 2-2), and was grown at 23 °C, 170 rpm for 8 hours. The starter culture was then inoculated into 8 flasks×0.7 litre LB media with the same antibiotics content (10 ml starter culture for each flask). The cells were further grown overnight at 23 °C, 150 rpm until the OD_{600nm} of the culture reaches 1.2~1.4. Then 1 mM IPTG was added into each flask to induce the expression of the target protein. After 4-hour induction at 15 °C, 170 rpm, the cells were harvested using a Sorvall RC5B centrifuge at 4 °C, 9,000 rpm for 20 min and the cell pellets were frozen at -20 °C ready for lysis.

2.3.4 Cell lysis

Frozen cell pellets from Section 2.3.3 were suspended with buffer A (see Table 2-4) (100 ml buffer A per 30 g pellet) plus 1 mM EDTA and 1 mM PMSF to inhibit the

proteinase. The cells were lysed by 8~10 bursts (20 seconds per burst) of 10~15 μm sonication on ice. The lysate was centrifuged in a Sorvall RC5B centrifuge at 4 °C, 19,000 rpm for 1 hour and the supernatant was collected for the next step.

Table 2-4 Buffers used during the purification.

Buffer label	Contents	pH
A	20 mM Tris-HCl	8.4
B	20 mM Tris-HCl + 500 mM NaCl	8.4
C	20 mM Tris-HCl + 50 mM K_2HPO_4	8.4
D	20 mM Tris-HCl + 100 mM K_2HPO_4	8.4
E	10 mM Imidazole + 100 mM NaCl 100 mM phosphate	8.0
F	250 mM Imidazole + 100 mM NaCl 100 mM phosphate	8.0

2.3.5 DE52 weak anion exchange

DE52 resin (diethylaminoethyl cellulose, Whatman®) was suspended in buffer A and packed into a 3 cm×10 cm column (diameter×height) which was then equilibrated with 5 column volumes of buffer A in a 4 °C cold room. Supernatant of cell lysate was loaded onto the DE52 column which was subsequently washed with 50 mM NaCl buffer (10-fold dilution of buffer B with buffer A) until the 280 nm absorbance (A_{280nm}) of the eluate became zero. The column was then eluted with 100 mM NaCl buffer (5-fold dilution of buffer B with buffer A) and the eluate was collected in 25-ml fractions. Fractions containing the target protein were identified by the heme-stained NuPAGE® gel and concentrated into a volume of 5-10 ml using the 30,000-Da MWCO tubes (VIVASCIENCE) centrifuged at 4 °C and 3,000 rpm. The DE52 resin was re-suspended after use and washed with 1 M NaCl and 1 M NaOH solution in a plastic beaker for 3-5 times until it turned white.

2.3.6 Q-sepharose strong anion exchange

Buffer A and B (1.8 litre each), 500 ml 1.5 M NaCl, 500 ml dH_2O and 500 ml 20% ethanol solution were filtered by flowing through a 0.2 μm nylon membrane filer (Whatman®) before use. A pre-packed Q-sepharose column (bed volume 53 ml) run by the ÄKTA purifier (Amersham Pharmacia Biotech) was washed with 100 ml dH_2O first and equilibrated with 200 ml buffer A at the flow-rate of 5.0 ml/min, room temperature. The concentrated protein sample from DE52 (stored on ice) was injected onto the column which was subsequently washed with 20% buffer B (containing 100 mM NaCl) for 6 bed volumes (around 300 ml). Then a continuous salt gradient of 20%-50% buffer B over 6 bed volumes was applied through the column. Eluate containing heme proteins during this gradient was collected in 20-ml fractions according to the A_{410nm}. Fractions containing the protein of interest were identified and concentrated as described in Section 2.3.5. The Q-sepharose column was then regenerated by washing it with 120 ml 1.5 M NaCl solution and 60 ml dH_2O before being stored in 20% alcohol.

2.3.7 Hydroxyapatite (HTP) chromatography

About 6 g hydroxyapatite powder (BIO-RAD®) was suspended in 200 ml dH_2O and the supernatant was decanted after the suspension was settled down in 5 min. The above step was repeated for 3 times to remove small particles and bubbles. The settled HTP was then suspended in 100 ml buffer A and packed into a 3 cm×5 cm column placed in the 4 °C cold room. After equilibrating the column with 5 bed volumes of buffer A, the concentrated protein sample from Q-sepharose (stored on ice) was loaded onto the HTP column surface. After the unbound proteins completely flew though (by monitoring the A_{280nm}), the column was washed with buffer C until no proteins was found in the eluate. Finally the column was eluted with buffer D and 5-ml fractions of the eluate were collected. Fractions containing the target protein was identified and concentrated into a volume of 100~300 μl before stored at -80 °C.

2.3.8 Superdex 75 gel-filtration

Concentrated protein sample from HTP was loaded into a pre-packed Superdex™ 75 HR 10/30 gel-filtration column (bed volume is 24ml) run by the ÄKTA purifier (Amersham Pharmacia Biotech) in buffer B at the flow-rate of 0.2 ml/min. The eluate was collected in 0.5 ml fractions and the target protein was identified and concentrated before stored at -80 °C.

2.3.9 Nickel affinity chromatography

The 6×His-tagged OTR was also expressed the same way as described in Section 2.3.3. Supernatant of cell lysate was loaded onto a Nickel column (3cm×6cm) which was pre-equilibrated with Buffer E. The column was then washed with 100 ml 20 mM Imidazole (24-fold dilution of Buffer F with Buffer E). The protein of interest was eluated with 40 mM Imidazole (8-fold dilution of Buffer F with Buffer E) and concentrated. The Nickel column was regenerated by washing it with 150 ml Buffer E. The imidazole in the protein sample was removed by running the sample through a G25 gel-filtration column.

2.4 Kinetic measurements of OTR-catalysed reactions

2.4.1 Reduced methyl viologen (MV^+) preparation

Reduced methyl viologen (MV^+) is a strong reducing agent ($E^o_{MV^{2+}/MV^+}$ = -446 mV) and has a large extinction coefficient of 13.6±0.5 $mM^{-1}\bullet cm^{-1}$ at 604 nm where its oxidised form (MV^{2+}) has nearly no absorbance (Mayhew, 1978). Therefore MV^+ was employed in this work as the artificial electron donor to measure the electron transfer rate in the OTR-catalysed reduction of various substrates.

6-10 mg methyl viologen crystal ($MVCl_2$, purchased from SIGMA-ALDRICH®) was dissolved in 5 ml 1.5 M NaCl solution (pre-degased) in a Nitrogen box ($[O_2]$<5 ppm). Methyl viologen was then reduced electronically driven by AutoLab Potentiostat. The working potential between the electrodes was increased gradually from zero to around -450 mV to generate MV^+, controlled by GPES (General Purpose Electrochemical System V4.9). The working potential was never lower than -500 mV to prevent formation of H_2 ($E^o_{H2O/H2}$ = -830 mV) or MV^0 ($E^o_{MV^+/MV^0}$ = -700 mV). When the current became constant the reaction was stopped and the dark-blue solution of MV^+ was sealed and stored in the Nitrogen box.

2.4.2 Steady-state assays of OTR-catalysed reduction of different substrates

The steady-state kinetics of the reduction of tetrathionate, nitrite, hydroxylamine and formate catalysed by wild-type OTR and its mutant forms were measured in the nitrogen box ($[O_2]$<5 ppm). Small amount of enzyme (<1 μM) and around 60-70 μM MV^+ was pre-incubated in 3 ml 50 mM Tris-HCl buffer (pH=7.0) for 1-2 min to allow the oxidised OTR to be fully reduced. Then appropriate amount of substrate was added into the solution and mixed to trigger the reaction. The absorbance at 604 nm (A_{604nm}) was monitored all the time and the electron transfer rate was obtained based on the linear change of A_{604nm} over time in the early stage of the reaction right after adding the substrate (see Figure 2-1).

As substrates may react with MV^+ without enzyme, the enzyme-free assays were also carried out as the controls. The enzyme-free reaction rates were measured and subtracted from the steady-state reaction rate in the presence of enzyme at the same substrate concentration, to obtain the observed reaction rate ($V_{steady\text{-}state}$). Notably in the absence of enzyme high concentrations of nitrite (>0.3 mM) could react with MV^+ drastically after a flat lag-phase which is more than 70 seconds under the assays conditions (see Appendices-3.1). Therefore all measurements of the steady-state reaction rates for nitrite reduction were taken within the first 60 seconds to minimise the errors.

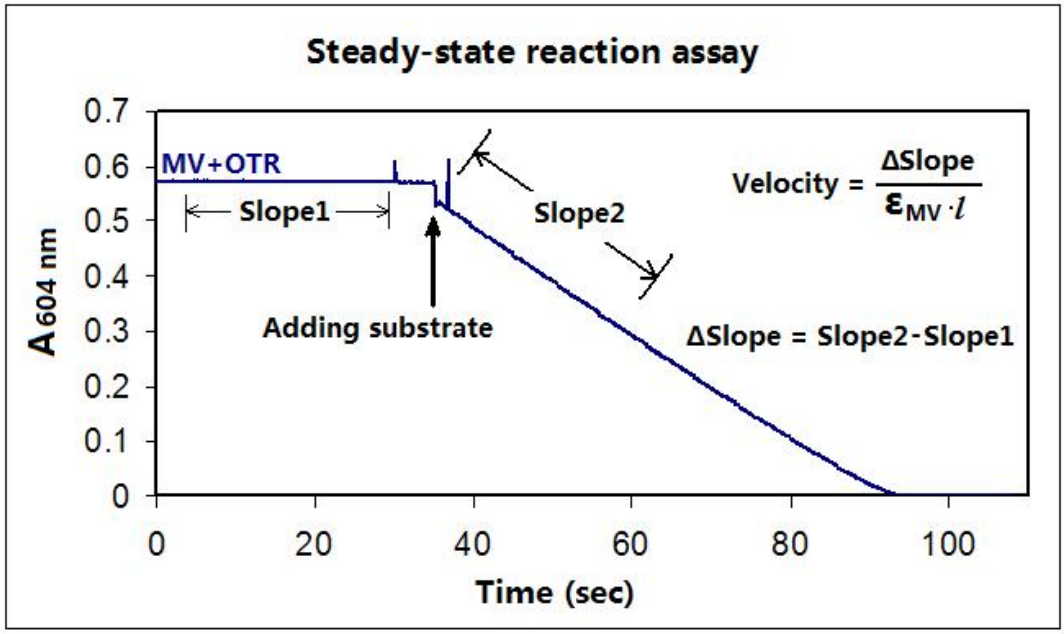

Figure 2-1. Time course of the reduction of the substrate (hydroxylamine in this case) catalysed by OTR. The blue curve is the changing course of the 604 nm absorbance of reduced methyl viologen (MV^+) over time. Slope1 reflects the background oxidation rate of MV^+, which is generally zero. Slope2 of the linear part of the curve after adding the substrate reflects the steady-state electron transfer rate. Rate of the enzymatic reduction could be calculated by the following equation: Velocity = (Slope2-Slope1)/($\varepsilon_{MV^+} \bullet l$), where l = 1 cm, ε_{MV^+} = 13.6 $mM^{-1} \bullet cm^{-1}$.

The observed reaction rates ($V_{steady\text{-}state}$) at different substrate concentrations could be fitted into the Michaelis-Menton equation by Origin® 7.5 to obtain the apparent dissociation constant K_m and the maximum reaction rate V_{max}:

$$\mathbf{V_{steady\text{-}state} = V_{max} \times [Substrate] / ([Substrate] + K_m)}$$

The turnover number (k_{cat}) was then calculated from $k_{cat} = V_{max}$ / [Enzyme], where the concentration of enzyme was obtained by measuring the 408 nm absorbance of the protein sample (ε_{408nm} = 952.4 $mM^{-1} \bullet cm^{-1}$ for oxidized OTR, Rothery, 2004).

2.4.3 Stopped-flow pre-steady-state kinetic assay

OTR was fully reduced by adding sodium dithionite into the protein sample which was then run through a G25 gel-filtration column in the Nitrogen box to remove the extra dithionite. Reactions between reduced OTR and one of its substrates (nitrite, hydroxylamine and tetrathionate) at different concentrations were carried out in the stopped-flow apparatus in the Nitrogen box. The whole wavelength (300-700 nm) spectral change of the reaction mixture was monitored over time. The 420 nm absorbance change (ΔA) over time (Δt) was used to calculate the initial electron transfer rate (V_{ini}) of the reaction. As the A_{420nm} change may not be proportional to the moles of electrons transferred all the time, a titration curve of the reduced OTR was made by gradually adding small amount of hydroxylamine (see Figure 2-2).

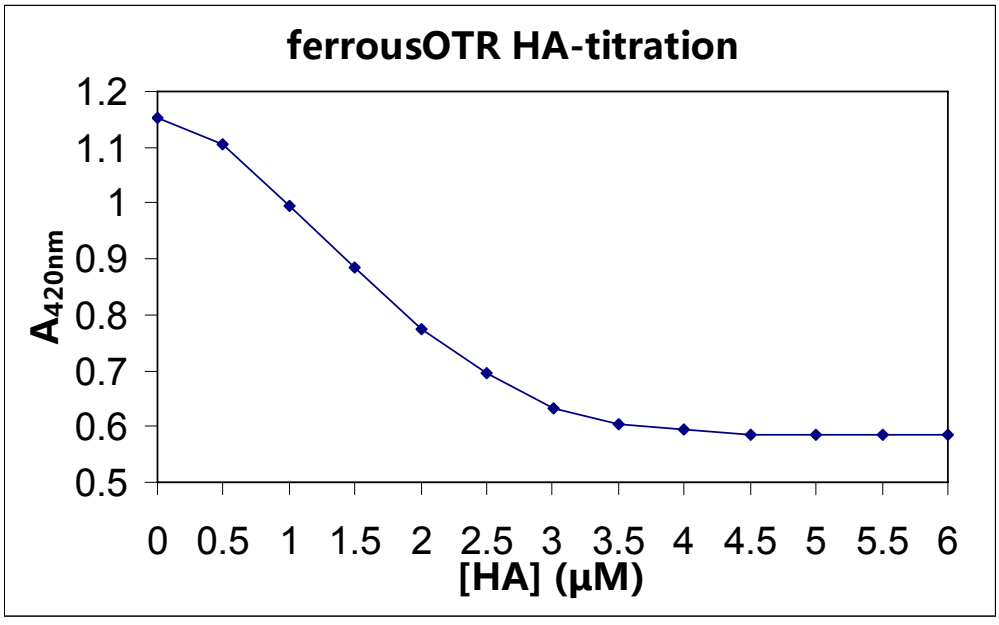

Figure 2-2. Titration curve of ferrous OTR. Fully reduced OTR (0.94 µM) was titrated with 0.5 µM hydroxylamine each time and the normalised A_{420nm} was recorded. The initial A_{420nm} is 1.154 and the A_{420nm} at 0.5 µM hydroxylamine (1 µM electron) is 1.104.

The initial stage of the pre-steady-state reaction was defined here by the absorbance change (ΔA) from the starting value (A_{ini}) when the first electron was transferred from one molecule of ferrous OTR to the substrate. From the titration curve (see Figure 2-2) it could be calculated that ΔA for the initial stage is A_{ini}*4.1%. Therefore the initial electron transfer rate could be calculated by the equation $V_{ini}=k*20$ (s^{-1}), where *k* is the slope of the straight line fitted to the initial-stage data points recorded by the stopped-flow (see Apendices-8.1 for detailed calculation).

2.5 Phenotype studies of *Shewanella oneidensis* MR-1 strains

2.5.1 Cell growth with defined terminal electron acceptors

Phenotypes of *Shewanella oneidensis* MR-1 strains, both the wild-type and Δ*otr*, were monitored by growing the cells in minimal media with defined sole electron donor and acceptor. Unless mentioned otherwise, Rifampicin was added to 10 μg/ml into the minimal media at any time before inoculation. The electron donor was always 40 mM lactate and the electron acceptors used in this work included fumarate, nitrite, nitrate, tetrathionate, thiosulfate, sulfite, elemental sulphur and oxygen, at appropriate concentrations. The cells were pre-cultured aerobically in minimal media at 30 °C overnight with 40 mM lactate as the electron donor and 1 ml of the overnight culture was centrifuged at 5,000 rpm. Cell pellets were re-suspended with around 50 μl minimal media base to make sure the OD_{600nm} of the suspension was the same (to 0.01) between the wild-type and the Δ*otr* strain. The cell suspension was then moved into a Nitrogen box and inoculated to the minimal media liquid or agar plate which contains the defined electron donor and acceptor. Sealed bottles or plates of minimal media with the inoculated cells were incubated at 30 °C and the growth was monitored for up to 5 weeks.

The media containing colloidal elemental sulphur was made by mixing small volume of 1 M polysulfide stock into the minimal media. The polysulfide stock was made by heating 1 M sodium sulphide solution containing 2 M elemental sulphur powder until the sulphur was completely dissolved.

2.5.2 Fe(III) reduction by *Shewanella oneidensis* MR-1

The insoluble Fe(III), hydrous ferric oxide (HFO), was synthesized by neutralising $FeCl_3$ solution with NaOH to precipitate HFO which was then washed with dH_2O for 3 times to remove Cl^- (Zachara *et al.*, 1998). Ferric citrate solution was made by heating ferric citrate aqueous suspension until complete dissolution and adjusting the solution pH to 6.5 after cooling down.

The Fe^{2+}-detecting agent Ferrozine was purchased from SIGMA-ALDRICH® and made into a 100 mM stock solution. The extinction coefficient of Ferrozine-Fe(II) complex at 562 nm was calibrated to be 29,514 $M^{-1} \bullet cm^{-1}$ with $FeSO_4$ solution at known concentration and 100 mM NaAc solution (pH=5.3) as the testing buffer.

Cells of wild-type *Shewanella oneidensis* MR-1 and the Δ*otr* strain were pre-cultured aerobically in 100 ml minimal media containing with 20 mM lactate and 10 μg/ml Rifampicin for 24 hours. The cells were then spin down and re-suspended with small volume of minimal media to OD_{600nm}=10.5 before inoculation into the testing culture.

The testing culture was prepared for each Bijou bottle following Table 2-5. After being inoculated with the cell suspension in a N_2-box, all the bottles were sealed with screw caps and Parafilm and moved outside the N_2-box to shake at 100 rpm, 30 °C.

Table 2-5. Content of the testing bottles in the Fe(III) reduction assays.

No. of bottle(s)	Minimal media	Electron donor	Electron acceptor	Cell inoculum
1	3 ml	20 mM Lactate	20 mM HFO	-
2, 3, 4	3 ml	20 mM Lactate	20 mM HFO	200 μl WT
5, 6, 7	3 ml	20 mM Lactate	20 mM HFO	200 μl Δ*otr*
1'	2 ml	20 mM Lactate	20 mM Fe(III)Citrate	-
2', 3', 4'	2 ml	20 mM Lactate	20 mM Fe(III)Citrate	130 μl WT
5', 6', 7'	2 ml	20 mM Lactate	20 mM Fe(III)Citrate	130 μl Δ*otr*

After incubation for 68 hours, testing bottles No.1-No.7 were assayed for Fe^{2+} concentration. Immediately after unsealing, 5 µl of culture from each bottle was added into a cuvette containing 985 µl 100 mM NaAc buffer (pH=5.3) and 10 µl 100 mM ferrozine stock (1 mM after mixing). The testing solution in each cuvette was then mixed by pipetting and settled for 30 seconds before reading its absorbance at 562 nm in a UV-visible spectrometer. During that 30-second period, 1 ml of culture from each bottle was added into 1 ml concentrated HCl to mix and left for one hour to extract the undissolved form of Fe(II) before reading the A_{562nm} (Zachara *et al.*, 1998). The Fe^{2+} concentration in the original culture was calculated by the following equation: $\mathbf{[Fe^{2+}] = 200*A_{562nm}/(\varepsilon_{562nm}*\mathit{l})}$, where l = 1 cm. Testing bottles No.1'-No.7' were assayed with the same method but only after 45-hour incubation.

2.6 MALDI-TOF mass spectroscopy

2.6.1 Protein peptide sample preparation

Porcine pancreas trypsin was purchased from SIGMA-ALDRICH® and made into 50 µl 25 mg/ml stock solution which was then divided into 10 aliquots (5 µl each) and stored at -20 °C for future use. Purified OTR sample (~20µM) was diluted by 10 times with 50 mM NH_4HCO_3 solution. Protein digestion was carried out by adding 1 µl trypsin stock into 49 µl protein-NH_4HCO_3 solution and the mixture was incubated at 30 °C for 12 hours.

2.6.2 Peptides treatment with DTT and/or IAA

Part of the trypsin-digested sample of OTR was further mixed with 50 mM DTT (Dithiothreitol) and incubated at 30 °C for 20 minutes. Part of the DTT-treated sample was mixed with 50 mM IAA (Iodoacetamide) in the dark at room temperature to alkylate the cysteine thiol group.

2.6.3 OTR treatment with Dimedone

Dimedone (5,5-Dimethyl-1,3-cyclohexanedione) powder was purchased from SIGMA-ALDRICH® and a 100 mM stock solution was made in pure ethanol. Sample-I was prepared by mixing 20 µM wild-type OTR with 4 M guanidine hydrochloride (GndCl) in an Eppendorf tube in a Nitrogen box. After the tube was incubated for 1 hour at room temperature, 2 mM dimedone was added and the tube was further incubated overnight in the box. Sample-II was prepared by first mixing the OTR sample (20 µM) with 2 mM dimedone and incubating the tube overnight in the Nitrogen box. Then 4 M GndCl was added into the tube to denature the protein for 4 hours. Sample I and II were then digested with trypsin as described in Section 2.6.1. Part of the digested sample was treated with DTT+IAA as described in Section 2.6.2.

2.6.4 MALDI-TOF mass spectrometer operation and data processing

The matrix used for MALDI-TOF (Matrix-assisted laser desorption/ionization) mass spectroscopy in this work was the CHCA (α-cyano-4-hydroxycinnamic acid) solution. 10 mg CHCA which was purchased from SIGMA-ALDRICH® was mixed with 400 µl dH_2O in an Eppendorf tube. 100 µl 3% TFA (trifluoroacetic acid) and 500 µl ACN (acetonitrile) were then added into the tube. After thorough mixing the tube was centrifuged at 13,000 rpm and stored at -20 °C. The supernatant was used as the matrix solution.

0.5 µl of each sample prepared in Section 2.6.1 to 2.6.3 was mixed with 0.5 µl matrix solution on one of the spots on the Symbiot I MALDI-plate. Triplicate spots were made for each sample. The air-dried plate was loaded into the Voyager-DE™ STR Biospectrometry™ Workstation mass spectrometer (PerSeptive Biosystems) and the data were collected within the *m/z* (mass over charge ratio) range of 800-3600. The results were viewed and processed with DataExplorer (PerSeptive Biosystems). Mass of peaks in the results was calibrated with the featured peptides with known mass (842.5 Da and 2283.2 Da) resulting from the auto-digestion of porcine trypsin. The data were not deisotoped because this process could introduce false peaks.

Theoretical mass of peptides of trypsin-digested OTR was calculated by PeptideMass from the ExPASy proteomics server of the Swiss Institute of Bioinformatics (SIB) which could be accessed by visiting http://www.expasy.ch/tools/peptide-mass.html. Because the calculation by PeptideMass does not take into account the *c*-type hemes which are still attached to the peptide flying in the MALDI-TOF chamber, the mass of the heme-attaching peptides from OTR calculated by PeptideMass were added 616.49 Da to identify the corresponding peaks in the MALDI-TOF data.

2.7 Electron Spray Ionization (ESI) mass spectroscopy

Pure sample of OTR (~22 μM) was prepared in 100 mM NH_4Ac buffer (pH=~6.4-7.2) and diluted with the loading solution which contains 50% (v/v) dH_2O, 49% methanol and 1% formic acid. The diluted protein sample was loaded into the Apex-Qe ESI-FT-ICR (Electron Spray Ionization Fourier Transform Ion Cyclotron Resonance) mass spectrometer equipped with 12 T magnet (BRUKER). Data were processed with DataAnalysis (BRUKER) by Dr David. J. Clarke (School of Chemistry, University of Edinburgh).

2.8 Crystallisation of OTR K56A

Pure OTR K56A sample was concentrated to 110 μM (~6 mg/ml) and stored on ice. Stock solutions used in crystallisation were 50% (w/v) PEG-4000, 1 M NaAc buffers with various pH, and 1 M NH_4Ac. Hanging-drop vaporisation crystallisation of K56A was carried out in the closed wells on a 24-well plate. Three 4×6 plates (24 wells each) were setup aerobically and each well was added 1 ml well solution which constantly contained 100 mM NaAc and 200 mM NH_4Ac but various amounts of PEG4000 and different pH values (see Table 2-6).

Table 2-6 PEG-4000 content and pH of each well.

Plate 1						
PEG / pH	15%	18%	21%	24%	27%	30%
5.3						
5.5						
5.7						
5.8						
Plate 2						
PEG / pH	15%	18%	21%	24%	27%	30%
5.9						
6.1						
6.3						
6.5						
Plate 3						
PEG / pH	24%	26%	28%	30%	32%	34%
6.1						
6.2						
6.3						
6.4						

The concentrated protein sample was mixed with the well solution into 3 drops (3 µl each) on a thin slide and the content of each drop is listed in Table 2-7.

Table 2-7 Contents of the drops on each slide.

	Protein sample (110 µM)	Well solution
Drop 1	1 µl	2 µl
Drop 2	1.5 µl	1.5 µl
Drop 3	2 µl	1 µl

The slide was then sealed onto the corresponding well with the drops facing inside. The plates were incubated at room temperature for 3-8 weeks to allow crystals to grow.

Chapter 3 – Results and Discussion

Mechanisms of OTR-catalysed reduction of *in vitro* substrates

As OTR has been found to catalyse the *in vitro* reduction of various substrates including nitrite (NO_2^-), hydroxylamine (NH_2OH), tetrathionate ($S_4O_6^{2-}$), trithionate ($S_3O_6^{2-}$) and hydrogen peroxide (H_2O_2), studies on the binding and reaction kinetics for these substrates could help clarify the mechanism of the catalysis at the active site of OTR, and thus potentially provide clues in identifying the physiological substrate(s) of this enzyme. In this chapter the spectroscopic features and enzymatic activities of several mutant forms of OTR are investigated in comparison with the wild-type protein. Each of these mutant enzymes, including N61A, K153A, C64A and D150A, has an active-site amino-acid residue replaced by alanine.

3.1 Spectroscopic features of OTR and its mutant forms

3.1.1 OTR expression and purification

OTR over-expressed in *Shewanella oneidensis* MR-1 was found difficult to be separated from the fumarate reductase (Fcc_3) in all methods tried in this work. Therefore all the plasmids encoding the OTRs of interest were transformed from *E. coli* SM10 into a Fcc_3-knock-out strain *Shewanella frigidimarina* EG301 through bacterial conjugation. OTR was then successfully expressed in this new host. The purity of the purified OTR sample was checked in SDS-PAGE (see Figure 3-1). The productivity for wild-type OTR is about 0.3 mg protein per litre LB medium, while for the mutant forms it is about 0.1 mg per litre LB medium.

3.1.2 Spectroscopic characters of wild-type OTR

OTR in solution at pH=7 has a UV-visible spectrum of a typical *c*-type cytochrome (see Figure 3-2). The freshly purified OTR is in the oxidised form which features a Soret band with the maximum absorbance at 408 nm and a β peak at ~532 nm, while

the fully reduced OTR has four peaks at 325 nm, 420 nm (Soret), 523 nm (β) and 551 nm (α), respectively. The 280 nm absorbance of the reduced OTR also slightly decreases after being oxidised by excess amount of hydroxylamine or nitrite.

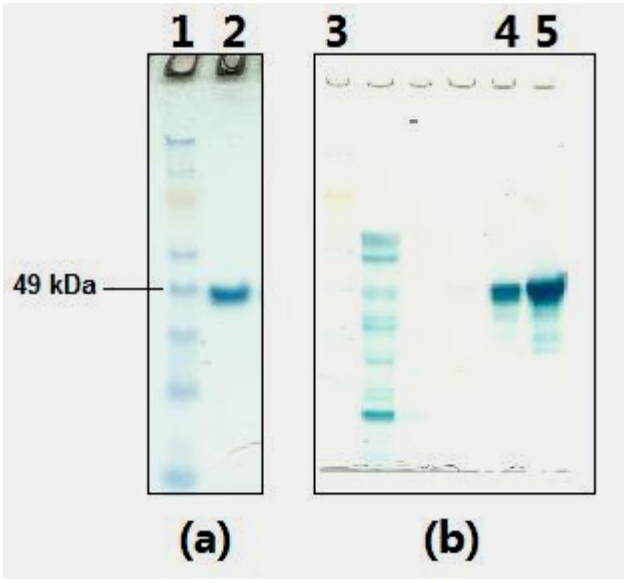

Figure 3-1. Purified OTR sample run in SDS-PAGE gels in (a) Coomassie-blue staining and (b) heme staining. Lane 1 and lane 3 are M_r ladders. Lane 2 and lane 5 are genetically unmodified wild-type OTR purified through 4 successive columns as described in Section 2.3. Lane 4 is the 6×His-tagged wild-type OTR purified through one-step column after cell lysis.

3.1.3 Spectral comparison between wild-type OTR and its mutant forms

Comparing the spectra of the oxidised OTR, there is no major difference observed between the wild-type and several of its mutant forms including N61A, D150A, C64A and K56A (see Figure 3-3a). However the mutant protein K153A displays a slightly different spectrum from that of the wild-type OTR (see Figure 3-3b). The spectrum of OTR K153A has: (i) a distinct peak at ~635 nm which is absent in the spectra of the wild-type and other mutant forms (see Figure 3-3d), (ii) lower absorbances in the region between 500 nm and 600 nm where the spectrum is closer to a single wide peak, whereas other forms of OTR including the wild-type have a slightly double-

peaked spectrum in this region, and (iii) a slightly violet-shifted Soret band compared to that of the wild-type OTR, featuring higher absorbances between 350 nm and 420 nm and lower absorbances between 420 nm and 470 nm. From the differential spectrum of K153A over the wild-type OTR (see Figure 3-3e) it can be seen that a small Soret band is shifted from around 420 nm to 380 nm.

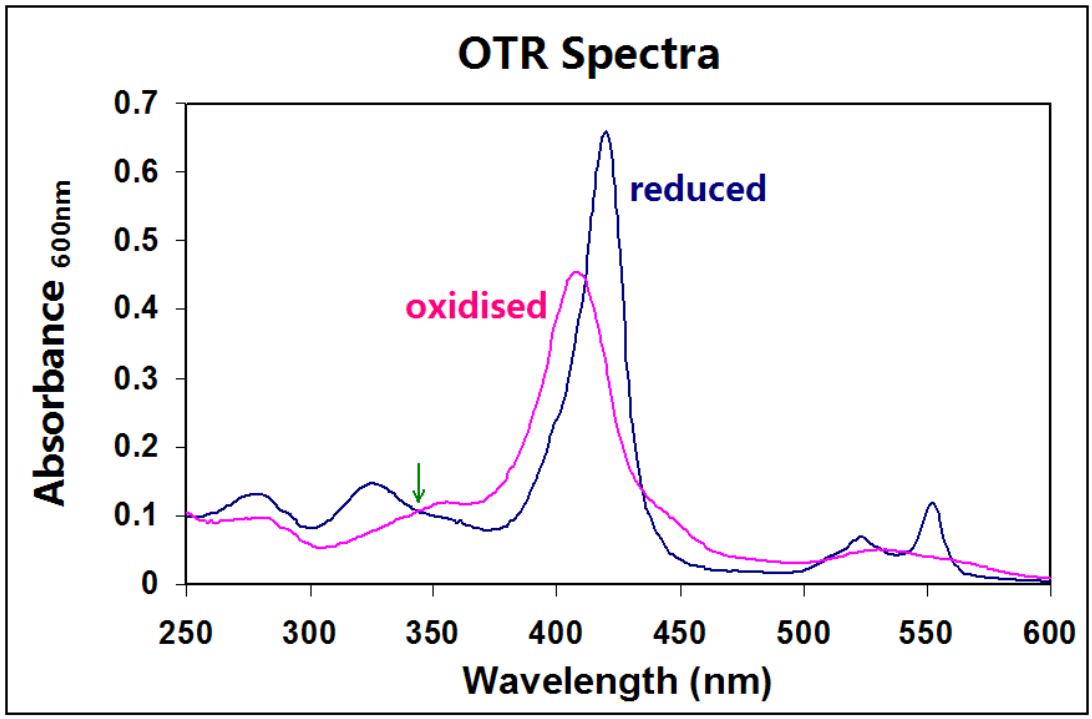

Figure 3-2. **UV-visible spectra of the fully oxidised (pink) and the fully reduced (blue) form of pure wild-type OTR.** About 0.65 µM reduced OTR was completely oxidised by 10 µM hydroxylamine within 15 minutes under anaerobic conditions. All spectra of OTR in different oxido-reduction states during this oxidation (not shown in the figure) share one obvious isosbestic point at around 342 nm as indicated by the green arrow.

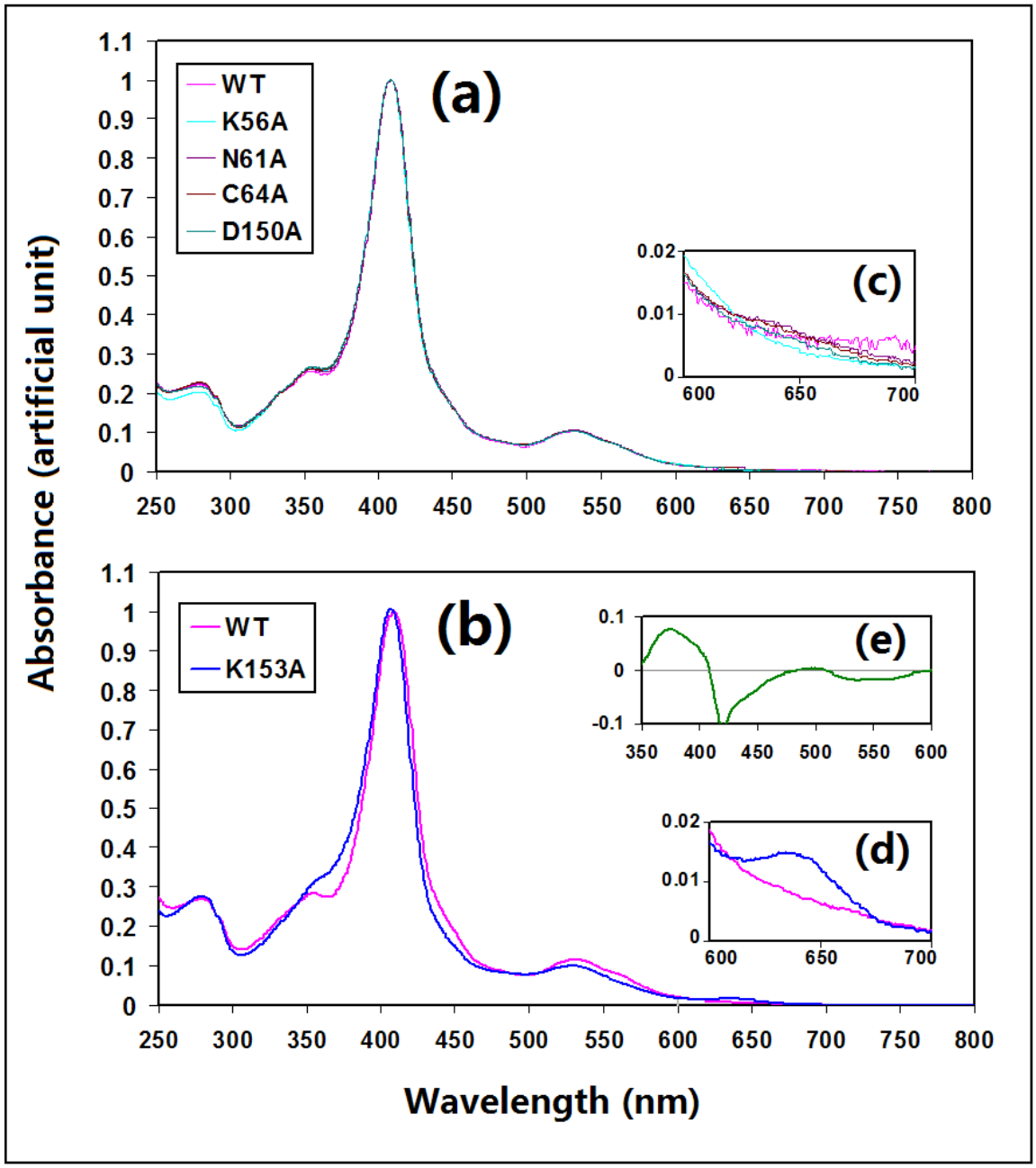

Figure 3-3. Spectroscopic comparison between wild-type OTR and various mutant forms. Spectra for oxidised protein samples with the concentration of around 6.5-7.0 μM were normalised to $A_{408\ nm}$ = 1.0 (in artificial unit) for comparison purpose. Panel (a) and (b) are the whole spectral comparison. Inset (c) and (d) are zoomed spectra between 600 nm and 700 nm. Inset (e) is the differential spectrum between wild-type OTR and K153A ($\Delta A=A_{K153A}-A_{WT}$) based on the spectra in panel (b).

3.2 Reduction of nitrite and hydroxylamine catalysed by OTR

3.2.1 Steady-state kinetics of OTR-catalysed reduction of nitrite

Using excess amount of reduced methyl viologen (MV^{+}•) as the artificial electron donor, the nitrite reduction catalysed by OTR and its mutant forms displays typical Michaelis-Menten kinetics (see Figure 3-4). The corresponding enzymatic parameters (K_m and k_{cat}) are listed in Table 3-1.

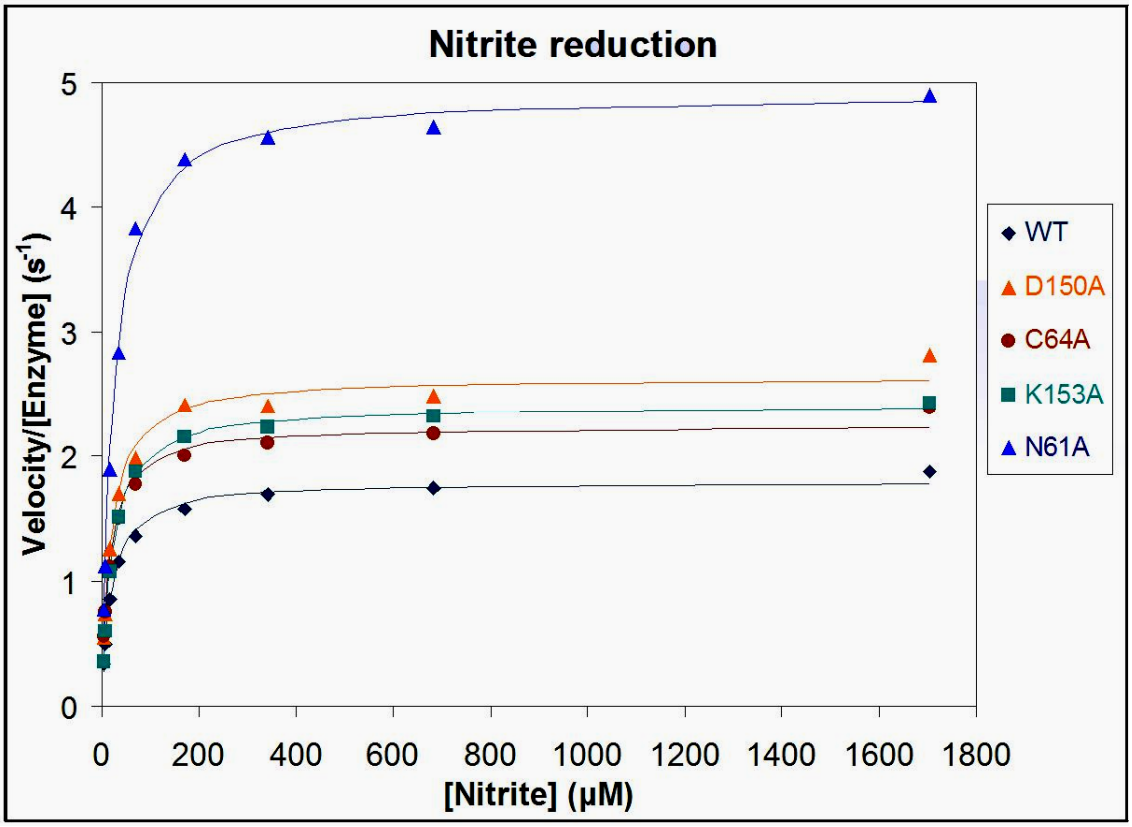

Figure 3-4. Reaction kinetics of the steady-state reduction of nitrite catalysed by wild-type OTR and its mutant forms. The velocity of the electron transfer (μM/s) for each assayed reaction has been divided by the corresponding enzyme concentration (μM) and the resulting values are presented in the diagram for comparison purposes. Data points (solid dots) for each enzyme are fitted into the Michaelis-Menten curves (solid lines).

Table 3-1. Kinetic parameters of OTR-catalysed nitrite reduction.

	K_m (μM)	k_{cat} (s^{-1})	k_{cat}/K_m ($M^{-1}•s^{-1}$)
WT	18.9 ± 1.5	1.8 ± 0.0	$0.95×10^5$
D150A	18.4 ± 2.2	2.6 ± 0.1	$1.4×10^5$
C64A	15.5 ± 1.9	2.2 ± 0.1	$1.4×10^5$
K153A	20.5 ± 0.7	2.4 ± 0.0	$1.2×10^5$
N61A	23.7 ± 1.7	4.9 ± 0.1	$2.1×10^5$

The nitrite reductase activities of wild-type OTR, D150A, C64A and K153A are basically at the same level. The mutation of Asp150, Cys64 and Lys153 into alanine does not impair the ability of OTR to reduce nitrite. N61A shows an even higher turn-over number compared to the wild-type. The K_m values for all these enzymes are around 20 μM.

3.2.2 Steady-state kinetics of OTR-catalysed reduction of hydroxylamine

OTR-catalysed hydroxylamine reduction also follows Michaelis-Menten kinetics but the velocity cap for reactions catalysed by wild-type OTR, N61A and K153A was not directly assayed due to the limitation of the measurement conditions. Data points from the assays are shown in Figure 3-5 and the enzymatic parameters are listed in Table 3-2.

Similar to the results of the nitrite reduction, no mutant protein shows a significantly decreased activity in catalysing the reduction of hydroxylamine. Compared to the wild-type OTR, C64A and D150A show some lower turn-over numbers, whereas N61A and K153A display a remarkable increase in the turn-over. The K_m values for all enzymes assayed are similar but much higher than a physiologically possible concentration of hydroxylamine.

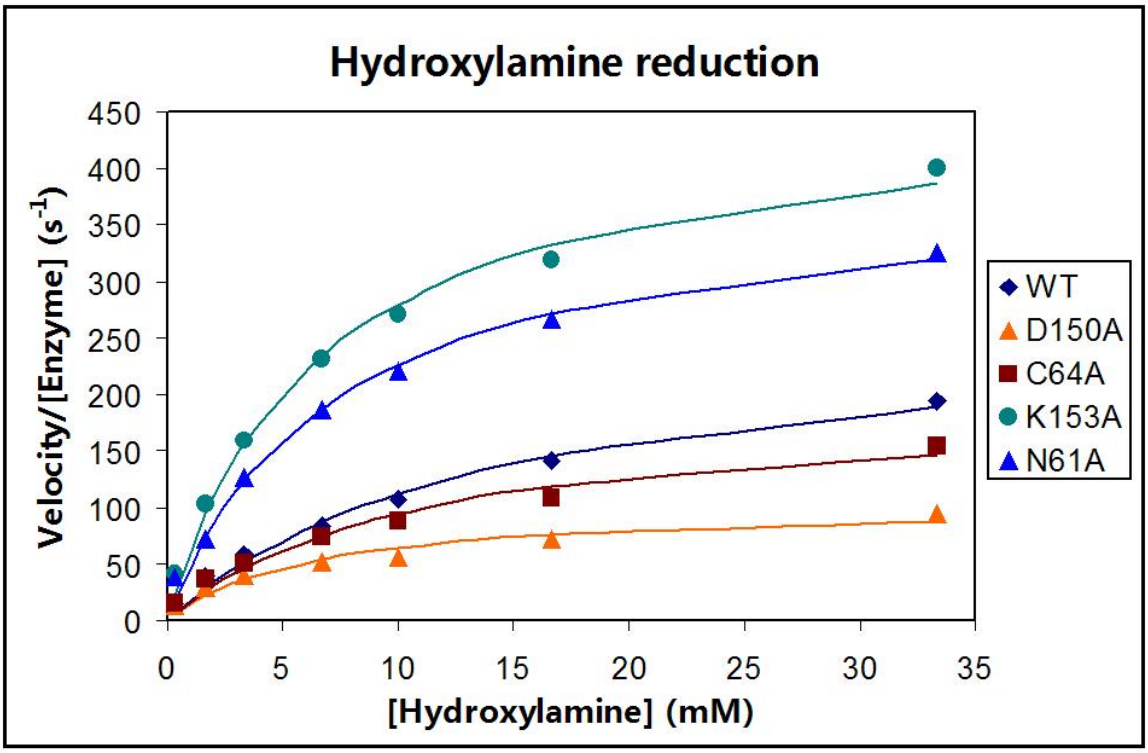

Figure 3-5. Reaction kinetics of the steady-state reduction of hydroxylamine catalysed by wild-type OTR and its mutant forms. The velocity of the electrons transfer (μM/s) for each assayed reaction has been divided by the corresponding enzyme concentration (μM) and the resulted values are presented in the diagram for comparison purpose. Data points (solid dots) for each enzyme are fitted into the Michaelis-Menten curve (lines).

Table 3-2. Kinetic parameters of OTR-catalysed hydroxylamine reduction.

	K_m (mM)	k_{cat} (s^{-1})	k_{cat}/K_m ($M^{-1}s^{-1}$)
WT	13.8 ± 2.5	267 ± 23	1.9×10^4
D150A	6.1 ± 1.8	104 ± 11	1.7×10^4
C64A	10.7 ± 2.8	194 ± 22	1.8×10^4
K153A	6.6 ± 0.8	463 ± 22	7.0×10^4
N61A	7.2 ± 0.9	389 ± 18	5.4×10^4

3.2.3 Binding of nitrite and hydroxylamine to OTR

Measurement of the substrate binding of OTR based on the spectral change in UV-visible spectrometer was found to be difficult, because incubating ferric OTR with excess amount of each of its *in vitro* substrates including nitrite, hydroxylamine, thiosulfate and tetrathionate did not cause detectable spectral change to OTR. Capture of the stable spectrum of ferrous OTR that is binding nitrite, hydroxylamine or tetrathionate was impossible in a spectrometer because immediate oxidation of OTR occurs as soon as these substrates were added.

However, the steady-state reduction rate of hydroxylamine catalysed by OTR is inhibited by imidazole under the O_2-free assay conditions (see Figure 3-6a), indicating that imidazole competes for the 6^{th} coordination position of heme II with hydroxylamine. Strong binding agent carbon monoxide (CO) also inhibits the activity of OTR under the same conditions (see Figure 3-6a) and could cause dramatic spectral shift to ferrous OTR which indicates an overall structural distortion to the protein (see Figure 3-6b).

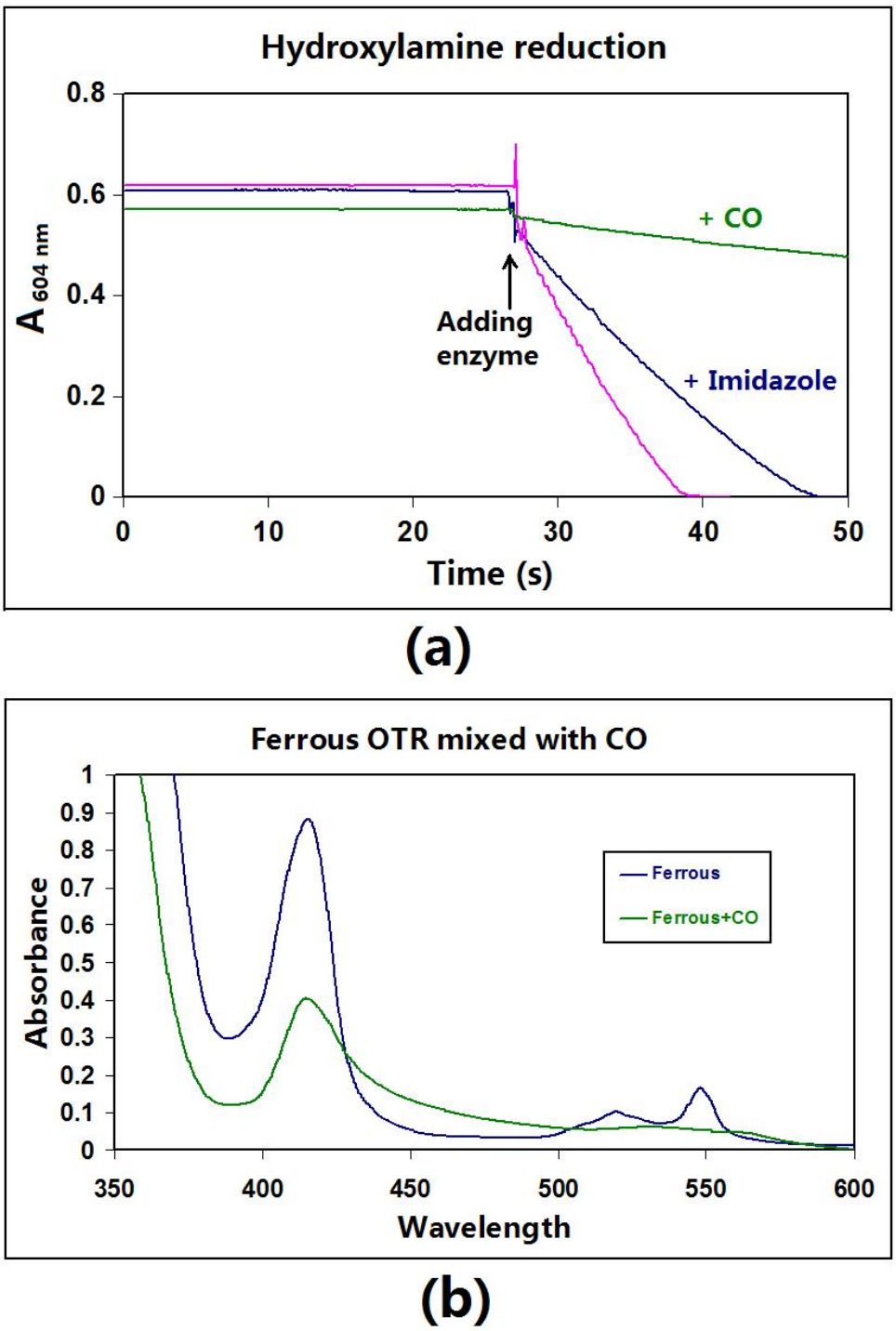

Figure 3-6. Effects of exogenous heme-binding agents on OTR. (a) The inhibition effect of imidazole and CO on the hydroxylamine reductase activity of OTR under anaerobic conditions. Reduced methyl viologen (~45 μM) and hydroxylamine (3.3 mM) was pre-incubated in 3 ml reaction buffer (pH 7.0). OTR was then added to trigger the reaction without any inhibitors added (pink line), or after adding imidazole (blue line), or after adding CO (green line). **(b)** The spectral change to ferrous OTR after adding CO under aerobic conditions. OTR was reduced by adding excess amount of sodium dithionite before adding CO.

3.2.4 Pre-steady-state kinetics of reactions between ferrous OTR and its substrates

To further investigate the reaction mechanism of the reduction of nitrite and hydroxylamine catalysed by OTR, pre-steady-state kinetics was assayed in stopped-flow spectroscopy in which ferrous OTR and nitrite/hydroxylamine were mixed and the absorbance at 420 nm (where the biggest spectral change happens) was recorded over time. The time course of A_{420nm} for nitrite reduction displays a clear initial climbing phase within the first 20 ms and a subsequent exponential decline, whereas the curve for hydroxylamine reduction shows a descending trend from the first moment after mixing which could be fitted into a double-exponential model (see Figure 3-7).

The approximate initial rate of the first electron transfer from ferrous OTR to nitrite or hydroxylamine was calculated with the method described in Section 2.4.3 and Appendices-8.1. Table 3-3 lists the observed pre-steady-state first-order reaction rates and the steady-state turnover rates at the same substrate concentrations which are calculated with the K_m and k_{cat} listed in Table 3-1 and 3-2.

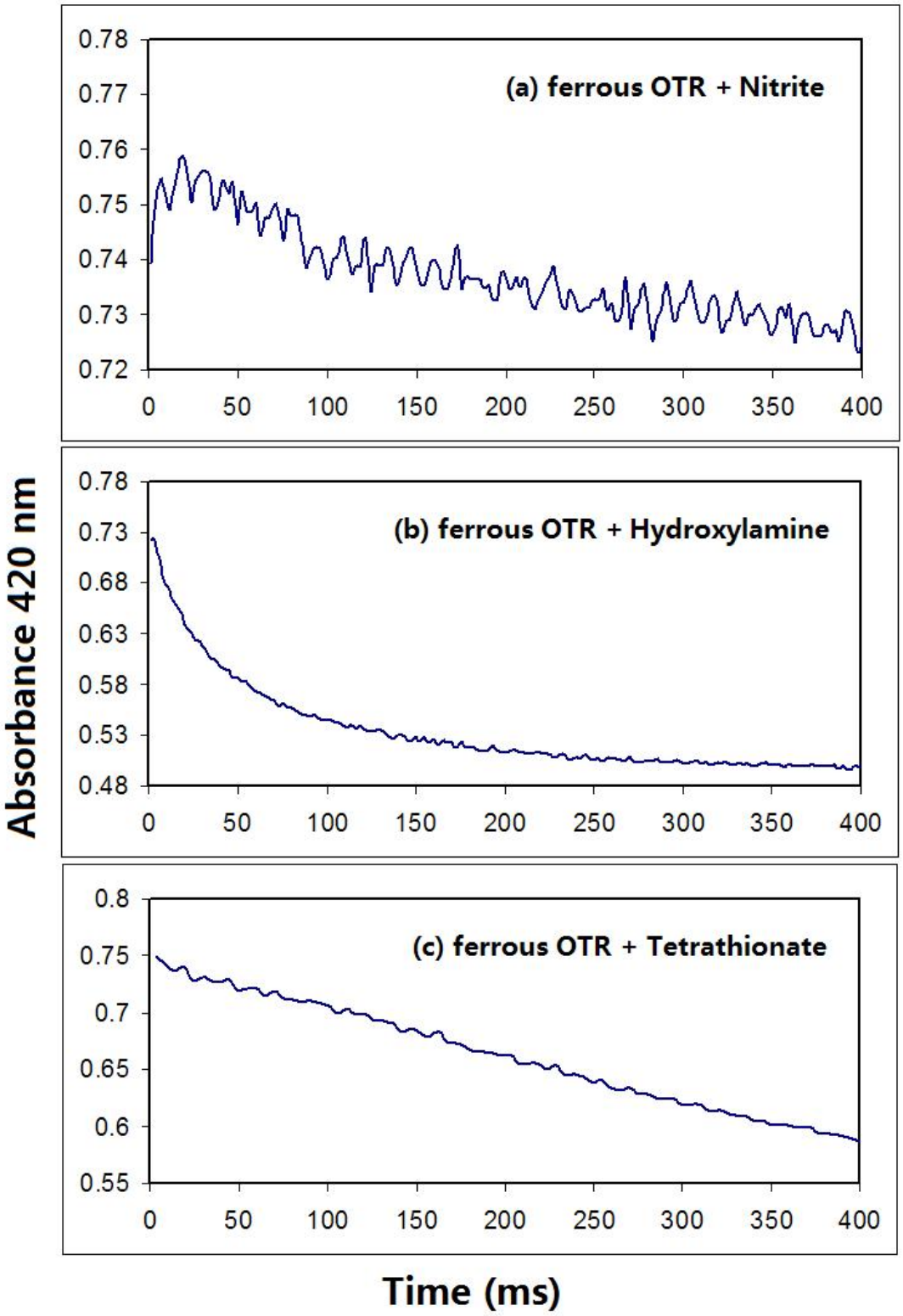

Figure 3-7. Pre-steady-state time courses of A_{420nm} for the reduction of nitrite, hydroxylamine and tetrathionate by ferrous OTR. All reactions were assayed by stopped-flow at pH = 7.0 and 25 ºC. The enzyme is about 0.6 µM after mixing. Substrate concentrations after mixing are (a) $[NO_2^-]$ = 0.5 mM, (b) $[NH_2OH]$ = 5 mM, and (c) $[S_4O_6^{2-}]$ = 5 mM.

Table 3-3. Comparison of reduction rates between pre-steady state and steady-state kinetics. Enzymes used are about 0.6 μM after mixing.

Substrate concentration (after mixing)	Observed pre-steady-state initial reaction rate (electron transferred s^{-1})	Calculated steady-state reaction rate (electron transferred s^{-1})
Hydroxylamine		
0.5 mM	**50**	**9.8**
5.0 mM	**99**	**73**
Nitrite		
0.5 mM	**1.6**	**1.7**
Tetrathionate		
0.5 mM	**0.1**	**19.3***
1.0 mM	**0.8**	**19.7***
2.5 mM	**3.1**	**19.9***
5.0 mM	**8.3**	**19.9***

* Calculation based on previously reported K_m and k_{cat} from Rothery, 2004.

3.3 Reduction of tetrathionate

3.3.1 Steady-state kinetics

The *in vitro* tetrathionate reductase activity of OTR could not be reproduced in this project, even using freshly made tetrathionate solution from first-time-unsealed bottle of solid tetrathionate salt crystal. The steady-state kinetic assay shows no catalytic activity of OTR at various concentrations of tetrathionate from 15 μM to 500 μM. The oxidation of thiosulfate and reduction of trithionate were also unable to be observed in presence of OTR.

3.3.2 Stopped-flow pre-steady-state kinetics

To investigate the nature of the reaction between OTR and tetrathionate, ferrous OTR and tetrathionate were mixed in the stopped-flow apparatus and the absorbance at 420

nm was record over time. The typical time course of enzyme oxidation is shown in Figure 3-7c. The observed initial oxidation rates of ferrous OTR by different concentrations of tetrathionate are listed in Table 3-3.

3.4 Reduction of other *in vitro* substrates catalysed by OTR

Besides the known *in vitro* substrates, OTR was also found to catalyse the reduction of formic acid with reduced methyl viologen (MV^+) as the electron donor, the kinetics of which also follows the Michaelis-Menten equation (see Figure 3-8). The product of this reaction is yet to be identified and the turnover rate is around 1 s^{-1}. The mutant C64A shows similar activity to the wild-type enzyme.

Some other potential substrates of OTR were also tried, including sulphite, thiosulfate, thiocyanide, cysteine, ethanol, colloidal elemental sulphur, and polysulphide (pH=8.5). However OTR showed no reduction activity for any of them.

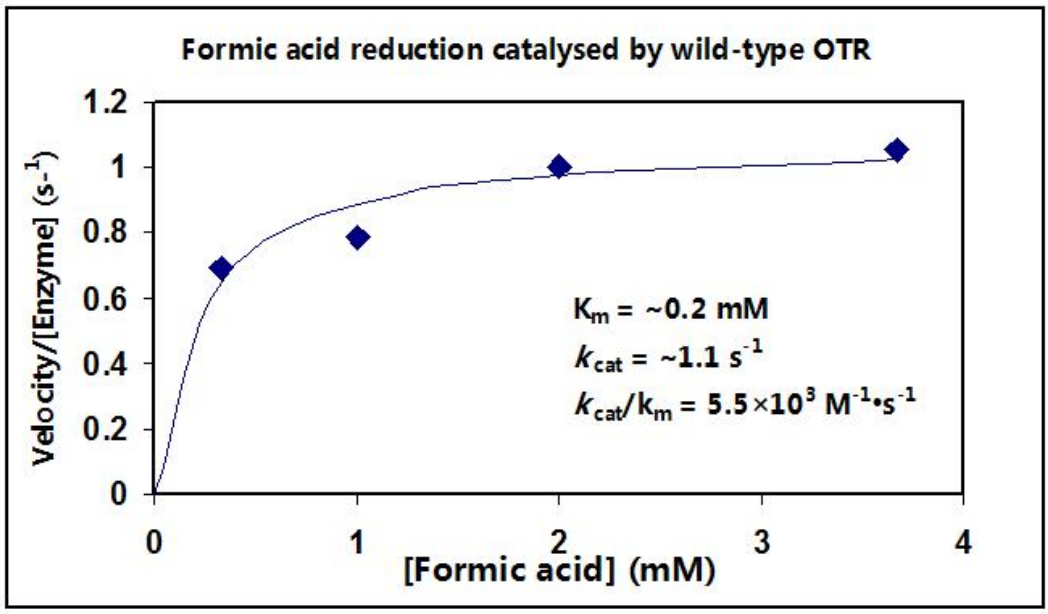

Figure 3-8. The steady-state reduction of formic acid catalysed by wild-type OTR. The velocity of the electrons transfer (μM/s) for each assayed reaction has been divided by the corresponding enzyme concentration (μM). Data points (blue squares) are fitted into the Michaelis-Menten curve (lines).

3.5 Discussion

3.5.1 Spectra reveal some structural features of OTR

All the mutant forms of OTR studied in this work show the final productivity of about only one-third of that of the wild-type, suggesting that the introduction of mutation to the active site of the wild-type OTR makes a negative impact on the cellular maturation of this protein. These structurally immature proteins could be either degraded in the cell or separated from the mature form during the purification.

As there is little difference among the spectra of wild-type OTR, N61A, K56A, D150A and C64A, the heme environments of these four mutant proteins seem not much distorted. Nevertheless OTR K153A exceptionally displays a characteristic peak at around 635 nm which is not seen in the spectra of the wild-type or any other mutant form (see Figure 3-3d). This peak appears to be the typical charge transfer band within the 600-650 nm region, as an indication of a high-spin ferric heme iron in a number of heme proteins such as mitochondrial cytochrome *c* (Bren and Gray, 1993; Silkstone *et al.*, 2005), cytochrome *c* peroxidise (Yonetani and Anni, 1987; Goodin *et al.*, 1991), cytochrome P450 (Jefcoate and Gaylor, 1969), coral allene oxide synthase (Abraham *et al.*, 2001), myoglobin and hemoglobin (Yoshida *et al.*, 1975). Therefore K153A potentially has a high-spin active site heme iron while the wild-type is low-spin. In the substrate-free crystal structure of wild-type OTR, the 6^{th} coordination position of the iron of heme II is occupied by a single-atom anion (potentially S^{2-} or Cl^{-}) which is hydrogen bonded to the amine group of K153 (Mowat, unpublished data). Considering that anion may come from the crystallisation solution, it could also be a water molecule or hydroxide anion that occupies the 6^{th} coordination place in wild-type OTR. The deletion of the long side chain of K153 could destabilise the anion ligand bound to the iron, and hence results in a percentage of 5-coordinated high-spin heme iron in K153A (see Figure 3-9). This model also favours the

hypothesis that K153 helps fit the substrate during the catalysis. However it needs further confirmation by EPR and crystallography studies.

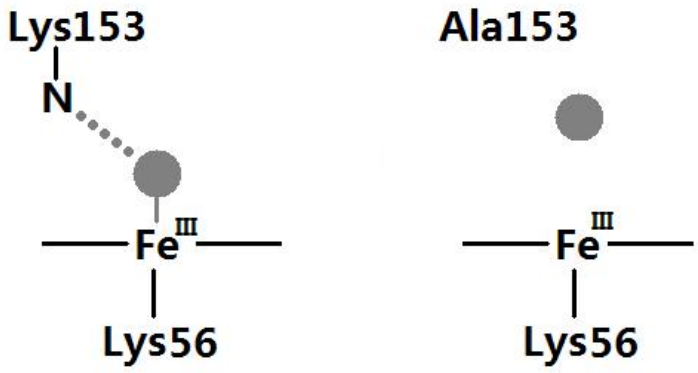

Figure 3-9. Model of the coordination state of the ferric iron of heme II in wild-type OTR and K153A. The left panel shows the low-spin heme iron of wild-type OTR binding an atom (S^{2-}, Cl^- or O from H_2O or OH^-) which is stabilised by the hydrogen-bond from the terminal nitrogen atom of the Lys153 side chain. The right panel shows the 5-coordinated high-spin heme iron in K153A.

3.5.2 Kinetic data analysis for nitrite/hydroxylamine reduction catalysed by OTR

The heme-binding agent, imidazole, inhibits the hydroxylamine reductase activity of OTR, suggesting that hydroxylamine and nitrite bind to the active site heme during the reaction, which is similar to the situation in NrfA. Under anaerobic conditions, fully reduced OTR is rapidly oxidised by added nitrite and hydroxylamine, which is consistent with the fact that the hemes of OTR have very negative redox potentials within the range of about -50 mV to -350 mV (Rothery, 2004). The pre-steady-state assays show that the 420 nm absorbance of OTR undergoes a two-phase time course after mixing with nitrite (see Figure 3-7a). The short initial increase of absorbance probably represents the spectral change caused by the formation of Fe^{II}-nitrite complex. The following descending phase should be the oxidation process of OTR by nitrite and its initial electron transfer rate is nearly equal to the steady-state turn-over

rate (see Table 3-3), suggesting that the rate-limiting step of nitrite reduction is in the early stage of the whole catalytic cycle.

The steady-state reaction curves (see Figure 2-1) and the fitted Michaelis-Menten curves (see Figure 3-4 and 3-5) indicate that in the OTR-catalysed reduction of nitrite and hydroxylamine, both substrates rapidly form the enzyme-substrate complex (ES) at constant concentration during the early stage of the reaction after mixing, and the ES complex turns into the product-enzyme complex (EP) via multiple intermediates.

The small K_m values of nitrite reduction (around 20 μM) reveals a tight binding of nitrite to the heme iron, which is partly due to the back-bonding from the iron(II) to the π^*-orbital of nitrite (Einsle *et al.*, 2002). Such a back-bonding will result in a relatively short Fe(II)-N distance (~2 Å, Einsle *et al.*, 2002) compared to the Fe(III)-S length (2.4 Å) observed in the crystal structure, and therefore potentially weaken the interaction between the side-chain amino group of lysine153 and the nitrogen atom of nitrite. This might explain why K153A does not significantly increase the K_m of nitrite reduction.

The high K_m of hydroxylamine reduction catalysed by OTR (around 10-20 mM) suggest that the interaction between hydroxylamine and heme iron is weaker than nitrite, possibly because hydroxylamine cannot receive the electron back-donation from the ferrous iron. In the assays the observed reaction rates of hydroxylamine reduction never reach the flat phase, i.e. the maximum velocity (see Figure 3-5), so the errors of K_m values could be much bigger than those shown in Table 3-2 which are obtained only from unsaturated enzymes. Therefore the milli-molar difference among the K_m values of different enzymes is not very reliable.

Lysine 153 is a highly conserved active site residue and is the closest to the heme centre. The terminal amino group of lysine153 hydrogen-bonds the sulphur atom that occupies the 6^{th} coordination place of the heme iron; it could potentially offer a hydrogen bond to the Fe(II)-bound nitrogen atom of nitrite and hydroxylamine, or to attack the oxygen atom of these two substrates. However the kinetic data show that the replacement of lysine 153 with alanine does not result in a decreased activity of the enzyme, indicating that the side chain of lysine 153 does not attack the oxygen of

nitrite or hydroxylamine. Surprisingly K153A has even an elevated turnover number (k_{cat}) in comparison with the wild-type, and the reason for that could be among the following points: (1) the deletion of the hydrophobic part of the side chain of lysine 153 facilitates proton access and could therefore speed up the proton-involved steps that limit the overall turn-over rates, (2) the hydrogen bond between the heme carboxyl group and lysine 153 disappears, causing the possible structural disturbance of the heme distal pocket that could also allow the substrates to access protons more easily, and (3) the active site heme of K153A has its redox-potential shifted compared to the wild-type and may affect the reaction rates. The last two reasons could also apply to the increased turn-over rate of N61A which also loses the hydrogen bond between Asn61 and the heme carboxyl group.

Cysteine 64 is a highly conserved, covalently modified active site amino acid residue which interacts with the SCN^- anion via a water molecule. It is therefore strongly suggested that Cys64 is important to the function of OTR by interacting with the substrate, although the identity and the purpose of its modification remains unknown. However C64A shows similar kinetic properties to the wild-type in both reactions, indicating that its side chain does not strongly interact with nitrite or hydroxylamine. This result is consistent with the substrate-docking modelling which shows that the bound nitrite or hydroxylamine is fairly distant from the terminal sulphur atom of Cys64 and it is not feasible for the effective hydrogen bond formation (see Figure 3-10).

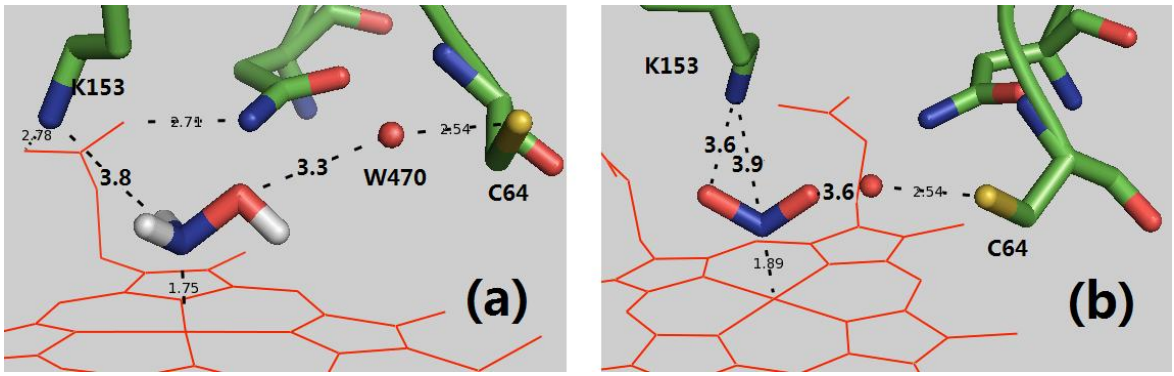

Figure 3-10. Modelling of OTR active site with (a) hydroxylamine and (b) nitrite bound respectively. The N-Fe^{II} distances are modelled based on the structures of substrate-binding NrfA (Einsle *et al.*, 2002). The labelled numbers are in Å. Models were built with PyMOL v0.99 RC6.

3.5.3 Mechanism model for OTR-catalysed nitrite reduction

As ammonium is the observed final product of the OTR-catalysed reduction of both nitrite and hydroxylamine (Atkinson, 2009), the whole catalytic cycle of nitrite reduction could be proposed in Figure 3-11, where hydroxylamine is one of several intermediates.

In this model, the rate-limiting step of the whole cycle should be within Steps 1-3 as the phase from hydroxylamine to ammonium shows a turn-over rate hundreds of times higher than the overall rate from nitrite to ammonium. Because the initial oxidation rate of ferrous OTR by nitrite in pre-steady-state was measured during the first electron transfer stage (see Section 2.4.3) and is similar to the steady-state electron transfer rate (see Table 3-3), the rate-limiting step is proposed to be Step 1.

The low turn-over rate of nitrite reduction in OTR (about 2 electrons per second) is much lower than that of NrfA which is several thousands of electrons per second (Stach *et al.*, 2000; Clarke *et al.*, 2006). This is not surprising because there seems no group from any side chains of the active-site residues attacking the oxygen atoms of the bound nitrite in OTR and the only force facilitating the first N-O bond cleavage is

the interaction between Fe(II) and the nitrogen atom of nitrite, whereas in NrfA the first oxygen atom of nitrite is directly attacked by the side chains of two amino-acid residues in the active site (Einsle *et al.*, 2002). A minor factor could be the redox-potential difference between the active site hemes of OTR and NrfA. Similar reasons could also explain why the turn-over rate of hydroxylamine in OTR is less than one-third of that in NrfA (Stach *et al.*, 2000) as there is an amino-acid side chain attacking the oxygen atom of the bound hydroxylamine molecule in NrfA (Einsle *et al.*, 2002).

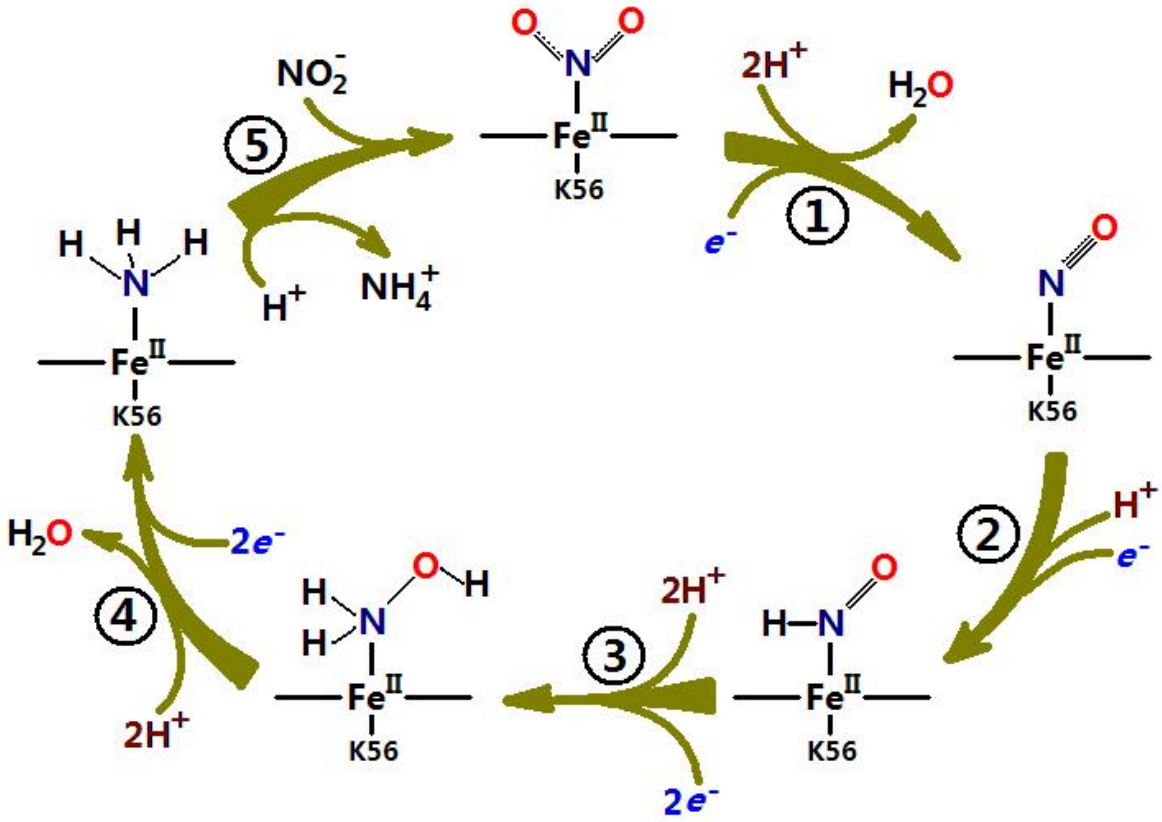

Figure 3-11. Proposed mechanism for the catalytic cycle of nitrite reduction at the active site of OTR. Step 1 involves the first N-O bond breaking of nitrite, water release and the formation of Fe^{II}-NO complex. In Step 2 the Fe^{II}-NO complex undergoes the single-electron reduction and protonation to generate the Fe^{II}-HNO intermediate, which then receives two protons and two electrons to turn into Fe^{II}-NH_2OH complex in Step 3. Hydroxylamine as an intermediate of nitrite reduction is reduced into ammonia in Step 4 and a water molecule is released simultaneously. The ammonia accepts a proton to form ammonium and replaced by nitrite molecule in Step 5.

3.5.4 OTR may not be a physiological nitrite/hydroxylamine reductase

There are several reasons to speculate that nitrite or hydroxylamine may not be the real physiological substrate of OTR:

(1) The activities of nitrite reduction and hydroxylamine reduction catalysed by OTR are not affected by the displacement of the side chain of highly conserved active-site amino-acid residues lysine153 and cysteine64. Especially the terminal sulphur atom of cysteine64 is covalently modified which strongly implies some functional purpose of this special structure.

(2) The *in vitro* nitrite or hydroxylamine reductase activities have been seen in many proteins featuring a 5-coordinated heme, including haemoglobin, myoglobin (Huang *et al.*, 2005a; Huang *et al.*, 2005b), neuroglobin (Petersen *et al.*, 2008), NOS (Gazor, unpublished data) and SHP-N88A (see Figure 3-12 and the legend), but their *in vivo* targets are other molecules.

(3) The specificity activity of nitrite reduction of OTR ($k_{cat}/K_m = 1.0\times10^5$ $M^{-1}\bullet s^{-1}$) is much lower than that of NrfA ($k_{cat}/K_m = \sim10^8$ $M^{-1}\bullet s^{-1}$) (Bamford *et al.*, 2002a; Tikhonova *et al.*, 2006), indicating that OTR cannot compete for nitrite *in vivo* against NrfA which is also encoded in the genome of *Shewanella oneidensis* MR-1 and located in the periplasmic space. OTR seems not designed to specifically reduce nitrite.

(4) The high similarity of the three-dimensional organisation of heme centres between OTR and NrfA/HAO reveals the conserved architecture of an electron transfer wire. Similar conservation is also found among many other cytochromes but not always means a closely related physiological function. For example, the four hemes of the bacterial Fe^{III}-induced periplasmic flavocytochrome c_3 (If_3), the four hemes of fumarate reductase (Fcc_3), and four of the 8 hemes of HAO are highly superposable to each other (Richardson, 2000), but they have completely different physiological functions.

Whether the physiological function of OTR is connected with nitrite or other nitrogenous compounds needs further studies to identify.

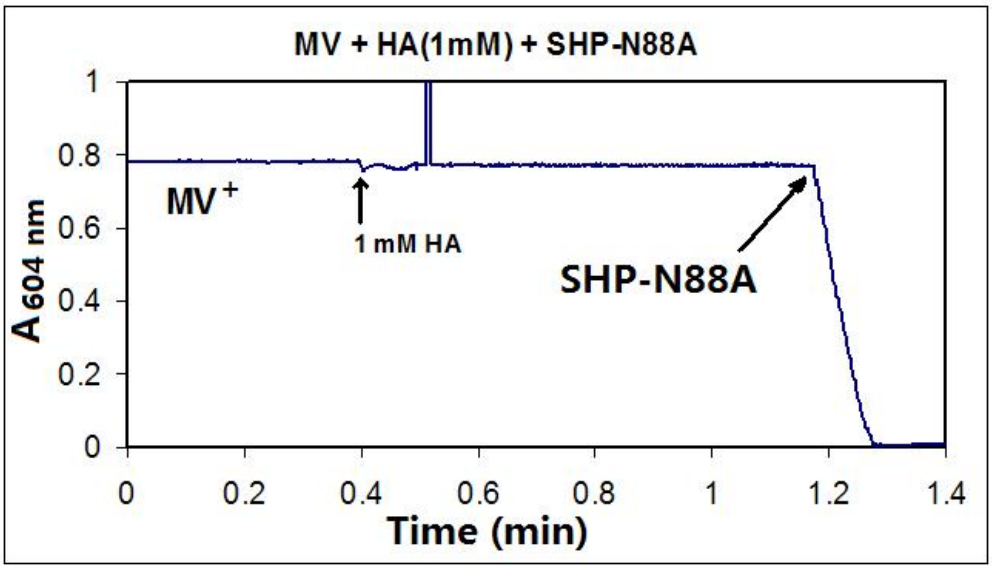

Figure 3-12. The hydroxylamine reductase activity shown by SHP-N88A. SHP is a heme protein capable of ligand binding with its active site heme and its mutant form N88A has a 5-coordinated active site heme which can reduce nitrite (Li, unpublished data) and hydroxylamine (this work).

3.5.5 The reduction of tetrathionate and other *in vitro* substrates

In this work, attempts have failed to reproduce the previously reported activity of tetrathionate reductase/thiosulfate oxidase of OTR in the steady-state assays. Although the pre-steady-state studies show that fully reduced OTR is oxidised by tetrathionate, the initial oxido-reduction rate is much lower than the reported steady-state rate at various tetrathionate concentrations (see Table 3-3) and the time course looks linear rather than exponential (see Figure 3-7c), indicating that under the experiment conditions ferrous OTR is not enzymatically oxidised by tetrathionate. The reason for the inconsistency with the previous results remains unknown. Ligand-docking programme generated 6 favoured positions for a tetrathionate molecule

bound to the active site of OTR, but all of the 6 molecules are perpendicular to the heme plane and protrude through the hole above the active site (see Figure 3-13), leaving no side chains able to attack the middle S-S bond. Because the hole that the tetrathionate fits in is probably artificial due to the missing structure of the six amino-acid residues GGGDAV, tetrathionate seems unable to be bound close to the active site heme.

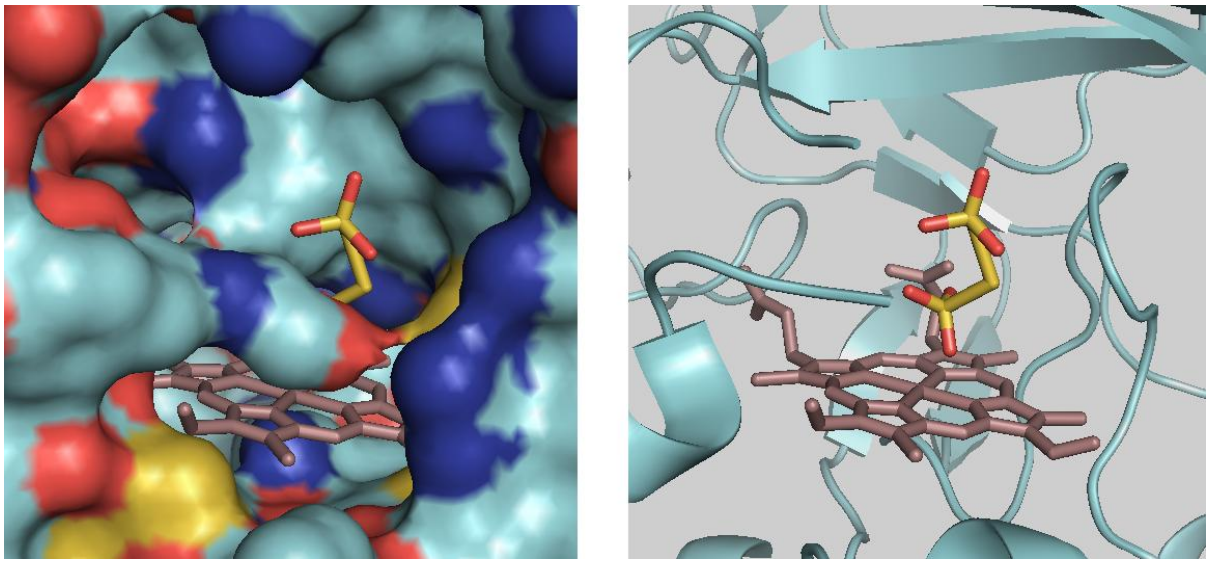

Figure 3-13. Modelling for a tetrathionate molecule fitted to the active site of OTR. The left panel is the surface view showing the hole above the heme that the tetrathionate fits in. The right panel is the carton view of the left panel indicating the missing segment in the structure. Molecular docking computation was carried out using AutoDockTools v1.5.4 and AutoDock Vina v2.0. The docking results were visualised by PyMOL v0.99 RC6.

Considering the structure of the active site of OTR, the real substrate could be speculated to interact with lysine153 and cysteine64, which requires the size to be larger than the so far identified *in vitro* substrates of OTR (NH_2OH, NO, NO_2^-, H_2O_2 and HCO_2^-). Although computing tools are available for ligand docking and active site searching, the major difficulty of detecting the best ligand for OTR is the structural blank of the six residues GGGDAV which could cause false results.

Chapter 4 – Results and Discussion

Function Investigation of OTR Based on Phenotype Studies

As the function of OTR has been proposed to be related to the metabolism of nitrogenous compounds (Atkinson, 2009), phenotype studies on the wild-type *Shewanella oneidensis* MR-1 and its OTR knock-out (Δ*otr*) strain could help confirm whether OTR is important for the bacterial cells to grow on or resist certain nitrogen-containing chemicals. Besides the identified *in vitro* substrates of OTR, the chemicals employed as potential electron acceptors for *Shewanella* also include solid metal oxides and some sulphur-containing compounds which could be potentially linked to the function of OTR.

4.1 Aerobic growth of *Shewanella oneidensis* MR-1 strains in response to toxic substrates

4.1.1 Cell growth in response to toxic amounts of hydrogen peroxide

[H_2O_2]-gradient plate screening of *S. oneidensis* MR-1 cells shows that neither the wild-type nor the Δ*otr* strain can survive the condition of [H_2O_2] > 0.4 mM when growing on LB-agar plates aerobically (see Table 4-1). Therefore 0.3 mM H_2O_2 was used as a toxic additive to the cells growing aerobically in LB liquid media. H_2O_2 effectively inhibits the growth of both wild-type and Δ*otr* strain of *S. oneidensis* MR-1 for at least the first 10 hours after mixing, but there is no difference observed between the two strains in their ability to resist H_2O_2 toxicity (see Figure 4-1). 24 hours later both wild-type and Δ*otr* strain treated with H_2O_2 recovered the growth and their OD_{600nm} reached 1.6, similar to the 1.7 of the H_2O_2-free controls of both strains.

Table 4-1. LB-agar plate screening of *S. oneidensis* MR-1 cell growth with various concentrations of hydrogen peroxide. "+" means positive growth on the plate, "-" means no growth, and "+/-" means positive growth on some plates but negative for others.

[H_2O_2] (mM)	0	0.1	0.2	0.3	0.4	0.5	0.6	0.8	1.0
Wild-type	+	+	+	+	+/-	-	-	-	-
Δ*otr*	+	+	+	+	+/-	-	-	-	-

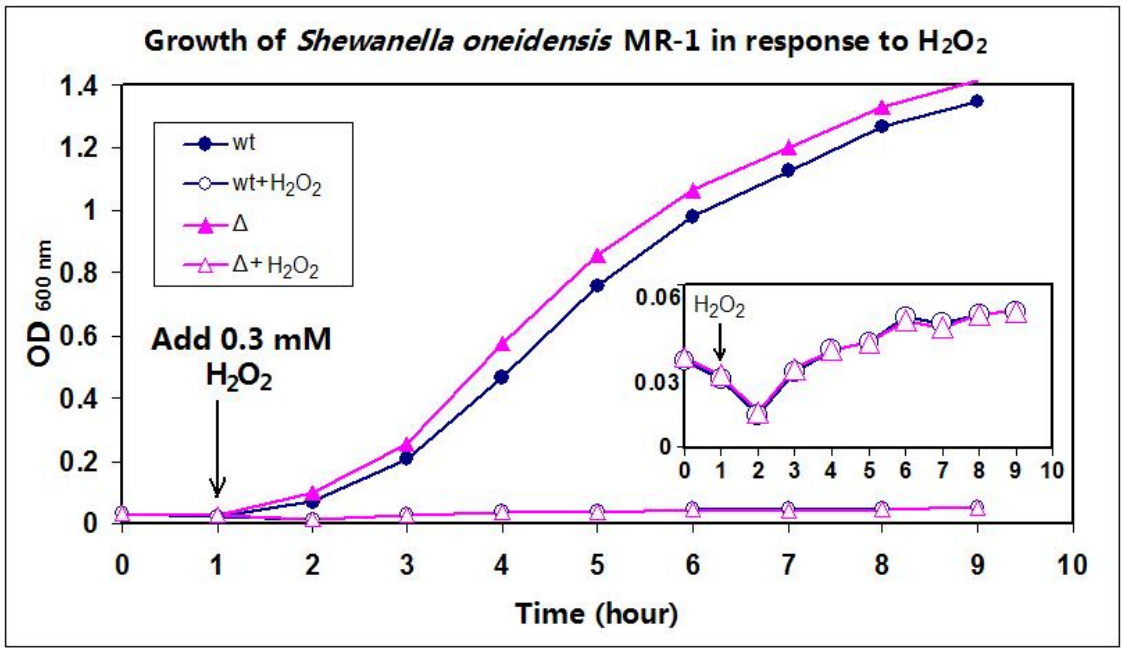

Figure 4-1. Aerobic growth of *S. oneidensis* MR-1 wild-type strain (wt) and OTR knock-out strain (Δ) in response to the toxic H_2O_2 in liquid LB media. The initial culture of each strain was taken from a mid-log-phase pre-culture with the same OD_{600nm} value. All flasks were shaken at 150 rpm at 30 °C. The inset is the zoomed area of the curves for H_2O_2 treated cell growth of both strains.

4.1.2 Cell growth in response to toxic amount of nitrite and hydroxylamine

Under aerobic conditions, the wild-type strain of *S. oneidensis* MR-1 and its OTR knock-out strain show no difference in growth after adding a toxic but non-lethal amount of nitrite (10 mM) or hydroxylamine (0.1 mM) into the corresponding medium, although the growth of both strains is inhibited (see Figure 4-2).

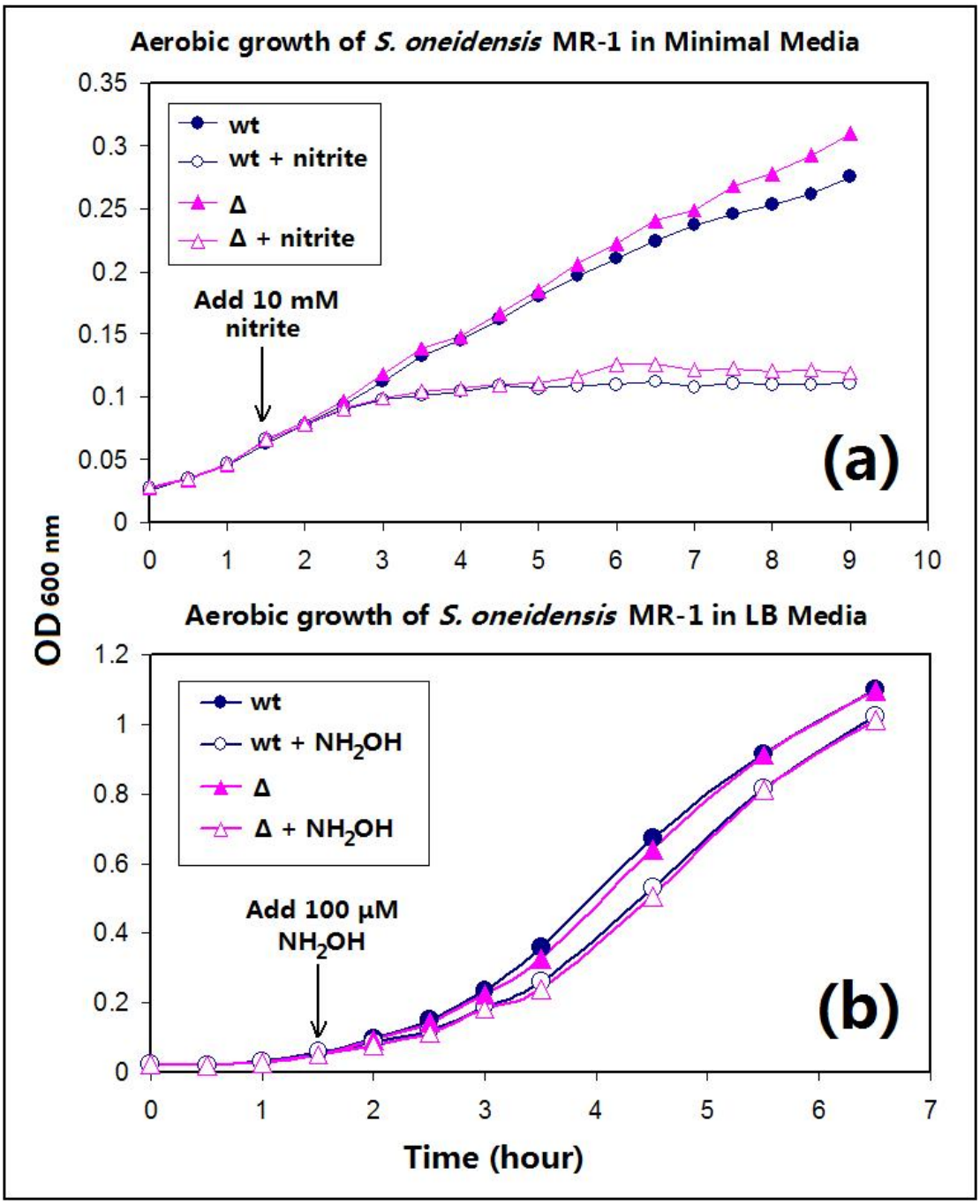

Figure 4-2. Aerobic growth of *S. oneidensis* MR-1 wild-type strain (wt) and OTR knock-out strain (Δ) in response to the toxic nitrite (Panel a) and hydroxylamine (Panel b). The initial culture of both strains was taken from the log-phase pre-culture with the same OD_{600nm} value. The minimal media used was supplied with 40 mM lactate as electron donor. All flasks were shaken at 150 rpm at 30 °C.

4.2 Anaerobic growth of *S. oneidensis* MR-1 with controlled terminal electron acceptors

Various chemicals were employed as the sole electron acceptor to support the anaerobic growth of *S. oneidensis* MR-1 on minimal media agar plates with lactate as the electron donor. However none of them could discriminate the growth between the wild-type strain and the OTR knock-out strain (see Table 4-2) as their colonies grow to the similar size (see Appendices-4.1 to 4.8). Growth in liquid minimal media shows similar results (see Table 4-2). Therefore the comparison screening experiment failed to provide any positive information that could reveal the physiological function of OTR.

When nitrite serves at the sole electron acceptor for *S. oneidensis* MR-1, its dose must be below the limit for the cells to overcome its toxicity during respiration, which is some value below 10 mM for agar plate growth as indicated in Table 4-2. Among the various electron acceptors tried in this work, *S. oneidensis* MR-1 cells show the best growth on fumarate besides O_2, which is consistent with the high level consecutive expression of the fumarate reductase (Fcc_3). Interestingly the cells could also grow on thiosulfate only without any supplied electron donor, suggesting that *S. oneidensis* MR-1 could ferment thiosulfate as the only energy source as do some sulphate reducing bacteria (Bak and Cypionka, 1987).

Table 4-2. Anaerobic growth of *S. oneidensis* MR-1 cells in minimal media with defined electron donor and electron acceptor. "+" means positive growth on agar plates compared to the lactate-only control, and "-" means no colony. The values for growth in liquid minimal media are OD_{600nm} after 24-hour incubation at 30 °C. The inoculants were taken from the mid-exponential cell culture in LB with OD_{600nm}=0.8.

Electron donor	Electron acceptor	Wild-type strain		Δ*otr* strain	
		Growth on Plate	Growth in Liquid	Growth on Plate	Growth in Liquid
40 mM lactate	1 mM NO_2^-	+	0.07	+	0.06
40 mM lactate	10 mM NO_2^-	-	N/A	-	N/A
40 mM lactate	20 mM Fumarate	+	0.36	+	0.36
40 mM lactate	1 mM NO_2^- 20 mM Fumarate	+	N/A	+	N/A
40 mM lactate	10 mM NO_2^- 20 mM Fumarate	-	N/A	-	N/A
40 mM lactate	10 mM NO_3^-	+	0.18	+	0.20
40 mM lactate	10 mM colloidal S(0)	+	0.43	+	0.30
40 mM lactate	20 mM $S_2O_3^{2-}$	+	0.11	+	0.14
40 mM lactate	20 mM $S_4O_6^{2-}$	+	0.22	+	0.17
40 mM lactate	20 mM SO_3^{2-}	+	0.27	+	0.26
	20 mM $S_2O_3^{2-}$	+	N/A	+	N/A

4.3 Anaerobic reduction of insoluble iron oxides by *S. oneidensis* MR-1

As it was previously reported that an OTR knock-out strain of *S. oneidensis* MR-1 showed significantly decreased ability in reducing insoluble iron oxide under anaerobic conditions (Bretschger *et al.*, 2007), OTR could be involved in Fe(III)

metabolism. However, in this project the wild-type *S. oneidensis* MR-1 and the Δ*otr* strain have basically the same ability in reducing both insoluble Fe(III) oxide (see Figure 4-3) and soluble Fe(III) (see Figure 4-4) under anaerobic conditions. Around 3×10^9/ml *S. oneidensis* MR-1 cells could reduce ~1.5 mM insoluble hydrous ferric oxide (HFO) after 68-hour incubation at 100 rpm and 30 °C, whereas the same density of cells could reduce ~8 mM ferric citrate after only 45-hour incubation under the same condition.

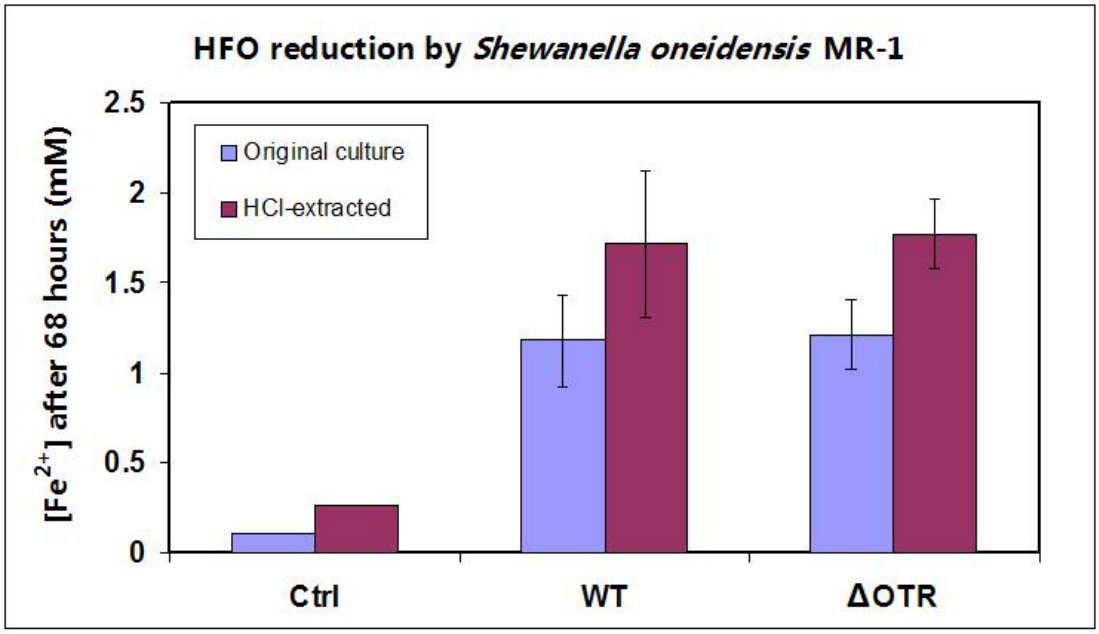

Figure 4-3. Fe^{2+} concentration resulting from the reduction of 20 mM ferric hydrous oxide (HFO) after 68-hour incubation with cells of wild-type *Shewanella oneidensis* MR-1 and the OTR knock-out strain. The media used is liquid minimal media containing 20 mM lactate as electron donor. Averages (the bar height) and standard deviations (the errors) of Fe^{2+} concentration were calculated based on the results of triplicate experiments.

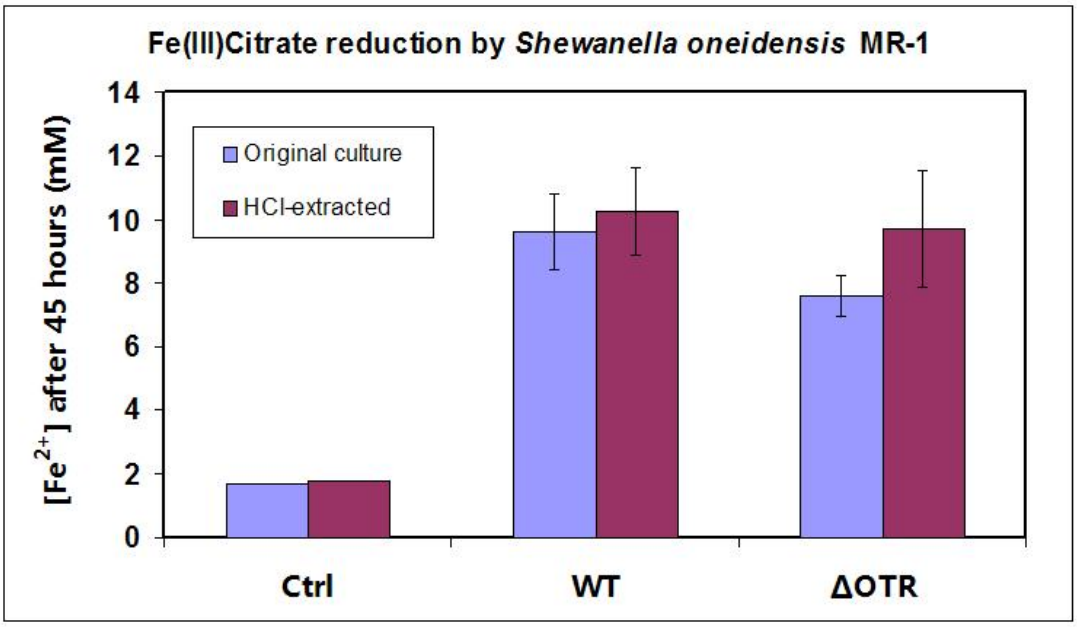

Figure 4-4. Fe^{2+} concentration resulting from the reduction of 20 mM ferric citrate after 45-hour incubation with the cells of wild-type *Shewanella oneidensis* MR-1 and its OTR knock-out strain. The media used is liquid minimal media containing 20 mM lactate as electron donor. Averages (the bar height) and standard deviations (the errors) of Fe^{2+} concentration were calculated based on the results of triplicate experiments.

4.4 Discussion

4.4.1 OTR and the nitrate/nitrite metabolism

Although OTR can reduce nitrite, hydroxylamine and hydrogen peroxide *in vitro*, it could not physiologically help the cells relieve the toxic stress caused by these three substrates under the experimental conditions used in this work.

Bacterial nitrate/nitrite respiration generally has two pathways: (i) the ammonification pathway in which nitrate is reduced into nitrite first and then the nitrite is directly reduced into ammonium without releasing any intermediate, and (ii) the

denitrification pathway in which nitrate is reduced stepwise to dinitrogen via nitrite, nitric oxide and nitrous oxide by four different enzymes (see Figure 1-2a). Both wild-type *S. oneidensis* MR-1 and the Δ*otr* strain grow equally well on the minimal media agar plate when nitrite or nitrate is the sole electron acceptor (see Table 4-2), suggesting that OTR is not involved in the nitrate/nitrite respiration pathway. This result is not surprising because the genome of *S. oneidensis* MR-1 does encode a NrfA protein which is the real respiratory nitrite reductase in this bacterium and accepts nitrite from the nitrate-reducing NAP system in the ammonification pathway (Gao *et al.*, 2009; Cruz-García *et al.*, 2007). As OTR is kinetically unable to compete with NrfA and both proteins are located in the periplasmic space of the cell, it is very unlikely that OTR is a physiological nitrite reductase, which has been confirmed by the result that the Δ*nrfA* strain of *S. oneidensis* MR-1 was unable to grow with 2 mM nitrite as the sole electron acceptor whereas the wild-type strain grew well under the same condition (Gao *et al.*, 2009). Although OTR could also reduce nitrous oxide *in vitro* (Atkinson, 2009), in the most recent report *S. oneidensis* MR-1 appears to lack the denitrification pathway and cannot grow with nitrous oxide as the sole electron acceptor (Cruz-García *et al.*, 2007), indicating that OTR is not a physiological respiratory nitrous oxide reductase.

Some other evidence from the literature also supports the idea that OTR is not involved in the nitrate/nitrite metabolism. In the genome of *Shewanella oneidensis* MR-1 the OTR gene is thought to belong to the 3-gene operon of SO4142-SO4143-SO4144 (see Cluster I in Figure 1.12a). Beliaev and his colleagues reported that when *S. oneidensis* MR-1 was supplied with nitrate as the sole electron acceptor, in comparison with the fumarate reference, the mRNA of SO4142 was down-regulated by 20% and the mRNA level of SO4143 showed little change (2% increase), whereas the mRNA of *nrfA* (SO3980) was 20-fold up-regulated (Beliaev *et al.*, 2005). In another report the similar nitrate/fumarate experiment shows that the expression of SO4142 and SO4144 (*otr*) is down-regulated by 44% and 56% respectively, whereas the mRNA level of *nrfA* is up-regulated by 4 times (Gao *et al.*, 2009), suggesting that OTR is not functionally related to the respiration of nitrate/nitrite. The NrfA knock-out strain of *Desulfovibrio vulgaris*, whose genome encodes an OTR homologue, suffers serious growth suppression after adding 5 mM nitrite compared to the wild-type, suggesting that OTR cannot function as a nitrite detoxifier as NrfA does in this

bacterium. Further more, transcriptional studies show that in response to added nitrite the expression level of the genes of OTR and its potential functional partner cytochrome *b* fluctuate by less than 2 fold around the control level in the wild-type *D. vulgaris*, and are down-regulated by less than 4 folds in the NrfA knock-out strain (see Table 4-3) (Haveman *et al.*, 2004), suggesting the OTR-Cyt*b* operon is not involved in nitrite detoxification in this species. In addition, *Rhodoferax ferrireducens* also encodes an OTR but not NrfA in its genome and cannot grow with nitrite as the sole electron acceptor (Finneran *et al.*, 2003), which may suggest that OTR does not function as a nitrite reductase. However the nitrite dose used in that work is 10 mM which could be too toxic for the cells to survive.

Table 4-3. Relative expression levels of the genes of OTR and the cytochrome *b* in the same operon (see Cluster II in Figure 1.12a) in wild-type *Desulfovibiro vulgaris* and the NrfA knock-out (Δ*nrfA*) strain in response to nitrite toxicity. Data are from Haveman *et al.*, 2004.

Gene tag	Protein encoded	Relative expression level for wild-type	Change in expression (fold)				
			WT + 5 mM NO_2^-	**WT + 0.1 mM NO_2^-**	**Δ*nrfA* (NO_2^- free)**	**Δ*nrfA*+ 5 mM NO_2^-**	**Δ*nrfA*+ 0.1 mM NO_2^-**
DVU3144	OTR	0.05	0.95	1.92	2.31	1.80	1.33
DVU3145	Cyt *b*	0.09	1.07	1.72	1.60	1.45	0.42

4.4.2 OTR and the sulphur compounds metabolism in *S. oneidensis* MR-1

The question of what OTR does *in vivo* is still yet to be answered. Some clues were found in previous reports that OTR may be related to the metabolism of sulphur-containing compounds. In some transcriptomic studies of *Shewanella oneidensis* MR-1, the gene of OTR seems to be up-regulated in response to thiosulfate as the sole electron acceptor. It was reported that the genes SO4142 and SO4143, encoding the

potential functional partner of OTR, were up-regulated by 7.21- and 2.02-fold respectively when thiosulfate was supplied as the sole electron acceptor in replacement of fumarate (Beliaev *et al.,* 2005). Further more, the expression level of the open reading frames in the genome of *S. oneidensis* MR-1 was assayed in several sets of experiments and the results can be retrieved from Many Microbe Microarrays Database (M^{3D}) (Faith *et al.*, 2007). The data for the *otr* operon (SO4142-SO4143-SO4144) from M^{3D} are presented in Table 4-4 and Figure 4-5. These data also reveal a positive correlation between the expression level of the *otr* operon and the growth condition with thiosulfate as the sole electron acceptor, suggesting that OTR may be linked to the metabolism of thiosulfate. The data from M^{3D} also show that the *otr* operon is up-regulated by DMSO (see Table 4-4 and Figure 4-5), whereas in the report by Beliaev and his colleagues DMSO does not cause an obvious up-regulation for SO4142 (-20%) and SO4143 (+35%) (Beliaev *et al.* 2005).

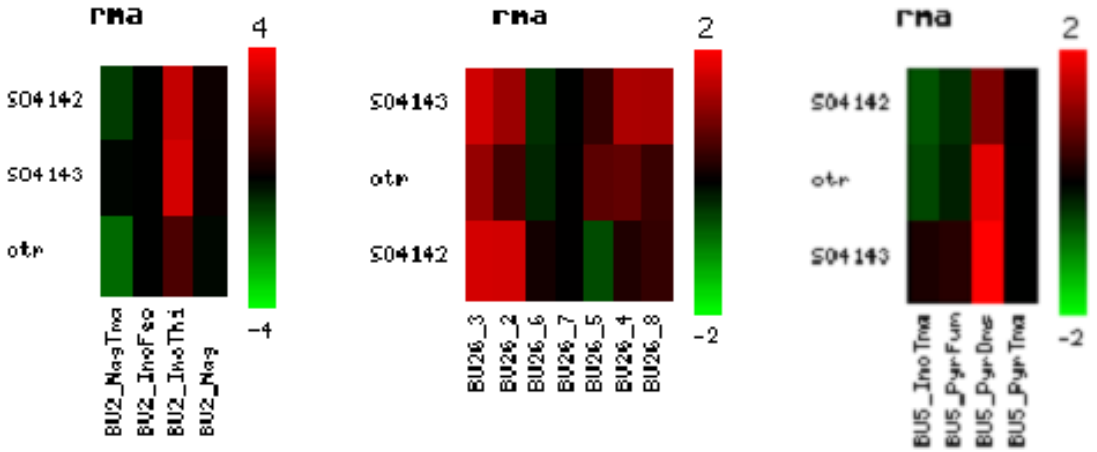

Figure 4-5. Heatmap for the mRNA levels of *otr*, SO4142 and SO4143 in *Shewanella oneidensis* MR-1 under different growth conditions. Panels from left to right represent the Experiment 1-3 respectively as indicated in Table 4-4. Red colour means up-regulation and green means down-regulation, and the numbers at the top and bottom of the red-green scale bar indicate the fold change. The labels below each map can be found in Table 4-4, corresponding to certain growth conditions. Data are from M^{3D}.

Table 4-4. Relative transcription level for genes SO4142, SO4143 and *otr* (SO4144) of *Shewanella oneidensis* MR-1 under different growth conditions. The first row of data for each experiment was set to 1 as the reference value for each gene (data from M^{3D}, Faith *et al.*, 2007).

Electron donor	Electron acceptor	Relative expression level (fold)			Label in Heatmap
		otr	SO4143	SO4142	
Experiment 1					
7.5 mM Inosine	10 mM Fe^{III} oxide	1	1	1	BU2_InoFeo
7.5 mM Inosine	10 mM $Na_2S_2O_3$	**2.25**	**9.92**	**8.30**	BU2_InoThi
7.5 mM NAG*	10 mM Mn^{IV} oxide	0.93	1.12	1.15	BU2_Nag
7.5 mM NAG	10 mM TMAO	0.32	0.9	0.53	BU2_NagTma
Experiment 2					
10 mM lactate 10 mM Inosine	6 mM Ferric citrate 5 mM KNO_3	1	1	1	BU26_7
10 mM Inosine	6 mM Ferric citrate 10 mM TMAO	1.45	2.33	3.12	BU26_2
3 mM Fe^{II} oxide	3 mM Ferric citrate 5 mM $Na_2S_2O_3$	**2.25**	**3.09**	**3.16**	BU26_3
10 mM Tween-20	3 mM Ferric NTA 5 mM $Na_2S_2O_3$	1.70	2.53	1.19	BU26_4
	6 mM Ferric NTA 3 mM Ferric citrate 10 mM $Na_2S_2O_3$	1.64	1.31	0.66	BU26_5
6 mM Fe^{II} oxide	5 mM KNO_3 10 mM DMSO	0.81	0.77	1.11	BU26_6
20 mM adenosine	6 mM Ferric NTA 5 mM TMAO	1.37	2.47	1.32	BU26_8
Experiment 3					
7.5 mM pyruvate	10 mM TMAO	1	1	1	BU5_PyrTma
7.5 mM Inosine	10 mM TMAO	0.68	1.15	0.64	BU5_InoTma
7.5 mM pyruvate	30 mM Fumarate	0.84	1.23	0.77	BU5_PyrFum
7.5 mM pyruvate	10 mM DMSO	**3.45**	**5.42**	**1.98**	BU5_PyrDms

*Abbreviations for compounds: NAG (N-Acetylglucosamine), NTA (Nitrilotriacetic acid), DMSO (Dimethyl sulfoxide), TMAO (Trimethylamine N-oxide).

However when tetrathionate, thiosulfate, sulphite or elemental sulphur are supplied as the sole electron acceptor, the anaerobic growth of cells of *S. oneidensis* MR-1 failed to show any detectable difference between the wild-type and the OTR knock-out strain (see Table 4-2), whish is consistent with the kinetic results (see Chapter 3) and

the previous report (Biddle *et al.*, 2008). In addition, the up-regulations of *otr* shown in Table 4-4 are only 2-3 fold. These results indicate that OTR does not directly function in the pathways responsible for the metabolism of those sulphur-containing substances.

4.4.3 OTR and the sulphate metabolism in *Desulfovibrio vulgaris*

In the sulphate reducing bacterium *Desulfovibrio vulgaris* Hildenborough growing in the minimal media, the OTR gene (DVU3144) was found 2.13-fold up-regulated in response to the sulphate-limiting (4 mM) condition in comparison with the sulphate-rich (40 mM) condition (Pereira *et al.*, 2008). Under this sulphate-limiting condition many energy metabolism genes, especially those involved in sulphate respiration, were also up-regulated, including the genes encoding adenosine-phosphosulphate (APS) reductase, some subunits of the quinone-interacting membrane-bound oxidoreductase (Qmo) complex and the dissimilatory sulphite reductase (Dsr) complex, Type-I cytochrome c_3 ($TpIc_3$), $[NiFe]_2$ hydrogenase and part of the high molecular weight cytochrome (Hmc) complex (see Figure 4-6) (Pereira *et al.*, 2008). This up-regulation may reflect an increased sulphate respiration activity as the reaction of the *D. vulgaris* cells to compete for limited energy source in the environment. The involvement of the up-regulation of the OTR gene in this response suggests it may have a function related to sulphate metabolism. However, the respiratory processes of sulphate reduction by *D. vulgaris* are all carried out in the cytoplasm and OTR is located on the periplasmic face of the plasma membrane (see Figure 4-6), indicating that OTR cannot directly participate in the reduction of sulphur-containing compounds. This conclusion is agreed by the anaerobic growth results in Table 4-2 and the report that the OTR-containing bacterium *Anaeromyxobacter dehalogenans* 2CP-C cannot grow on sulphate or thiosulfate as the sole electron acceptor (Sanford *et al.*, 2002). Assuming that OTR carries out the same local function in both *S. oneidensis* MR-1 and *D. vulgaris* Hildenborough, the common micro-environment for OTR is a sulphide-rich periplasmic space, which could be the condition inducing the up-regulation of *otr*.

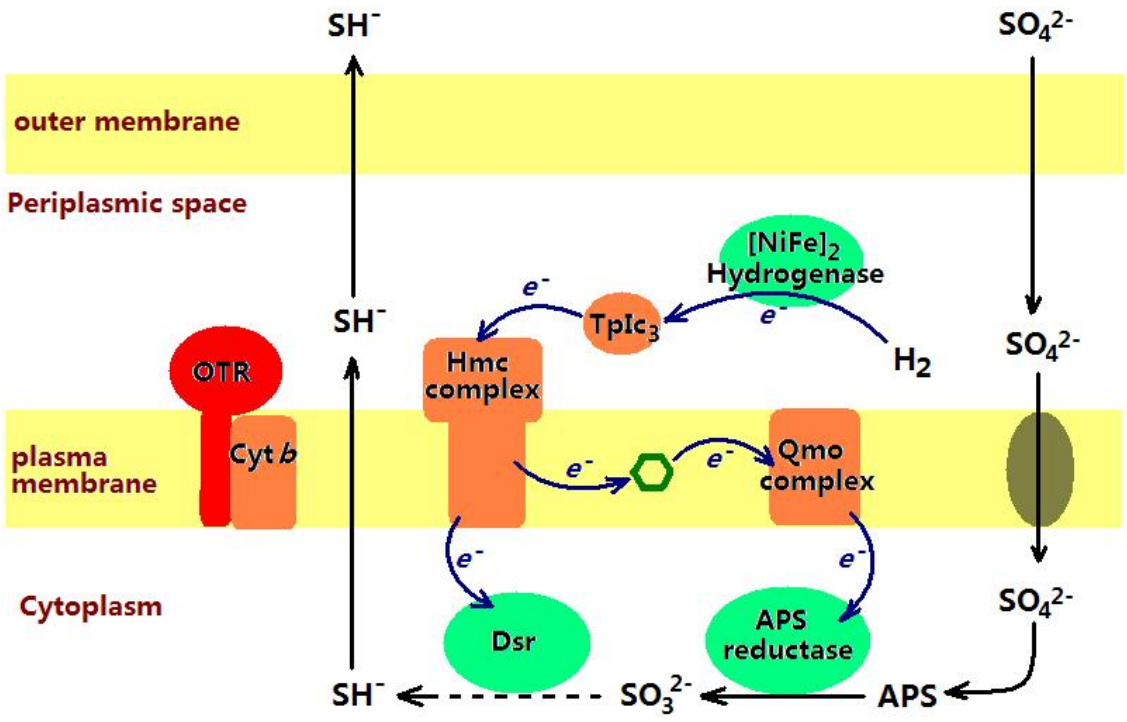

Figure 4-6. Model for the sulphate respiration pathway in *Desulfovibrio vulgaris* Hildenborough. Blocks are functional proteins that are up-regulated by limited source of sulphate. Green hexagon represents the membrane quinone pool. Blue arrows outline the electron flows.

To further investigate the potential functions of OTR, 38 bacterial species encoding an integral *otr* operon were reviewed and the phylogenetic tree based on the OTR sequences from these bacteria species is shown in Figure 4-7. As introduced in Chapter I, these species could be categorised into three groups based on the 3 types of *otr*-containing clusters (see Figure 1.12a), which is also well presented by the branches in the phylogenetic tree (see Figure 4-7). Most of these OTR-containing species are either sulphide producing or sulphide oxidising bacteria, indicating that their cells may frequently face the sulphide-rich surroundings which could influence the environmental redox conditions and induce the expression of certain genes to sustain the energy acquisition. However, whether the OTR gene is really stimulated by thiosulfate respiration needs further RT-PCR or microarray assays to confirm.

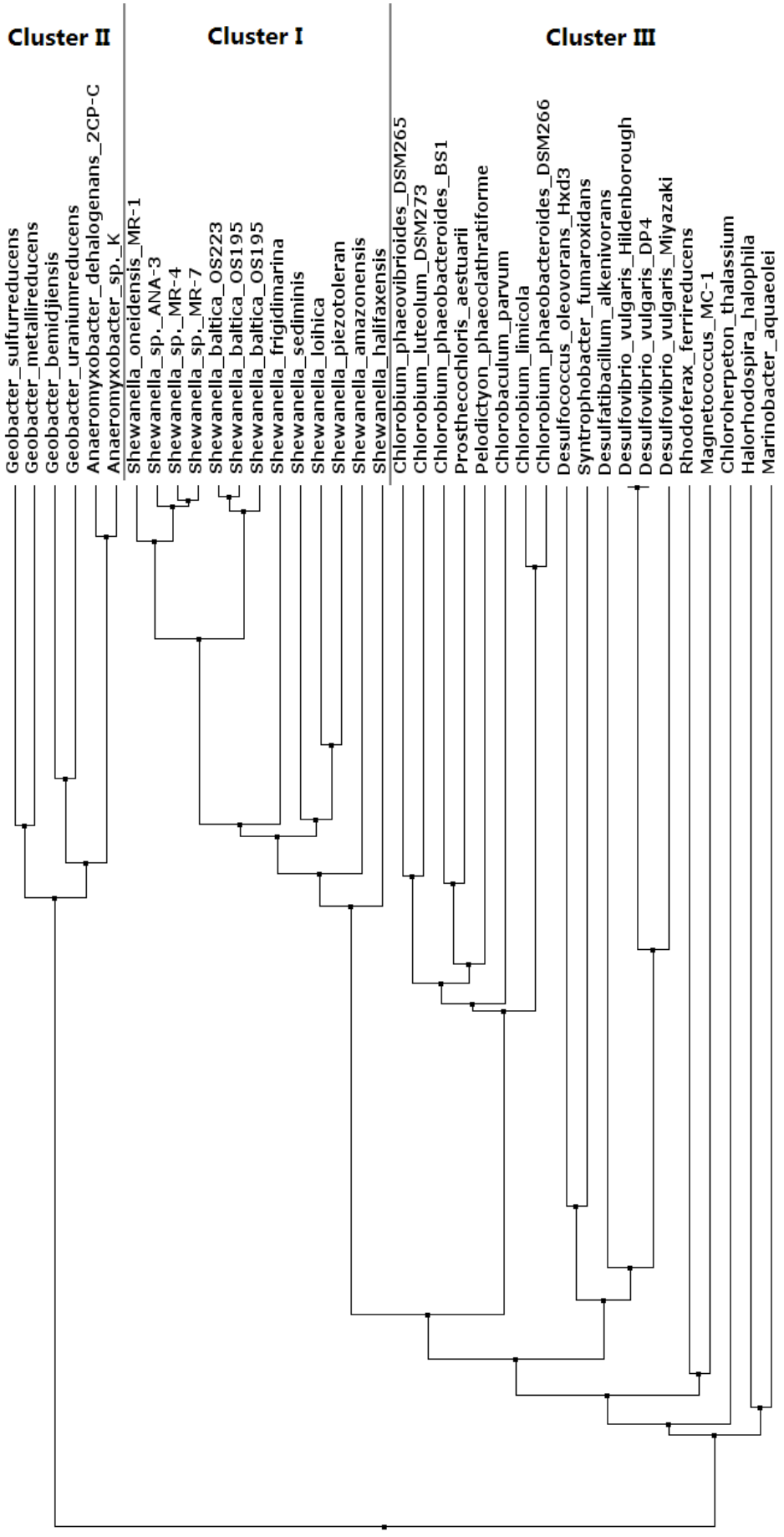

Figure 4-7. Phylogenetic tree for OTR-containing bacteria species based on the OTR sequence alignment.
Sequences of OTR are aligned with CLUSTAL W 1.83 and the phylogenetic tree is constructed with Jalview 2.5.1.

Based on the above information, the possible function of OTR could be speculated as one of the following:

(1) An enzyme catalysing the reduction of certain periplasmic substance. This pathway could be either respiratory reduction which is activated when the source of electron acceptor is limited, or the reduction which is used to consume the excess reducing power.

(2) An enzyme catalysing the oxidation of certain periplasmic substance. The electrons are then transferred to the membrane quinone pool to support the respiratory reduction of other electron acceptors, possibly sulphur-containing compounds.

(3) The electron transferring cytochrome in certain pathway(s) which is associated to the sulphur compounds metabolism but not essential in *S. oneidensis* MR-1. The heme II of OTR could be the binding site of its redox partner, considering the fact that a 5-coordinated heme does not always mean an enzyme active site, as happened in the NrfH whose heme 4 is the connection point between NrfH and NrfA (Rodrigues *et al.*, 2006).

4.4.4 OTR and Fe(III) reduction

The ability of *S. oneidensis* MR-1 cells to reduce HFO and ferric citrate remains unchanged after the deletion of OTR, indicating that OTR is not important to the Fe(III) reduction by the cell. The huge difference in Fe^{2+} production between the wild-type *S. oneidensis* MR-1 and the Δ*otr* strain previously reported by Bretschger and his colleagues could be because of the death of the Δ*otr* cells.

In the present work the soluble ferric citrate is much easier to be reduced by the cells than the insoluble HFO as expected. Adding the HCl-extracted culture sample into the assay solution in the cuvette did cause a pH jump from 5.3 to 4.6, which however should not affect the results as within the pH range of 4-6 the molar absorbance of Fe(II)-ferrozine complex remains unchanged (Stookey, 1970; Ceriotti and Ceriotti, 1980). The HCl-extracted samples show higher concentration of Fe^{2+} than the original culture as expected, and that difference could be from small amount of $FeCO_3$ and $Fe_3(PO4)_2$, or the Fe(II) sorbed to the surface of HFO (Fredrickson *et al.*, 1998).

Chapter 5 - Results and Discussion

Studies on the modification of Cysteine 64 of OTR

Cysteine 64 of OTR is a highly conserved active-site amino acid residue and its terminal sulphur atom is covalently modified into a Cys-S-X structure shown by the crystal structure of OTR. However the electron density map can only predict the added atom (X) is either sulphur or oxygen. As cysteine 64 is thought to be crucial to the function of OTR, identification of this intriguing modification will provide important information for predicting the real substrate of OTR and the mechanism of the interaction between them.

5.1 MALDI-TOF Mass Spectra Studies on Cysteine 64

5.1.1 The peptide mass spectra of trypsin-digested OTR

The pure OTR samples were digested with trypsin and scanned in a MALDI-TOF mass spectrometer. The calibrated peaks of the peptides in the *m/z* (mass/charge ratio) range of 1710-1850 for wild-type OTR and C64A are shown in Figure 5-1. Nearly all the peptides are single-charged (z=1) under the experimental conditions and each peptide species in the spectra is presented as a cluster of isotopic single peaks. The peptide that contains cysteine 64 is NSINNFCVAISSNEPR (residues 58-73), which is expected to have a molecular weight of 1764.8 Da if the cysteine is unmodified. In the peptide mass spectra of wild-type OTR, a peak that has the *m/z* value of 1764.3 (see Figure 5-1a) is observed and assigned to the cysteine 64-containing peptide with the unmodified Cys64 residue. The peptide mass spectra profile of the wild-type protein also shows some other peaks, including the m/z=1828.1 peak which is the peptide attaching heme II, and the two peaks with m/z=1748.2 and m/z=1804.2 respectively which do not match any predictable peptide species but also exist in the profile of C64A (see Figure 5-1b and Appendices-5.1) indicating that they are not Cys64-dependent. Interestingly, two peaks specific to the wild-type (m/z=1780.3 and m/z=1796.3) are exactly 16 Da and 32 Da more than the weight of Cys64-containing peptide (1764.3 Da), indicating that they could be the cysteine sulfenic acid (Cys64-SOH) and the cysteine sulfinic acid (Cys64-SO_2H). In the peptide mass profile of

C64A, a distinct peak with *m/z*=1733.3 matches the Alanine 64-containing peptide which has the theoretical molecular weight of 1732.8 Da. The two minor peaks with *m/z*=1772.1 and *m/z*=1791.1 in Figure 5-1b are not observed in other C64A samples (see Appendices-5.1).

5.1.2 The peptide mass spectra of DTT-treated OTR

The pure wild-type OTR sample was digested with trypsin, half of the digested sample was treated with DTT (Dithiothreitol), and part of the DTT-treated sample was incubated with IAA (Iodoacetamide) before being applied to MALDI-TOF mass spectrometer (see Section 2.6.2 for details). The results of the above three samples were shown in Figure 5-2, which were all obtained from the same experiment. It can be seen that after treatment with the reducing agent DTT, the population of the peptide that contains Cys64-SH (*m/z*=1764.2) increased significantly but no any other peak showed apparently diminished intensity (see Appendices-5.2 & 5.3). The peptide that contains the carboxyamidomethylated cysteine 64 (Cys64-S-CAM, M_r=1821.8) is distinct in the spectrum (*m/z*=1822.2, see Figure 5-2c), which is expected as the IAA modifies the thiol group of cystein64:

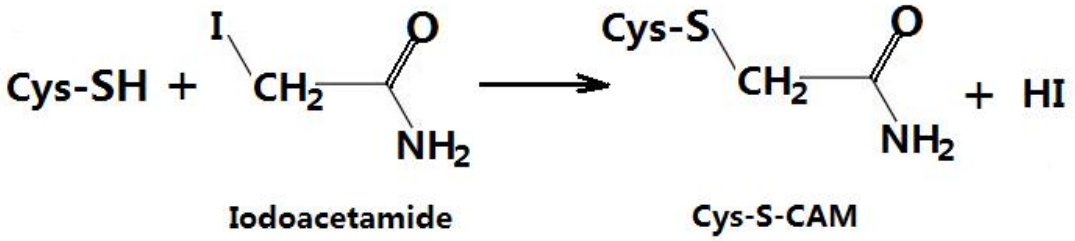

Surprisingly the big band of heme II-containing peptide (*m/z*=1828) is missing in the spectra of the "DTT+IAA"-treated sample (see Figure 5-2c), together with other heme-containing peptides (see Appendices-5.2). The sample treated with DTT-only or IAA-only retains the heme-containing bands (see Appendices-5.3).

5.1.3 The peptide mass spectra of Dimedone-treated OTR

The wild-type OTR was treated with 100 equimolar dimedone either before or after denatured by 4 M Guanidine hydrochloride (GndCl), and digested with trypsin before applied to MALDI-TOF mass spectrometer. If the modified structure of cysteine 64 is cysteine sulfenic acid (Cys-SOH), it could react specifically with dimedone to form the stable Cys-S-Dimedone complex which is DTT-resistant (Ellis and Poole, 1997):

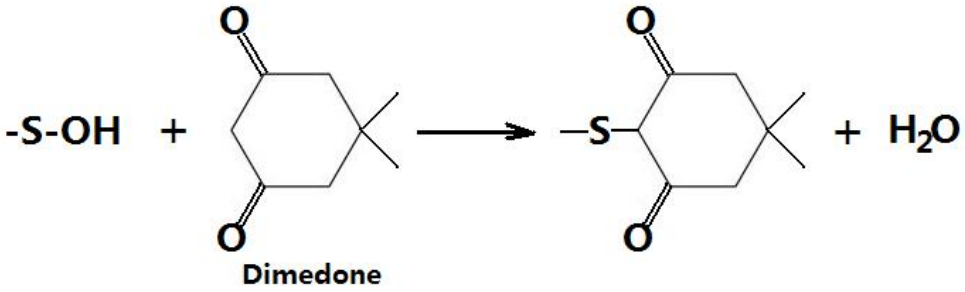

The expected mass of the dimedone-modified peptide is 1902.8 Da for the amino acid residues 58-73 or 2030.9 Da if the cutting site is occasionally between K56 and K57. However, no peptide band corresponding to the above mass (Mr=1902.8 Da or 2030.9 Da) was observed in the mass spectra. On the other hand, the dimedone-treated OTR sample showed distinct Cys64-S-CAM band in the mass spectra after further treated with DTT+IAA.

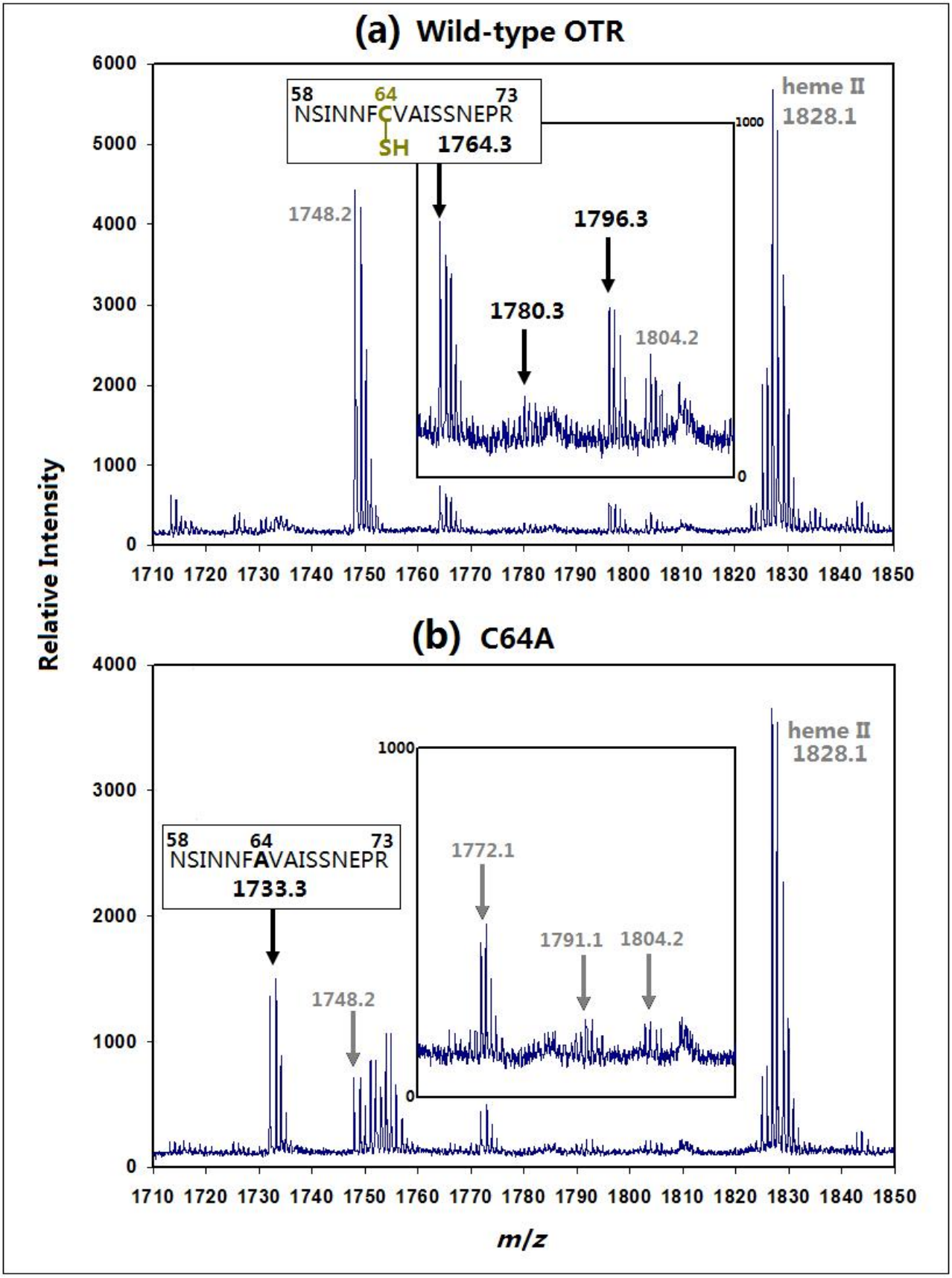

Figure 5-1. Mass spectra profile for the peptides of trypsin-digested wild-type OTR (a) and C64A (b) in selected *m/z* range. Insets in both panel (a) and (b) are zoomed areas within the *m/z* range of 1760-1820. Numbers indicated by arrows are the *m/z* values for corresponding peaks.

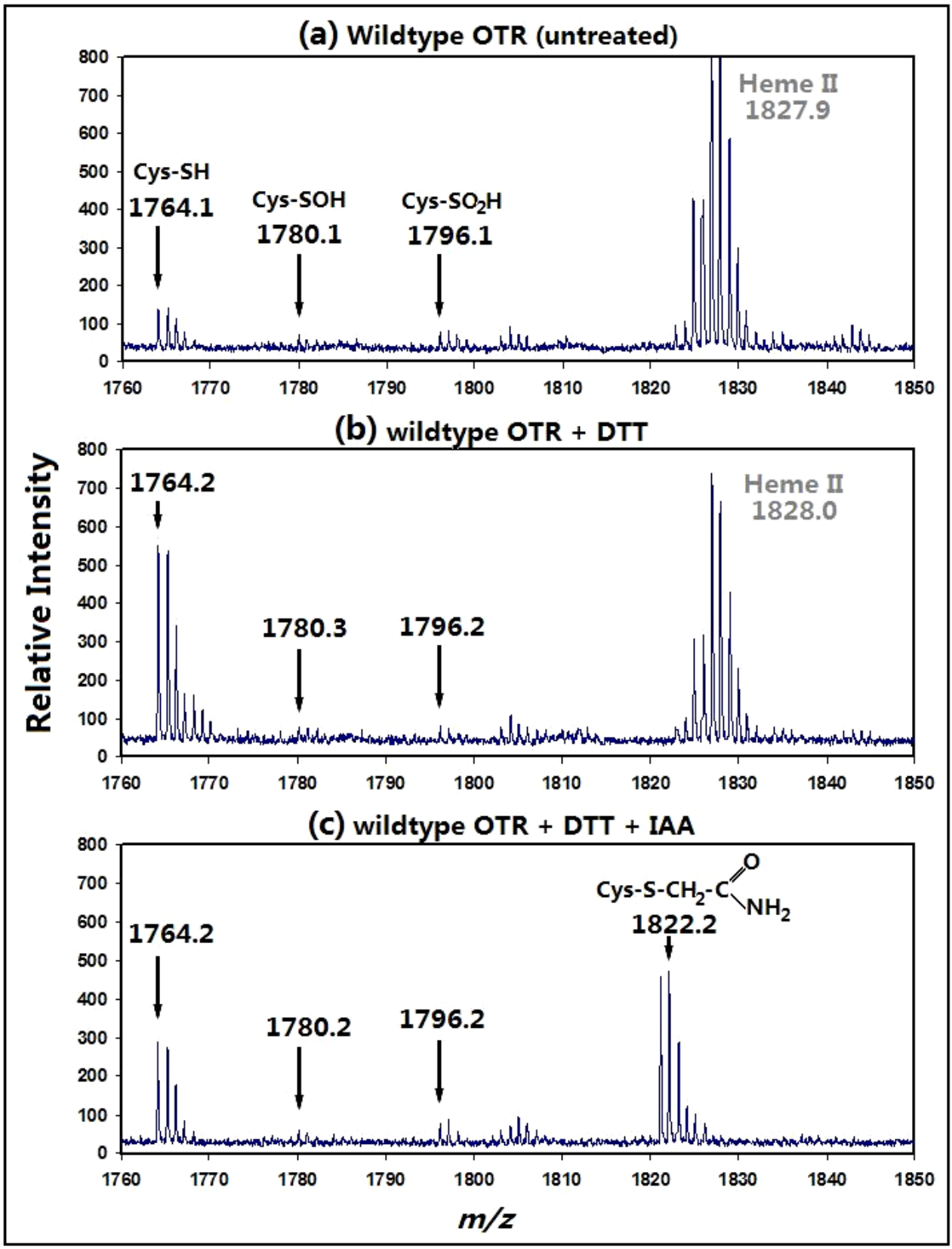

Figure 5-2. Mass spectra profile for the peptides of trypsin-digested wild-type OTR (a), the DTT-treated OTR (b) and the "DTT+IAA"-treated OTR (c) in selected *m/z* range. Numbers indicated by arrows are the *m/z* values for corresponding peaks. All samples were made from the same original OTR stock and scanned in the same experiment.

5.2 Electron Spray Ionization (ESI) Mass Spectra Studies on Cysteine 64

5.2.1 ESI Mass spectrum for wild-type OTR

To measure the mass of the intact protein, the pure sample of native wild-type OTR was applied to the Electron Spray Ionization (ESI) mass spectrometer and the result is shown in Figure 5-3. The spectra clearly show two distinct bands for each protonated protein species ($M+nH^{n+}$). The observed masses for these two bands of the 27-protonated OTR ($M+27H^{+}$) are 54449.1 ± 1.0 Da and 54497.0 ± 1.0 Da, respectively (see Figure 5-3). As the 27-protonated OTR ($M+27H^{+}$) has an extra mass of 27.2 Da from the added protons, the uncharged protein corresponding to the first band is 54421.9 ± 1.0 Da (54449.1 minus 27.2), which matches the average formula weight of the wild-type OTR (54422.8 Da, $C_{2435}H_{3540}O_{698}N_{638}S_{33}Fe_8$) very well. The uncharged species represented by the second band has a mass of 54469.8 ± 1.0 Da, 47.9 Da more than the mass of the wild-type OTR with unmodified cysteine 64. The population of the first band is around 40% and the second is 60%. The red and blue dots in Figure 5-3 are possible candidates predicted for these two bands. On the right-hand side of the two distinct bands, there is another poorly-defined small band (see Figure 5-3) which indicates a species with the mass of about 54489 Da, around 67 Da more than mass of the unmodified OTR.

5.2.2 ESI Mass spectrum for C64A

The ESI mass spectrum for C64A is shown in Figure 5-4. There is only one distinct band identified for each protonated protein species ($M+nH^{n+}$). The observed mass for the band of the 25-protonated species is 54416.2 ± 1.0 Da, i.e. the mass of the neutral protein is 54391.0 ± 1.0 Da, which matches the formula weight of C64A very well (54390.7 Da, $C_{2435}H_{3540}O_{698}N_{638}S_{32}Fe_8$). Comparing the spectra of wild-type OTR and C64A, the second distinct band of wild-type OTR (*m/z*=54497.0) should be the cysteine 64-modified form of OTR.

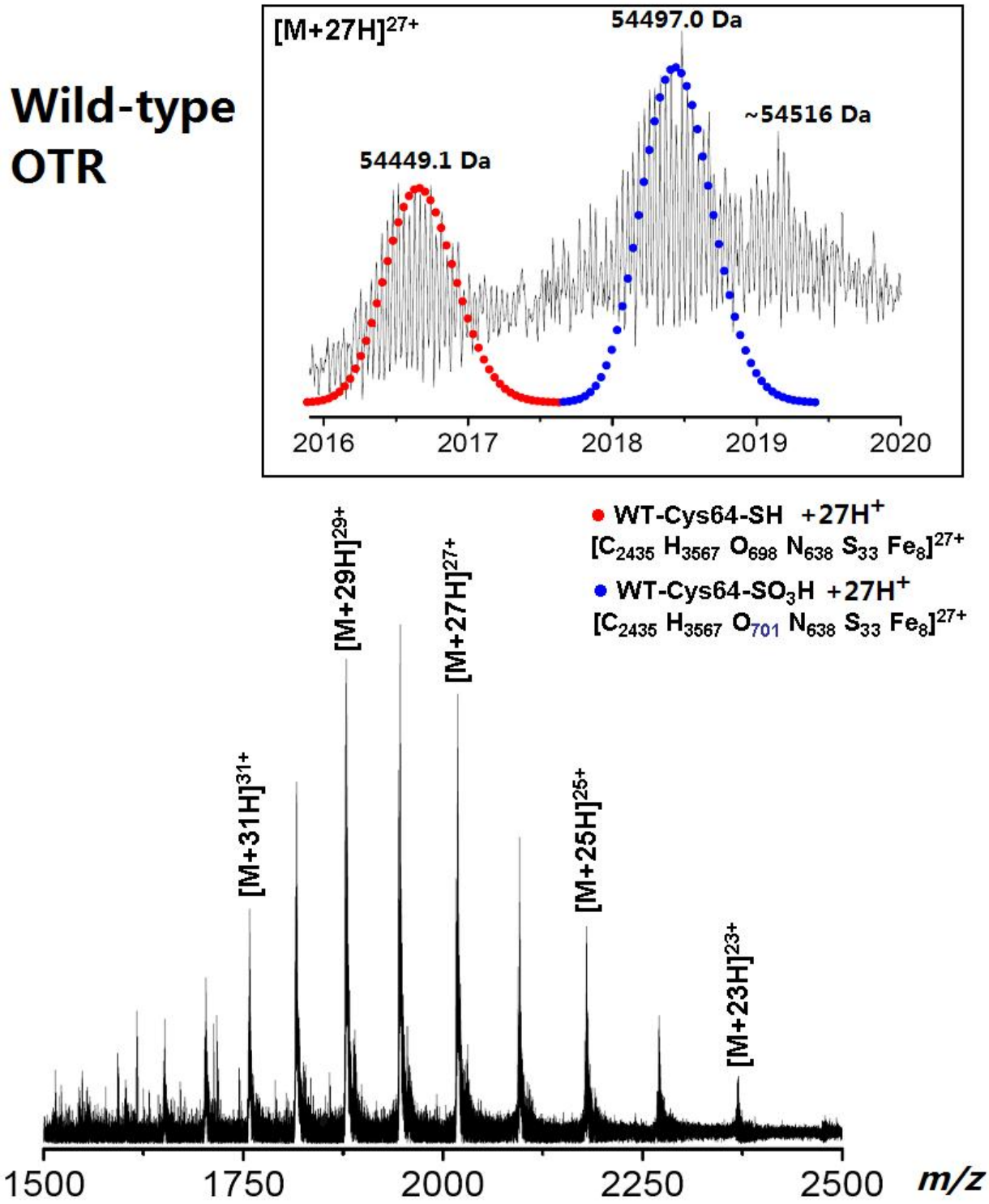

Figure 5-3. The ESI mass spectra for wild-type OTR. "M" represents the neutral protein. The inset is the zoomed band of 27-protonated OTR ($M+27H^+$). Molecular weights labelled in the inset are the calculated average mass of each band. Red dots are the formula-based theoretical isotopic masses for the OTR with its Cys64 unmodified (WT-Cys-SH), and blue dots are the theoretical isotopic masses for the OTR with its Cys64 modified into Cys-SO_3H.

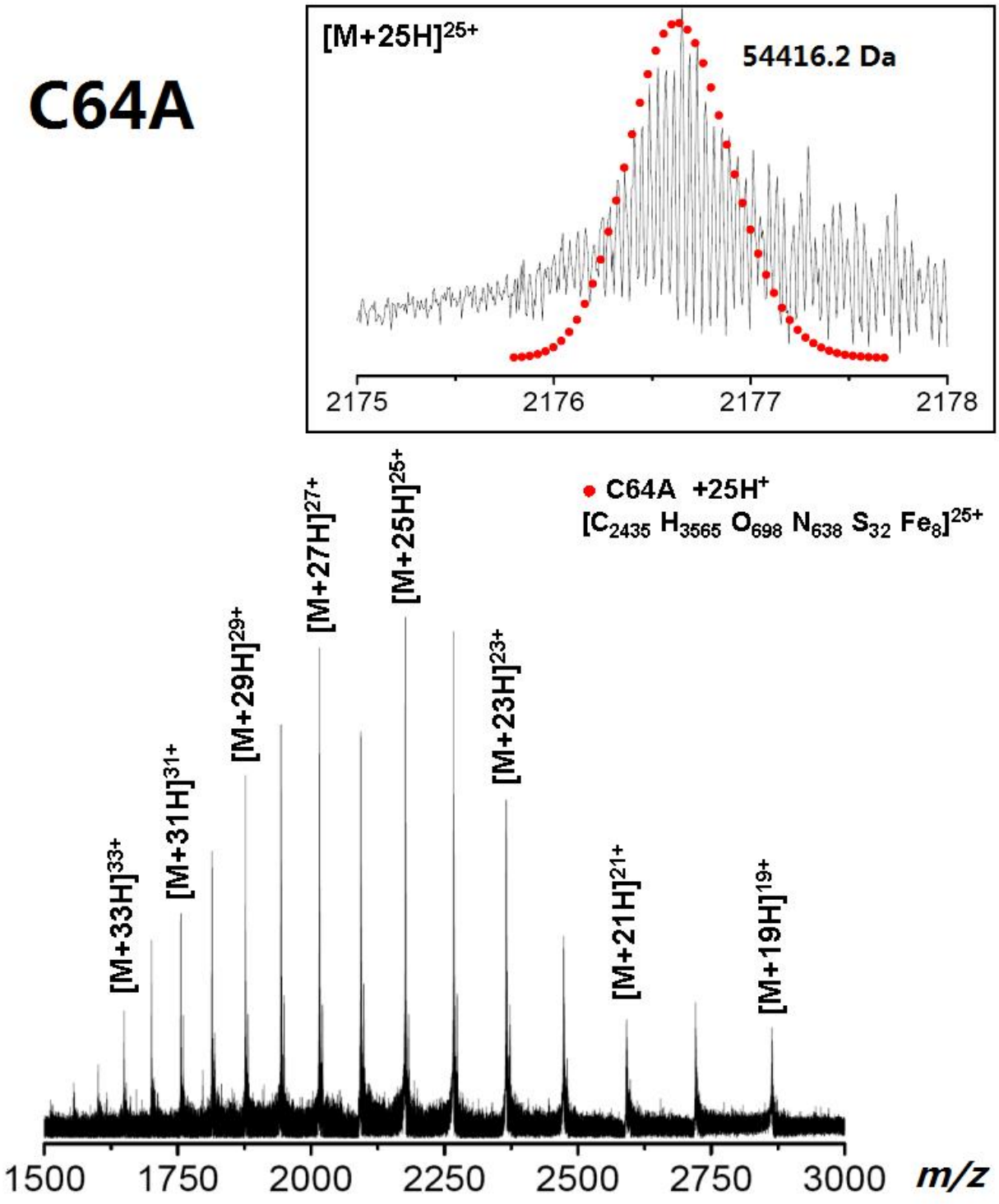

Figure 5-4. The ESI mass spectra for C64A. "M" represents the neutral protein. The inset is the zoomed band of 25-protonated C64A ($M+25H^+$). The molecular weight labelled in the inset is the calculated average mass of the band. Red dots represent the formula-based theoretical isotopic masses for C64A.

5.3 Structural studies with respect to Lysine 56

5.3.1 K56A retains integral heme II cavity

Previous studies on *c*-type heme maturation show that replacement of the proximal ligand (histidine) of the heme *c* result in a large amount of immature heme-free apoprotein (Allen *et al.*, 2003) or rapid degradation of the protein if the proximal ligand is replaced with leucine which cannot ligate the heme iron (Pisa *et al.*, 2002). As the only axial amino acid ligand of the heme II, lysine 56, is replaced with an alanine residue in the OTR K56A mutant form, this may disrupt the structure around the heme and result in heme loss or further degradation. Purified K56A shows the same productivity (0.1 mg per litre media) as other mutant forms of OTR and there is little spectral difference between K56A and wild-type OTR (see Figure 3-2), implying that K56A is not particularly degraded or disrupted. The heme integrity of K56A was investigated by identifying the existence of the covalently attached heme II in the protein. MALDI-TOF mass spectra for the trypsin-digestion sample of K56A shows a clear 1828 Da band which corresponds to the peptide covalently attaching the heme II (see Figure 5-5), indicating the purified K56A sample retains the heme II, although the axial ligand of this heme is unknown.

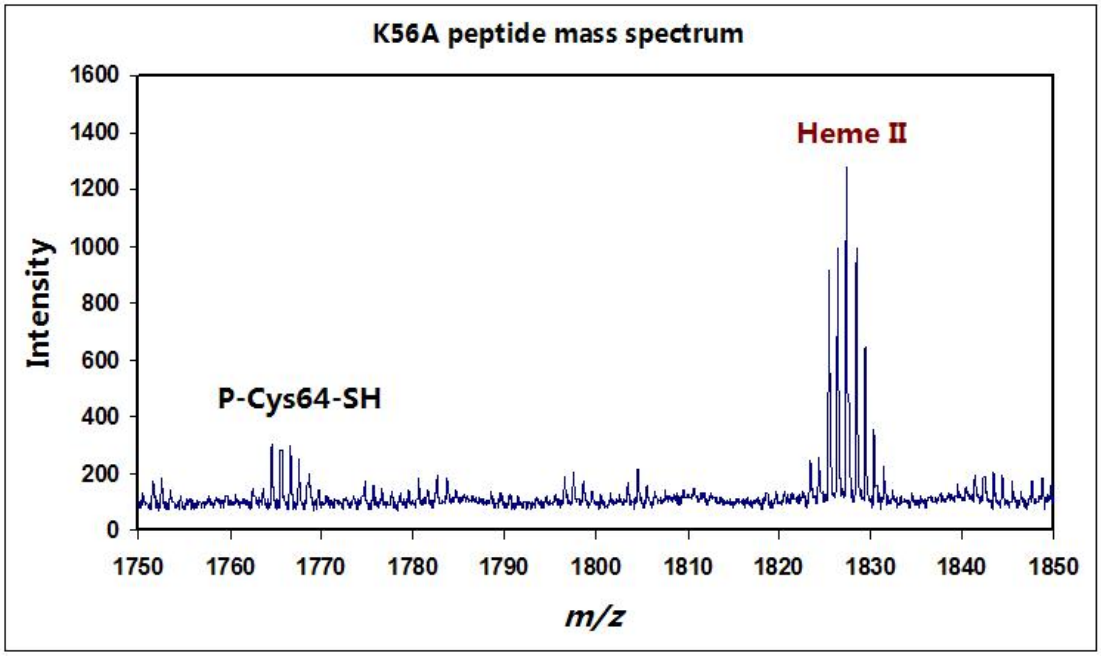

Figure 5-5. Mass spectra profile for the peptides of trypsin-digested OTR K56A in selected *m/z* range. The peptide attaching the heme II is labelled above the corresponding band.

5.3.2 Crystallisation of K56A

The best way to identify the axial ligand of heme II in K56A is to obtain the crystal structure. However in the present work only needle crystals were obtained which are not good enough for data collection (see Appendices-6.1). The crystal growth is fairly reproducible under the conditions of pH=6.1~6.3 and 30%~34% PEG4000 at room temperature (see more details in Section 2-8).

5.4 Discussion

5.4.1 MALDI-TOF data analysis in respect to the cysteine 64 modification

In the MALDI-TOF mass spectra of OTR, the existence of the peptide containing unmodified cysteine 64 (P-Cys-SH, where P represents the peptide of residues 58-73) in the peptide fingerprint of the wild-type OTR indicates that (i) the wild-type OTR has naturally a percentage of unmodified cysteine 64 in its structure in equilibrium with the modified form (P-Cys-S-X, where X=S or O), or (ii) the modification on cysteine 64 (P-Cys-S-X) is 100% in the native protein but becomes unstable after OTR is unfolded and hence partially decayed into P-Cys-SH. The other two small peptides specific to wild-type OTR that are 16 and 32 Daltons heavier than the P-Cys-SH are most possibly the one- and two-oxygen additives of Cys64, i.e. the cysteine sulfenic acid (P-Cys-SOH) and sulfinic acid (P-CysSO_2H) (see Figure 5-1 & 5-2). These two derivatives could result from the exposure of P-Cys-SH to the O_2 in the air on the sample plate, as some methionine-containing peptides are also partially oxidised on their sulphur atom in the methionine side-chain (see Appendices-5.4). The low signal intensity of the band of P-Cys-SOH in comparison with those of the P-Cys-SH and P-Cys-SO_2H (see Figure 5-1 & 5-2) reflects the poor stability of cysteine sulfenic acid which is easily further oxidised into the stable sulfinic acid. No peak corresponding to the cysteine sulfonic acid derivative (P-Cys-SO_3H) was ever found in the peptide mass spectra, indicating that the oxidising force under the experimental conditions, presumably the air O_2, may be not sufficient to further oxidise the sulfinic acid.

The population of P-Cys-SH significantly increased after treatment with excess amount of DTT, indicating that the unmodified Cys64 could be retrieved by reducing some unknown species that was not observed in the peptide mass spectra of OTR but contains the majority of Cys64.

As this unknown complex that contains the modified cysteine 64 in the MALDI peptide sample can be reduced by DTT to generate a free thiol group, it is highly

possibly in the form of -Cys-S-Y- where Y could be a sulphur, oxygen or nitrogen atom but not a carbon atom. The -Cys-S-Y- structure probably results from the original modified Cys64 (-Cys-S-X, X=O or S), which is fairly reactive and could be covalently connected to other structure during the unfolding of OTR or after being mixed with other peptides. The possibility of a disulfide bridge between two P-Cys-SH or two P-Cys-SOH peptides is less favourable as no peptide corresponding to the mass of P-Cys-S-S-Cys-P (from P-Cys-SH) or P-Cys-S(=O)-S-Cys-P (from P-Cys-SOH) was ever observed. No other peptide that is specific to wild-type could be identified in comparison with the spectra of C64A in the data range (*m/z*=800-4000), suggesting that the modified cysteine 64 (P-Cys-S-X) may react with some large peptide to form a complex over 4000 Daltons, or for some reason the P-Cys-S-X peptide does not fly well in MALDI-TOF. Nevertheless the modified form in the digested sample appears not to be cysteine sulfinic acid (P-Cys-SO_2H) or sulfonic acid (P-Cys-SO_3H) as they are DTT-resistant and cannot be converted to the P-Cys-SH form by DTT (Hamann *et al.*, 2002).

5.4.2 Electron spray ionization data analysis

The electron spray ionization mass spectra show the bands of the intact protein. C64A provide a good negative control to rule out other modifications on OTR which are not Cys64-dependent. Therefore the band with *m/z*=54497.0 in the spectra of wild-type OTR (see Figure 5-3) represents the Cys64-specific modification in wild-type OTR.

Although the size of this modified form is very close to the three-oxygen additive of unmodified OTR (54449.1 Da) and this model could be explained by the oxidation of the possible cysteine sulfenic acid (Cys64-SOH), it is practically highly unlikely to be cysteine sulfonic acid (Cys64-SO_3H) for some reasons: (1) Assuming the modification is cysteine sulfenic acid, it is stable in the native form as observed in the crystal structure and its oxidation to sulfonic acid can only happen after the protein is denatured and exposed to the air. However the oxygen-access time for the denatured protein sample is very limited in the experiment (< 1 min) before being applied to the ESI mass spectrometer in which the chamber is in vacuum. (2) Oxidation from Cys64-SOH to Cys64-SO_3H should leave significant amount of stable Cys64-SO_2H

which is however not observed in the ESI spectra. (3) No peptide corresponding to Cys64-SO_3H was observed in the MALDI-TOF peptide mass spectra of OTR and its existence could be ruled out as significant amount of Cys64-SH was retrieved by DTT from some complex (-Cys-S-Y-) other than Cys64-SO_3H. Therefore the modification on the Cys64 seems to be something else that has a total mass of around 48 Daltons. As predicted by the electron density in the crystal structure, the modification on Cys64 is either an oxygen or sulphur atom. There are few possibilities that could allow a ~32 Da add-on on the cysteine sulfenic acid (Cys64-SOH) in the native protein if the modified form is not sulfonic acid as discussed above. Therefore the cysteine persulfide (Cys-S-SH) model is more favoured as the sulphur atoms could possibly bind an adjacent water molecule or hydroxide anion which could be retained within the heme structure that is not completely disrupted under the ESI conditions. This model is consistent with the result that no dimedone modified species was detected in the MALDI-TOF peptide mass spectra. The poorly defined band in the ESI spectra of wild-type OTR which is ~67 Da heavier than the unmodified form may result from the attachment of another water molecule in the heme cavity of the protein.

In both the MALDI-TOF and ESI mass spectra, there is the signal for the existence of unmodified cysteine 64 (-Cys-SH), indicating that the modification on Cys64 is not very stable during or after the denaturation of OTR, no matter whether the free thiol group pre-exists in the native protein in equilibrium with the modified form or it is generated from the bond-breaking of the modified form by the harsh conditions in mass spectroscopy. This is agreed by the result that the free thiol form could be retrieved by reducing agent DTT in the peptide samples.

5.4.3 The role of Lysine 56

Lysine 56, a highly conserved residue in OTR, does not play an important role in the heme maturation or protein folding as the results show. This is consistent with the theory that the heme attachment is based on the protein sequence recognition of the CXXCH signature by the bacterial Type I Ccm system in Gram-negative bacteria (Allen *et al.*, 2003; Ferguson *et al.*, 2008). Although histidine 78 of the CXXCH motif in OTR does not ligate the heme iron, it may still participate in the maturation of

heme II. After the hemes are all attached to the apoprotein of OTR, K56 ligates the heme iron in the final folding process.

The role of K56 is probably to provide an appropriate redox potential for the heme or heme-substrate complex, as the proximal lysine in NrfA does. Although nitrite or hydroxylamine maybe not the real substrates of OTR, the reductase activities of K56A for these two substrates decrease significantly compared to the wild-type (see Table 5-1), indicating that the redox properties of the active site heme have been modified and K56 is responsible for the functional redox potential of the active site heme.

Table 5-1. Kinetic parameters of K56A-catalysed reduction of nitrite and hydroxylamine compared to the wild-type OTR (data from Atkinson, 2009).

	K_m (μM)	k_{cat} (s^{-1})	k_{cat}/K_m ($M^{-1}•s^{-1}$)
Nitrite reduction			
WT	5.2	2.8	5.3×10^5
K56A	65600	0.5	7.7
Hydroxylamine reduction			
WT	2200	849	3.9×10^5
K56A	10800	349	3.5×10^4

Assuming that both NrfA and OTR employ a proximal lysine ligand to the active site heme for redox-potential purpose, the question arises about why they use different assembling approach. In NrfA the proximal lysine is in the conserved heme-attaching CXXCK motif but in OTR the proximal lysine is distant from the CXXCH motif that attaches the active site heme. In NrfA the maturation of the active site heme needs specific enzyme other than the Type I Ccm system, namely NrfI expressed from the *nrf* operon (Pisa *et al.*, 2002). This extra energy and material input suggests a highly specific and efficient enzyme system responsible for nitrite metabolism in certain bacteria. In OTR the heme II seems potentially matured by Type I Ccm system in *Shewanella* and such a non-specific process implies a less evolved mechanism to adjust the redox potential of the active centre.

Chapter 6 – Conclusions and Future Work

6.1 The function of OTR

In this thesis I conclude that the physiological function of the novel octa-heme cytochrome *c* tetrathionate reductase (OTR) is very unlikely to be involved in the respiration or detoxification of nitrite or nitrite-derived compounds, which is against the previous proposal (Atkinson, 2009). Contrary to the previous results, OTR seems not a tetrathionate reductase either *in vitro* or *in vivo*. OTR might play a role in some metabolic pathway linked to (but not directly within) the respiration of sulphur-containing compounds, which still needs further investigation to confirm.

OTR was named after its previously reported *in vitro* tetrathionate reductase activity (Mowat *et al.*, 2004; Rothery, 2004). However the kinetic assays and phenotype studies carried out in this work show that OTR cannot reduce tetrathionate enzymatically and does not function as the respiratory tetrathionate reductase in *Shewanella oneidensis* MR-1, which is in agreement with a previous report (Biddle *et al.*, 2008).

OTR has been proposed to function in the nitrogen cycle in *S. oneidensis* MR-1 as it exhibits *in vitro* nitrite and hydroxylamine reductase activities and bears some structural similarities to NrfA (bacterial penta-heme cytochrome *c* nitrite reductase) and HAO (octa-heme hydroxylamine oxidoreductase). Kinetic data show that the reductase activities of OTR for nitrite ($k_{cat}/K_m = 1.0\times10^5$ $M^{-1}\bullet s^{-1}$) and hydroxylamine ($k_{cat} = 267$ s^{-1}) are much lower than those of NrfA ($k_{cat}/K_m = \sim10^8$ $M^{-1}\bullet s^{-1}$ for nitrite, $k_{cat} = \sim980$ s^{-1} for hydroxylamine, Stach *et al.*, 2000), and the activities are all similar among the wild-type OTR and its mutant forms. Each of these mutant forms has one active-site residue replaced by alanine. These results indicate that OTR is not naturally adapted to reduce nitrite. Phenotype studies also show that the absence of OTR caused no detectable difference in the ability of *S. oneidensis* MR-1 cells to detoxify or respire on nitrite, which is consistent with some reports that bacteria strains encoding OTR homologues in their genome cannot detoxify (Haveman *et al.*, 2004) or respire on nitrite (Finneran *et al.*, 2003). Further more, transcriptome reports show that the expression of genes in the *otr* operon does not response to the

conditions that nitrite or nitrate serves as the sole electron acceptor, or nitrite as a toxic additive. Therefore OTR appears not to be involved in the metabolism of nitrite or nitrate.

There are clues suggesting that OTR may be related to the metabolism of sulphur-containing compounds as its gene expression is up-regulated when thiosulfate is supplied as the sole electron acceptor of *S. oneidensis* MR-1. However kinetic and phenotype studies in this work show that OTR cannot reduce elemental sulphur or various sulphur-containing compounds including thiosulfate, sulfite and polysulfide *in vitro*, and the OTR-knock out strain does not show a decreased ability in respiring on these substances. Therefore OTR seems not to directly participate in the respiratory reduction of these electron acceptors, and the transcription of *otr* may be positively induced by some other conditions generated during the sulphur-metabolism in bacteria cells, for example the sulphide-rich condition which introduces a low environmental redox-potential.

6.2 The modification of cysteine 64

As a potentially important feature to the function of OTR, the modification on the side-chain sulphur atom of cysteine 64 appears to be either a sulphur or an oxygen atom as observed in the crystal structure (Mowat *et al*., 2004). Electron spray ionization mass spectra of the intact protein show that the modified form (Cys-SX) is ~48 Daltons heavier than the unmodified form (Cys-SH). However this modified form (Cys-SX) is less likely a cysteine sulfonic acid (Cys-SO_3H) because the oxygen access to the protein was very limited and there is no signal of the stable intermediate cysteine sulfinic acid (Cys-SO_2H) in the ESI mass spectra. In addition, Cys-SO_3H was never observed in the MALDI-TOF peptide mass spectra of trypsin-digested OTR in this work. MALDI peptide mass spectra results show that the unmodified form (Cys-SH) can be largely retrieved from some unobserved modified form (Cys-SY) by adding DTT, indicating that in this modified form, maybe different from the original Cys-SX, the side-chain sulphur of cysteine 64 is still single-bonded to an unknown atom in Y. As there is little possibility for a stable 48-Dalton adduct to derive from a

cysteine sulfenic acid (Cys-SOH) if it is not a cysteine sulfonic acid, the modification is modelled in this thesis to be a cysteine persulfide (Cys-S-SH) which attaches an extra water molecule or a hydroxide anion in the native protein.

6.3 Crystallisation of OTR K56A

UV-visible and MALDI-TOF spectroscopic data show that the purified OTR K56A retains the heme II and the overall tertiary structure very well despite that its proximal ligand lysine 56 is replaced with alanine. To identify the proximal ligand of heme II, K56A was crystallised but unfortunately the needle-shaped crystals do not diffract well enough under the X-ray.

6.4 Future work

Future work will aim to identify the physiological function of OTR and there could be two major approaches. The first one is to find the physiological substrate of OTR by chemistry and computational techniques. Using molecular docking programme like Autodock Vina or LIDAEUS (Ligand discovery at Edinburgh University), potential substrates that fit well into the active site of OTR could be predicted and then identified in subsequent kinetic assays. However reliable molecular docking necessitates the exact structure of the binding site which is unfortunately incomplete for the active site of OTR due to the missing electron density map of the six consecutive amino-acid residues. Therefore further crystallisation of OTR is required for molecular docking, which could be challenged by the possibility that the missing segment is fairly flexible and may never settle for a stable structure until an appropriate substrate is bound.

The second approach is to monitor the transcription level of the gene of OTR in response to various growth conditions. Following the reports that the gene expression of OTR is positively induced by some sulphur-containing compounds like thiosulfate, further investigations to confirm such an up-regulation are necessary. Possible techniques could be 2-D gel protein electrophoresis, RT-PCR or micro-chip mRNA

screening. RT-PCR is a preferred method to provide reliable data of the mRNA level of certain gene. The testing conditions for the cells could be expanded to sulphide-rich condition and other sulphur-containing compounds as the sole electron acceptor. And the selected OTR-containing bacteria strain could be switched from *S. oneidensis* MR-1 to some other species which has a smaller genome size and less complex metabolism network in order to minimise the possible functional overlap.

Identification of the exact structure of the modification of cysteine 64 could help predict the potential substrate which may specifically interact with cysteine 64. This can be achieved by solving the crystal structure with a higher resolution which however could not be guaranteed. On the other hand mass spectroscopy technique can still be applied in further studies. OTR could be treated with some reagents like DTT before being scanned in ESI-MS. Identification of the products from the reaction between OTR and DTT could also help elucidate the original modification, which may need a relatively large amount of protein.

OTR may function *in vivo* by binding some other proteins, potentially the two putative proteins encoded by the genes adjacent to *otr* in Cluster I in *Shewanella* species (see Section 1.4.5). Expression of these two putative proteins and studies of their interaction with OTR *in vitro* may help reveal if they are the physiological partners of OTR.

Solving the crystal structure of K56A is still an intriguing project as it may show some amino-acid residue proximally ligating the heme iron in replacement of the mutated lysine 56. It will be very interesting if the new ligand is histidine 78, the conserved residue in the CXXCH motif that attaches heme II. Based on the current crystallisation results, further methods could be tried as following: (1) making a soup like suspension of the available needle crystals by vortexing the drops, and then setting up a new plate with the soup as the protein stock, or (2) setting up a completely new plate with the same conditions except that the protein sample (~100 μM) is centrifuged at 13,000 rpm before being added onto the slides.

References

Abboud, R., Popa, R., Souza-Egipsy, V., Giometti, C.S., Tollaksen, S., Mosher, J.J., Findelay, R.H. and Nealson, K.H. (2005) Low-temperature growth of *Shewanella oneidensis* MR-1. *Appl. EnViron. Microbiol.*, **71**:811-816.

Abraham, B.D., Sono, M., Boutaud, O., Shriner, A., Dawson, J.H., Brash, A.R. and Gaffney, B.J. (2001) Characterization of the coral allene oxide synthase active site with UV-visible absorption, magnetic circular dichroism, and electron paramagnetic resonance spectroscopy: evidence for tyrosinate ligation to the ferric enzyme heme iron. *Biochemistry*, **40**:2251-2259.

Allen, J.W., Daltrop, O., Stevens, J.M. and Ferguson, S.J. (2003) *C*-type cytochromes: diverse structures and biogenesis systems pose evolutionary problems. *Philos. Trans. R. Soc. Lond. B. Biol. Sci.*, **358**:255-266.

Allen, J.W., Leach, N. and Ferguson, S.J. (2005) The histidine of the *c*-type cytochrome CXXCH haem-binding motif is essential for haem attachment by the *Escherichia coli* cytochrome *c* maturation (Ccm) apparatus. *Biochem. J.*, **389**:587–592.

Arnesano, F., Banci, L., Bertini, I., Ciofi-Baffoni, S., Woodyear, T.L., Johnson, C.M. and Barker, P.D. (2000) Structural consequences of *b*- to *c*-type heme conversion in oxidized *Escherichia coli* cytochrome b_{562}. *Biochemistry*, **39**:1499-1514.

Atkinson, S.J. (2009) Studies of multiheme proteins from the dissimilatory metal reducing bacteria *Shewanella oneidensis* MR-1 and *Geobacter sulfurreducens* (Ph.D. thesis), *the University of Edinburgh*.

Atkinson, S.J., Mowat, C.G., Reid, G.A. and Chapman, S.K. (2007) An octaheme *c*-type cytochrome from *Shewanella oneidensis* can reduce nitrite and hydroxylamine, *FEBS. Lett.*, **581**:3805-3808.

Baar, C., Eppinger, M., Raddatz, G., Simon, J., Lanz, C., Klimmek, O., Nandakumar, R., Gross, R., Rosinus, A., Keller, H., Jagtap, P., Linke, B., Meyer, F., Lederer, H.

and Schuster, S.C. (2003) Complete genome sequence and analysis of *Wolinella succinogenes*. *Proc. Natl. Acad. Sci. U.S.A.*, **100**:11690-11695.

Bak, F. and Cypionka, H. (1987) A novel type of energy metabolism involving fermentation of inorganic sulphur compounds. *Nature*, **326**:891-892.

Bamford, V.A., Angove, H.C., Seward, H.E., Thomson, A.J., Cole, J.A., Butt, J.N., Hemmings, A.M. and Richardson, D.J. (2002a) Structure and spectroscopy of the periplasmic cytochrome *c* nitrite reductase from *Escherichia coli*. Biochemistry, **41**:2921-2931.

Bamford, V.A., Bruno, S., Rasmussen, T., Appia-Ayme, C., Cheesman, M.R., Berks, B.C. and Hemmings, A.M. (2002b) Structural basis for the oxidation of thiosulfate by a sulfur cycle enzyme. *EMBO. J.*, **21**:5599-5610.

Berks, B.C., Page, M.D., Richardson, D.J., Reilly, A., Cavill, A., Outen, F. and Ferguson, S.J. (1995) Sequence analysis of subunits of the membrane-bound nitrate reductase from a denitrifying bacterium: the integral membrane subunit provides a prototype for the dihaem electron-carrying arm of a redox loop. *Mol. Microbiol.*, **15**:319-331.

Beliaev, A.S., Klingeman, D.M., Klappenbach, J.A., Wu, L., Romine, M.F., Tiedje, J.M., Nealson, K.H., Fredrickson, J.K. and Zhou, J. (2005) Global transcriptome analysis of *Shewanella oneidensis* MR-1 exposed to different terminal electron acceptors. *J. Bacteriol.*, **187**:7138-7145.

Biddle, E., Shirodkar, S. and Saffarini, D. (2008) Identification and analysis of components of the electron transport chains that lead to reduction of S-components in *S. oneidensis* MR-1. Genomics: GTL awardee workshop and metabolic engineering working group interagency conference on metabolic engineering, February 2008, Bethesda, Maryland, the U.S.A.

Bordo, D., Deriu, D., Colnaghi, R., Carpen, A., Pagani, S. and Bolognesi, M. (2000) The crystal structure of a sulfurtransferase from *Azotobacter vinelandii* highlights the

evolutionary relationship between the rhodanese and phosphatase enzyme families. *J. Mol. Biol.*, **298**:691-704.

Bren, K.L. and Gray, H.B. (1993) Structurally engineered cytochromes with novel ligand-binding sites : oxy and carbon monoxy derivatives of semisynthetic horse heart Ala80 cytochrome *c*, *J. Am. Chem. Soc.*, **115**:10382-10383.

Bretschger, O., Obraztsova, A., Sturm, C.A., Chang, I.S., Gorby, Y.A., Reed, S.B., Culley, D.E., Reardon, C.L., Barua, S., Romine, M.F., Zhou, J., Beliaev, A.S., Bouhenni, R., Saffarini, D., Mansfeld, F., Kim, B.H., Fredrickson, J.K. and Nealson, K.H. (2007) Current production and metal oxide reduction by *Shewanella oneidensis* MR-1 wild type and mutants. *Appl. Environ. Microbiol.*, **73**:7003-7012.

Carpentier, W., De Smet, L., Van Beeumen, J. and Brigé, A. (2005) Respiration and growth of *Shewanella oneidensis* MR-1 using vanadate as the sole electron acceptor. *J. Bacteriol.*, **187**:3293-3301.

Ceriotti, F. and Ceriotti, G. (1980) Improved direct specific determination of serum iron and total iron-binding capacity. *Clin. Chem.*, **26**:327-331.

Chain, P., Lamerdin, J., Larimer, F., Regala, W., Lao, V., Land, M., Hauser, L., Hooper, A., Klotz, M., Norton, J., Sayavedra-Soto, L., Arciero, D., Hommes, N., Whittaker, M. and Arp, D. (2003) Complete genome sequence of the ammonia-oxidizing bacterium and obligate chemolithoautotroph *Nitrosomonas europaea*. *J. Bacteriol.*, **185**:2759-2773.

Claiborne, A., Mallett, T.C., Yeh, J.I., Luba, J. and Parsonage, D. (2001) Structural, redox, and mechanistic parameters for cysteine-sulfenic acid function in catalysis and regulation. *Adv. Protein. Chem.*, **58**:215-276.

Claiborne, A., Yeh, J.I., Mallett, T.C., Luba, J., Crane, E.J.III, Charrier, V. and Parsonage, D. (1999) Protein-sulfenic acids: diverse roles for an unlikely player in enzyme catalysis and redox regulation. *Biochemistry*, **38**:15407-15416.

Clarke, T.A., Hemmings, A.M., Burlat, B., Butt, J.N., Cole, J.A. and Richardson, D.J. (2006) Comparison of the structural and kinetic properties of the cytochrome *c* nitrite reductases from *Escherichia coli*, *Wolinella succinogenes*, *Sulfurospirillum deleyianum* and *Desulfovibrio desulfuricans*. *Biochem. Soc. Trans*., **34**:143-145.

Cruz-García, C., Murray, A.E., Klappenbach, J.A., Stewart, V. and Tiedje, J.M. (2007) Respiratory nitrate ammonification by *Shewanella oneidensis* MR-1. *J. Bacteriol.*, **189**:656-662.

De Windt, W., Aelterman, P. and Verstraete, W. (2005) Bioreductive deposition of palladium (0) nanoparticles on *Shewanella oneidensis* with catalytic activity towards reductive dechlorination of polychlorinated biphenyls. *Environ. Microbiol.*, **7**:314-325.

Eaves, D.J., Grove, J., Staudenmann, W., James, P., Poole, R.K., White, S.A., Griffiths, I. and Cole, J.A. (1998) Involvement of products of the nrfEFG genes in the covalent attachment of haem *c* to a novel cysteine-lysine motif in the cytochrome c_{552} nitrite reductase from *Escherichia coli*. *Mol. Microbiol.*, **28**:205-216.

Einsle, O., Messerschmidt, A., Huber, R., Kroneck, P.M. and Neese, F. (2002) Mechanism of the six-electron reduction of nitrite to ammonia by cytochrome *c* nitrite reductase. *J. Am. Chem. Soc.*, **124**:11737-11745.

Einsle, O., Messerschmidt, A., Stach, P., Bourenkov, G.P., Bartunik, H.D., Huber, R. and Kroneck, P.M. (1999) Structure of cytochrome *c* nitrite reductase. *Nature*, **400**:476-480.

Ellis, H.R. and Poole, L.B. (1997) Novel application of 7-chloro-4-nitrobenzo-2-oxa-1,3-diazole to identify cysteine sulfenic acid in the AhpC component of alkyl hydroperoxide reductase. *Biochemistry*, **36**:15013-15018.

Faith, J.J., Driscoll, M.E., Fusaro, V.A., Cosgrove, E.J., Hayete, B., Juhn, F.S., Schneider, S.J., and Gardner, T.S. (2007) Many Microbe Microarrays Database: uniformly normalized Affymetrix compendia with structured experimental metadata. *Nucleic Acids Research*. http://m3d.bu.edu/cgi-bin/web/array/index.pl?section=home .

Ferguson, S.J. (2001) Keilin's cytochromes: how bacteria use them, vary them and make them. *Biochem. Soc. Trans.*, **29**:629-640.

Ferguson, S.J., Stevens, J.M., Allen, J.W. and Robertson, I.B. (2008) Cytochrome *c* assembly: a tale of ever increasing variation and mystery? *Biochim. Biophys. Acta.*, **1777**:980-984.

Finneran, K.T., Johnsen, C.V. and Lovley, D.R. (2003) *Rhodoferax ferrireducens* sp. nov., a psychrotolerant, facultatively anaerobic bacterium that oxidizes acetate with the reduction of Fe(III). *Int. J. Syst. Evol. Microbiol.*, **53**:669-673.

Fredrickson, J.K., Romine, M.F., Beliaev, A.S., Auchtung, J.M., Driscoll, M.E., Gardner, T.S., Nealson, K.H., Osterman, A.L., Pinchuk, G., Reed, J.L., Rodionov, D.A., Rodrigues, J.L., Saffarini, D.A., Serres, M.H., Spormann, A.M., Zhulin, I.B. and Tiedje, J.M. (2008) Towards environmental systems biology of *Shewanella*. *Nat. Rev. Microbiol.*, **6**:592-603.

Fredrickson, J.K., Zachara, J.M., Kennedy, D.W., Dong, H., Onstott, T.C., Hinman, N.W. and Li, S. (1998) Biogenic iron mineralization accompanying the dissimilatory reduction of hydrous ferric oxide by a groundwater bacterium. *Geochim. Cosmochim. Acta.*, **62**:3239-3257.

Gao, H., Yang, Z.K., Barua, S., Reed, S.B., Romine, M.F., Nealson, K.H., Fredrickson, J.K., Tiedje, J.M. and Zhou, J. (2009) Reduction of nitrate in *Shewanella oneidensis* depends on atypical NAP and NRF systems with NapB as a preferred electron transport protein from CymA to NapA. *ISME. J.*, **3**:966-976.

Goodhew, C.F., Brown, K.R. and Pettigrew, G.W. (1986) Heme staining in gels, a useful tool in the study of bacterial *c*-type cytochromes. *Biochim. Biophys. Acta.*, **852**:288-294.

Goodin, D.B., Davidson, M.G., Roe, J.A., Mauk, A.G. and Smith, M. (1991) Amino acid substitutions at tryptophan-51 of cytochrome *c* peroxidase: effects on

coordination, species preference for cytochrome *c*, and electron transfer. *Biochemistry*, **30**:4953-4962.

Gordon, E.H., Pealing, S.L., Chapman, S.K., Ward, F.B. and Reid, G.A. (1998) Physiological function and regulation of flavocytochrome *c*3, the soluble fumarate reductase from *Shewanella putrefaciens* NCIMB 400. *Microbiology*, **144**:937-945.

Gralnick, J.A., Vali, H., Lies, D.P. and Newman, D.K. (2006) Extracellular respiration of dimethyl sulfoxide by *Shewanella oneidensis* strain MR-1. *Proc. Natl. Acad. Sci. U.S.A.*, **103**:4669-4674.

Guiral, M., Leroy, G., Bianco, P., Gallice, P., Guigliarelli, B., Bruschi, M., Nitschke, W. and Giudici-Orticoni, M.T. (2005) Interaction and electron transfer between the high molecular weight cytochrome and cytochrome c_3 from *Desulfovibrio vulgaris* Hildenborough: kinetic, microcalorimetric, EPR and electrochemical studies. *Biochim. Biophys. Acta.*, **1723**:45-54.

Gupte, S.S. and Hackenbrock, C.R. (1988a) Multidimensional diffusion modes and collision frequencies of cytochrome *c* with its redox partners. *J. Biol. Chem.*, **263**:5241-5247.

Gupte, S.S. and Hackenbrock, C.R. (1988b) The role of cytochrome *c* diffusion in mitochondrial electron transport. *J. Biol. Chem.*, **263**:5248-5253.

Hackenbrock, C.R., Chazotte, B. and Gupte, S.S. (1986) The random collision model and a critical assessment of diffusion and collision in mitochondrial electron transport. *J. Bioenerg. Biomembr.*, **18**:331-368.

Hamann, M., Zhang, T., Hendrich, S. and Thomas, J.A. (2002) Quantitation of protein sulfinic and sulfonic acid, irreversibly oxidized protein cysteine sites in cellular proteins. *Methods. Enzymol.*, **348**:146-156.

Hau, H.H. and Gralnick, J.A. (2007) Ecology and biotechnology of the genus *Shewanella*. *Annu. Rev. Microbiol.*, **61**:237-258.

Hauska, G., Schoedl, T., Remigy, H. and Tsiotis, G. (2001) The reaction center of green sulfur bacteria. *Biochim. Biophys. Acta.*, **1507**:260-277.

Haveman, S.A., Greene, E.A., Stilwell, C.P., Voordouw, J.K. and Voordouw, G. (2004) Physiological and gene expression analysis of inhibition of *Desulfovibrio vulgaris* hildenborough by nitrite. *J. Bacteriol.*, **186**:7944-7950.

Heidelberg, J.F., Paulsen, I.T., Nelson, K.E., Gaidos, E.J., Nelson, W.C., Read, T.D., Eisen, J.A., Seshadri, R., Ward, N., Methe, B., Clayton, R.A., Meyer, T., Tsapin, A., Scott, J., Beanan, M., Brinkac, L., Daugherty, S., DeBoy, R.T., Dodson, R.J., Durkin, A.S., Haft, D.H., Kolonay, J.F., Madupu, R., Peterson, J.D., Umayam, L.A., White, O., Wolf, A.M., Vamathevan, J., Weidman, J., Impraim, M., Lee, K., Berry, K., Lee, C., Mueller, J., Khouri, H., Gill, J., Utterback, T.R., McDonald, L.A., Feldblyum, T.V., Smith, H.O., Venter, J.C., Nealson, K.H., and Fraser, C.M. (2002) Genome sequence of the dissimilatory metal ion-reducing bacterium *Shewanella oneidensis*. *Nat. Biotechnol.*, **20**:1118-1123.

Heidelberg, J.F., Seshadri, R., Haveman, S.A., Hemme, C.L., Paulsen, I.T., Kolonay, J.F., Eisen, J.A., Ward, N., Methe, B., Brinkac, L.M., Daugherty, S.C., Deboy, R.T., Dodson, R.J., Durkin, A.S., Madupu, R., Nelson, W.C., Sullivan, S.A., Fouts, D., Haft, D.H., Selengut, J., Peterson, J.D., Davidsen, T.M., Zafar, N., Zhou, L., Radune, D., Dimitrov, G., Hance, M., Tran, K., Khouri, H., Gill, J., Utterback, T.R., Feldblyum, T.V., Wall, J.D., Voordouw, G. and Fraser, C.M. (2004) The genome sequence of the anaerobic, sulfate-reducing bacterium *Desulfovibrio vulgaris* Hildenborough. *Nat. Biotechnol.*, **22**:554-559.

Hensel, M., Hinsley, A.P., Nikolaus, T., Sawers, G. and Berks, B.C. (1999) The genetic basis of tetrathionate respiration in *Salmonella typhimurium*. *Mol. Microbiol.*, **32**:275-287.

Hinsley, A.P. and Berks, B.C. (2002) Specificity of respiratory pathways involved in the reduction of sulfur compounds by *Salmonella enterica*. *Microbiology*, **148**:3631-3638.

Huang, K.T., Keszler, A., Patel, N., Patel, R.P., Gladwin, M.T., Kim-Shapiro, D.B. and Hogg, N. (2005a) The reaction between nitrite and deoxyhemoglobin. Reassessment of reaction kinetics and stoichiometry. *J. Biol. Chem.*, **280**:31126-31131.

Huang, Z., Shiva, S., Kim-Shapiro, D.B., Patel, R.P., Ringwood, L.A., Irby, C.E., Huang, K.T., Ho, C., Hogg, N., Schechter, A.N. and Gladwin, M.T. (2005b) Enzymatic function of hemoglobin as a nitrite reductase that produces NO under allosteric control. *J. Clin. Invest.*, **115**:2099-2107.

Igarashi, N., Moriyama, H., Fujiwara, T., Fukumori, Y. and Tanaka, N. (1997) The 2.8 Å structure of hydroxylamine oxidoreductase from a nitrifying chemoautotrophic bacterium, *Nitrosomonas europaea*. *Nat. Struct. Biol.*, **4**:276-284.

Jefcoate, C.R. and Gaylor, J.L. (1969) Ligand interactions with hemoprotein P-450. II. Influence of phenobarbital and methylcholanthrene induction processes on P-450 spectra. *Biochemistry*, **8**:3464-3472.

Jormakka, M., Törnroth, S., Byrne, B. and Iwata, S. (2002) Molecular basis of proton motive force generation: structure of formate dehydrogenase-N. *Science*, **295**:1863-1868.

Khashe, S. and Janda, J.M. (1998) Biochemical and pathogenic properties of *Shewanella alga* and *Shewanella putrefaciens*. *J. Clin. Microbiol.*, **36**:783-787.

Klamt, S., Grammel, H., Straube, R., Ghosh, R. and Gilles, E.D. (2008) Modeling the electron transport chain of purple non-sulfur bacteria. *Mol. Syst. Biol.*, **4**:156.

Klonowska, A., Heulin, T. and Vermeglio, A. (2005) Selenite and Tellurite Reduction by *Shewanella oneidensis*. *Appl. Environ. Microbiol.*, **71**:5607-5609.

Lenaz, G. and Genova, M.L. (2009) Mobility and function of coenzyme Q (ubiquinone) in the mitochondrial respiratory chain. *Biochim. Biophys. Acta.*, **1787**:563-573.

Li, B.R., Anderson, J.L., Mowat, C.G., Miles, C.S., Reid, G.A. and Chapman, S.K. (2008) *Rhodobacter sphaeroides* haem protein: a novel cytochrome with nitric oxide dioxygenase activity. *Biochem. Soc. Trans.*, **36**:992-995.

Liu, C., Gorby, Y.A., Zachara, J.M., Fredrickson, J.K. and Brown, C.F. (2002) Reduction kinetics of Fe(III), Co(III), U(VI), Cr(VI), and Tc(VII) in cultures of dissimilatory metal-reducing bacteria. *Biotechnol. Bioeng.*, **80**:637-649.

Marietou, A., Griffiths, L. and Cole, J. (2009) Preferential reduction of the thermodynamically less favorable electron acceptor, sulfate, by a nitrate-reducing strain of the sulfate-reducing bacterium *Desulfovibrio desulfuricans* 27774. *J. Bacteriol.*, **191**:882-889.

Matias, P.M., Coelho, A.V., Valente, F.M., Plácido, D., LeGall, J., Xavier, A.V., Pereira, I.A. and Carrondo, M.A. (2002) Sulfate respiration in Desulfovibrio vulgaris Hildenborough. Structure of the 16-heme cytochrome *c* HmcA at 2.5-Å resolution and a view of its role in transmembrane electron transfer. *J. Biol. Chem.*, **277**:47907-47916.

Mayhew, S.G. (1978) The redox potential of dithionite and SO_2^- from equilibrium reactions with flavodoxins, methyl viologen and hydrogen plus hydrogenase, *Eur. J. Biochem.*, **85**:535-547.

Meyer, T.E., Tsapin, A.I., Vandenberghe, I., de Smet, L., Frishman, D., Nealson, K.H., Cusanovich, M.A. and van Beeumen, J.J. (2004) Identification of 42 possible cytochrome *c* genes in the *Shewanella oneidensis* genome and characterization of six soluble cytochromes. *OMICS*, **8**:57-77.

Michel, L.O., Sandkvist, M. and Bagdasarian, M. (1995) Specificity of the protein secretory apparatus: secretion of the heat-labile enterotoxin B subunit pentamers by different species of Gram negative bacteria. *Gene*, **152**:41-45.

Middleton, S.S., Latmani, R.B., Mackey, M.R., Ellisman, M.H., Tebo, B.M. and Criddle, C.S. (2003) Cometabolism of Cr(VI) by *Shewanella oneidensis* MR-1 produces cell-associated reduced chromium and inhibits growth. *Biotechnol. Bioeng.*, **83**:627-637.

Moser, C.C., Farid, T.A., Chobot, S.E. and Dutton, P.L. (2006a) Electron tunneling chains of mitochondria. *Biochim. Biophys. Acta.*, **1757**:1096-1109.

Moser, C.C., Page, C.C. and Dutton, P.L. (2006b) Darwin at the molecular scale: selection and variance in electron tunnelling proteins including cytochrome *c* oxidase. *Philos. Trans. R. Soc. Lond. B. Biol. Sci.*, **361**:1295-1305.

Moser, D.P. and Nealson, K.H. (1996) Growth of the facultative anaerobe *Shewanella putrefaciens* by elemental sulfur reduction. *Appl. Environ. Microbiol.*, **62:** 2100–2105.

Mowat, C.G. and Chapman, S.K. (2005) Multi-heme cytochromes—new structures, new chemistry. *Dalton. Trans.*, **21**:3381-3389.

Mowat, C.G., Rothery, E., Miles, C.S., McIver, L., Doherty, M.K., Drewette, K., Taylor, P., Walkinshaw, M.D., Chapman, S.K. and Reid, G.A. (2004) Octaheme tetrathionate reductase is a respiratory enzyme with novel heme ligation. *Nat. Struct. Mol. Biol.*, **11**:1023-1024.

Muyzer, G. and Stams, A.J. (2008) The ecology and biotechnology of sulphate-reducing bacteria. *Nat. Rev. Microbiol.*, **6**:441-454.

Myers, C.R. and Nealson, K.H. (1988) Bacterial manganese reduction and growth with manganese oxide as the sole electron acceptor. *Science*, **240**:1319-1321

Nogi, T., Fathir, I., Kobayashi, M., Nozawa, T. and Miki, K. (2000) Crystal structures of photosynthetic reaction center and high-potential iron-sulfur protein from Thermochromatium tepidum: thermostability and electron transfer. *Proc. Natl. Acad. Sci. U.S.A.*, **97**:13561-13566.

Page, C.C., Moser, C.C. and Dutton, P.L. (2003) Mechanism for electron transfer within and between proteins. *Curr. Opin. Chem. Biol.*, **7**:551-556.

Page, C.C., Moser, C.C., Chen, X. and Dutton, P.L. (1999) Natural engineering principles of electron tunnelling in biological oxidation-reduction. *Nature*, **402**:47-52.

Paoli, M., Marles-Wright, J. and Smith, A. (2002) Structure-function relationships in heme-proteins. *DNA. Cell. Biol.*, **21**:271-280.

Payne, A.N. and Dichristina, T.J. (2006) A rapid mutant screening technique for detection of technetium [Tc(VII)] reduction-deficient mutants of *Shewanella oneidensis* MR-1. *FEMS. Microbiol. Lett.*, **259**:282-287.

Pereira, I.A., LeGall, J., Xavier, A.V. and Teixeira, M. (2000) Characterization of a heme *c* nitrite reductase from a non-ammonifying microorganism, *Desulfovibrio vulgaris* Hildenborough. *Biochim. Biophys. Acta.*, **31**:119-130.

Pereira, P.M., He, Q., Valente, F.M., Xavier, A.V., Zhou, J., Pereira, I.A. and Louro, R.O. (2008) Energy metabolism in *Desulfovibrio vulgaris* Hildenborough: insights from transcriptome analysis. *Antonie Van Leeuwenhoek*, **93**:347-362.

Perry, K.A., Kostka, J.E., Luther III G.W. and Nealson, K.H. (1993) Mediation of sulfur speciation by a Black Sea facultative anaerobe. *Science*, **259:** 801–803.

Petersen, M.G., Dewilde, S. and Fago, A. (2008) Reactions of ferrous neuroglobin and cytoglobin with nitrite under anaerobic conditions. *J. Inorg. Biochem.*, **102**:1777-1782.

Pickard, C., Foght, J.M., Pickard, M.A. and Westlake, D.W.S. (1993) Oil field and freshwater isolates of *Shewanella putrefaciens* have lipopolysaccharide polyacrylamide gel profiles characteristic of marine bacteria. *Can. J. Microbiol./Rev. Can. Microbiol.*, **39**:715-717.

Pisa, R., Stein, T., Eichler, R., Gross, R. and Simon, J. (2002) The *nrfI* gene is essential for the attachment of the active site haem group of *Wolinella succinogenes* cytochrome *c* nitrite reductase. *Mol. Microbiol.*, **43**:763-770.

Poock, S.R., Leach, E.R., Moir, J.W., Cole, J.A. and Richardson, D.J. (2002) Respiratory detoxification of nitric oxide by the cytochrome *c* nitrite reductase of *Escherichia coli. J. Biol. Chem.*, **277**:23664-23669.

Richardson, D.J. (2000) Bacterial respiration: a flexible process for a changing environment. *Microbiology*, **146**:551-571.

Richardson, D.J. and Ferguson, S.J. (1992) The influence of carbon substrate on the activity of the periplasmic nitrate reductase in aerobically grown *Thiosphaeva pantotropha*. *Arch. Microbial.*, **157**:535-537.

Rodrigues, M.L., Oliveira, T.F., Pereira, I.A. and Archer, M. (2006) X-ray structure of the membrane-bound cytochrome *c* quinol dehydrogenase NrfH reveals novel haem coordination. *EMBO. J.*, **25**:5951-5960.

Rothery, E.L. (2004) Mechanistic studies on multiheme cytochromes from *Shewanella* (Ph.D. thesis), *the University of Edinburgh*.

Ruebush, S.S., Icopini, G.A., Brantley, S.L. and Tien, M. (2006) In vitro enzymatic reduction kinetics of mineral oxides by membrane fractions from *Shewanella oneidensis* MR-1. *Geochimica et Cosmochimica Acta*, **70**:56-70.

Sanford, R., Cole, J. and Tiedje, J. (2002) Characterization and Description of *Anaeromyxobacter dehalogenans* gen. nov., sp. nov., an Aryl-Halorespiring Facultative Anaerobic Myxobacterium. *Appl Environ Microbiol.*, **68**:893–900.

Schwalb, C., Chapman, S.K. and Reid, G.A. (2003) The tetraheme cytochrome CymA is required for anaerobic respiration with dimethyl sulfoxide and nitrite in *Shewanella oneidensis*. *Biochemistry*, **42**:9491-9497.

Sears, H.J., Spiro, S. and Richardson, D.J. (1997) Effect of carbon substrate and aeration on nitrate reduction and expression of the periplasmic and membrane-bound nitrate reductases in carbon-limited continuous cultures of *Paracoccus denitrificans* Pd1222. *Microbiology*, **143**:3767-3774.

Serres, M.H. and Riley, M. (2006) Genomic analysis of carbon source metabolism of *Shewanella oneidensis* MR-1: Predictions versus experiments. *J Bacteriol.*, **188**:4601-4609.

Silkstone, G.G., Cooper, C.E., Svistunenko, D. and Wilson, M.T. (2005) EPR and optical spectroscopic studies of Met80X mutants of yeast ferricytochrome *c*. Models for intermediates in the alkaline transition. *J. Am. Chem. Soc.*, **127**:92-99.

Spaar, A., Flöck, D. and Helms, V. (2009) Association of cytochrome *c* with membrane-bound cytochrome *c* oxidase proceeds parallel to the membrane rather than in bulk solution. *Biophys. J.*, **96**:1721-1732.

Stach, P., Einsle, O., Schumacher, W., Kurun, E. and Kroneck, P.M. (2000) Bacterial cytochrome *c* nitrite reductase: new structural and functional aspects. *J. Inorg. Biochem.*, **79**:381-385.

Stevens, J.M., Daltrop, O., Allen, J.W. and Ferguson, S.J. (2004) *C*-type cytochrome formation: chemical and biological enigmas. *Acc. Chem. Res.*, **37**:999-1007.

Stookey, L.L. (1970) Ferrozine--a new spectrophotometric reagent for iron. *Anal. Chem.*, **42**:779–781.

Tadokoro, T., You, D., Abe, Y., Chon, H., Matsumura, H., Koga, Y., Takano, K. and Kanaya, S. (2007) Structural, thermodynamic, and mutational analyses of a psychrotrophic RNase HI. *Biochemistry*, **46**:7460 -7468.

Tikhonova, T.V., Slutsky, A., Antipov, A.N., Boyko, K.M., Polyakov, K.M., Sorokin, D.Y., Zvyagilskaya, R.A. and Popov, V.O. (2006) Molecular and catalytic properties of a novel cytochrome *c* nitrite reductase from nitrate-reducing haloalkaliphilic sulfur-oxidizing bacterium *Thioalkalivibrio nitratireducens*. *Biochim. Biophys. Acta.*, **1764**:715-723.

Tomlinson, E.J. and Ferguson, S.J. (2000) Conversion of a *c* type cytochrome to a *b* type that spontaneously forms *in vitro* from apo protein and heme: implications for *c* type cytochrome biogenesis and folding. *Proc. Natl. Acad. Sci. U.S.A.*, **97**:5156-5160.

Unden, G. and Bongaerts, J. (1997) Alternative respiratory pathways of *Escherichia coli*: energetics and transcriptional regulation in response to electron acceptors. *Biochim. Biophys. Acta.*, **1320**:217-234.

Venkateswaran, K., Moser, D.P., Dollhopf, M.E., Lies, D.P., Saffarini, D.A., MacGregor, B.J., Ringelberg, D.B., White, D.C., Nishijima, M., Sano, H., Burghardt, J., Stackebrandt, E. and Nealson, K.H. (1999) Polyphasic taxonomy of the genus *Shewanella* and description of *Shewanella oneidensis* sp. nov. *Int. J. Syst. Bacteriol.*, **49**:705-724.

Vonck, J. and Schäfer, E. (2009) Supramolecular organization of protein complexes in the mitochondrial inner membrane. Biochim. Biophys. Acta., **1793**:117-124.

Wiatrowski, H.A., Ward, P.M. and Barkay, T. (2006) Novel reduction of mercury (II) by mercury-sensitive dissimilatory metal reducing bacteria. *Environ. Sci. Technol.*, **40**:6690-6696.

Xiong, Y., Shi, L., Chen, B., Mayer, M.U., Lower, B.H., Londer, Y., Bose, S., Hochella, M.F., Fredrickson, J.K. and Squier, T.C. (2006) High-affinity binding and

direct electron transfer to solid metals by the *Shewanella oneidensis* MR-1 outer membrane *c*-type cytochrome OmcA. *J. Am. Chem. Soc.*, **128**:13978-13979.

Yonetani, T. and Anni, H. (1987) Yeast cytochrome *c* peroxidase. Coordination and spin states of heme prosthetic group. *J. Biol. Chem.*, **262**:9547-9554.

Yoshida, S., Iizuka, T., Nozawa, T. and Hatano, M. (1975) Studies on the charge transfer band in high spin state of ferric myoglobin and hemoglobin by low temperature optical and magnetic circular dichroism spectroscopy. *Biochim. Biophys. Acta.*, **405**:122-135.

Yurkov, V. and Beatty, J. (1998) Aerobic Anoxygenic Phototrophic Bacteria. *Microbiol. Mol. Biol. Rev.*, **62**:695–724.

Zachara, J.M., Fredrickson, J.K., Li, S.M., Kennedy, D.W., Smith, S.C. and Gassman, P.L. (1998) Bacterial reduction of crystalline Fe^{3+} oxides in single phase suspensions and subsurface materials. *American Mineralogist*, **83**:1426-1443.

Appendices

Part 1 – Protein sequence of OTR

Appendices-1.1 The sequence of OTR from *Shewanella oneidensis* MR-1. The heme-attaching motifs (CXXCH) are in red. The signal peptide is in green.

MKQLLFIALAGMALQAQA-

```
          10        20        30        40        50        60
ANPHKDVLKG PFTTGSEVTT QCLTCHEEQA TDMMKTSHWT WELEQKLPDR TVVRGKKNSI

          70        80        90       100       110       120
NNFCVAISSN EPRCTSCHAG YGWKDNTFDF KDKTKVDCLI CHDTTGTYVK DPAGAGEPMA

         130       140       150       160       170       180
KLDLAKIAQN VGAPVRDNCG SCHFYGGGGD AVKHGDLDSS MAYPDKATDV HMDSDGNNFQ

         190       200       210       220       230       240
CQNCHTTEKH QISGNAMGVS PGGIDHIGCE NCHDSAPHSN KKLNTHTATV ACQTCHIPFF

         250       260       270       280       290       300
AKNEPTKMQW DWSTAGDDKP ETVDQYGKHT YQKKKGNFVW EKMVKPQYAW YNGTANAYMA

         310       320       330       340       350       360
GDKMDSNVVT KLTYPMGDIN DAKAKIYPFK VHTGKQIYDK KLNIFITPKT YGKGGYWSEF

         370       380       390       400       410       420
DWNLAAKLGM EANPTMLEKG IKYSGEYDFA ATEMWWRINH MVSPKEQALN CNDCHNKGTR

         430       440
LDWQALGYQG DPMKNKQGPK HKQ
```

Part 2 – OTR and Fcc_3 in protein purification

Appendices-2.1 Heme-stained gels showing the purification process of OTR N61A expressed from *Shewanella oneidensis* MR-1 Δ*otr* strain. Black arrows indicate the target protein OTR N61A and red arrows point to the contaminant protein Fcc_3.

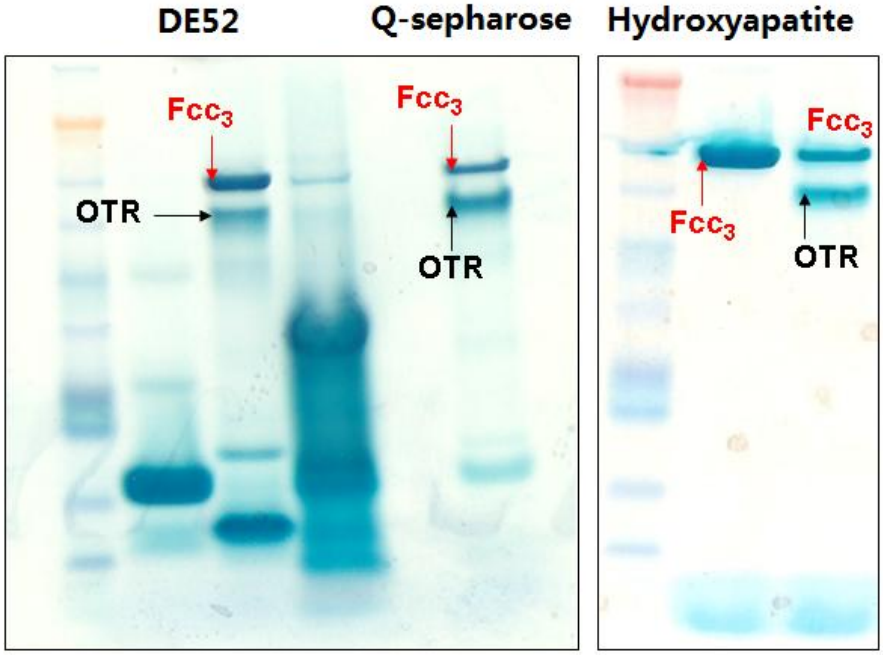

Appendices-2.2 Purification of OTR N61A expressed from *Shewanella oneidensis* MR-1 Δ*otr* strain with (a) SP-sepharose cation exchange (after DE52 purification) and (b) ammonium sulfate gradient precipitation (after cell lysis). Both gels were heme-stained.

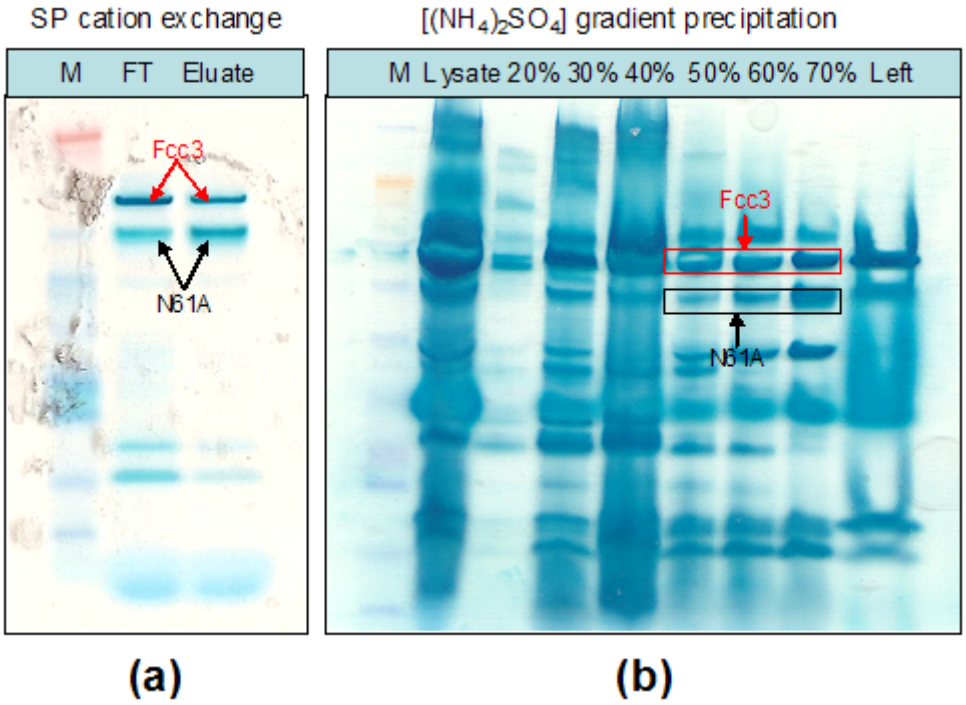

Part 3 – Nitrite and reduced methyl viologen (MV^+)

Appendices-3.1 Auto-reduction of nitrite by MV^+ in the absence of enzyme. 1.7 mM nitrite shown in the figure starts to react with MV^+ after a flat lag-phase of around 50 seconds. The lag-phase for 1 mM nitrite is 70 seconds and for lower concentrations of nitrite is longer (not shown in the figure).

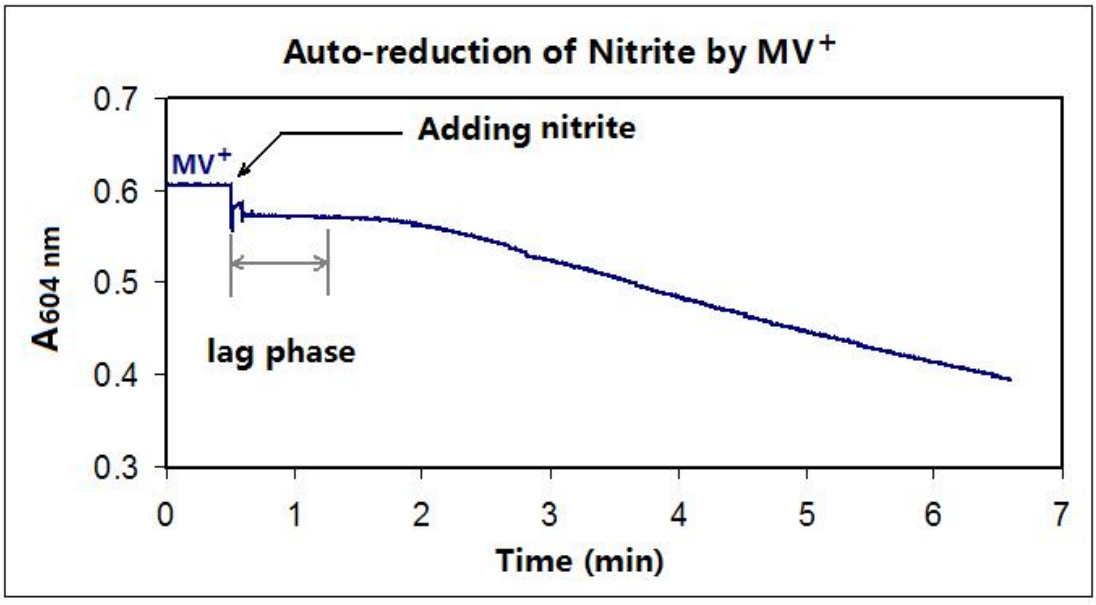

Part 4 – Anaerobic growth on minimal media plates

Appendices-4.1 Anaerobic growth (3 weeks) of wild-type *Shewanella oneidensis* MR-1 and its Δ*otr* strain on minimal media plates with 20 mM tetrathionate as the sole electron acceptor and 40 mM lactate as the electron donor.

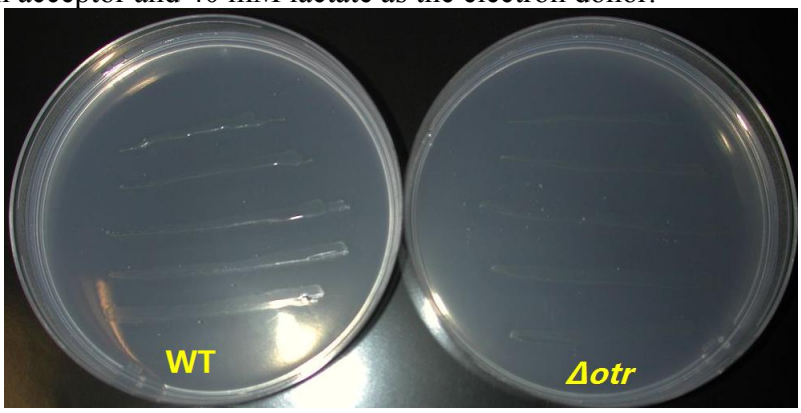

Appendices-4.2 Anaerobic growth (2 weeks) of wild-type *Shewanella oneidensis* MR-1 and its Δ*otr* strain on minimal media plates with 20 mM fumarate plus 1 mM nitrite as the electron acceptor and 40 mM lactate as the electron donor.

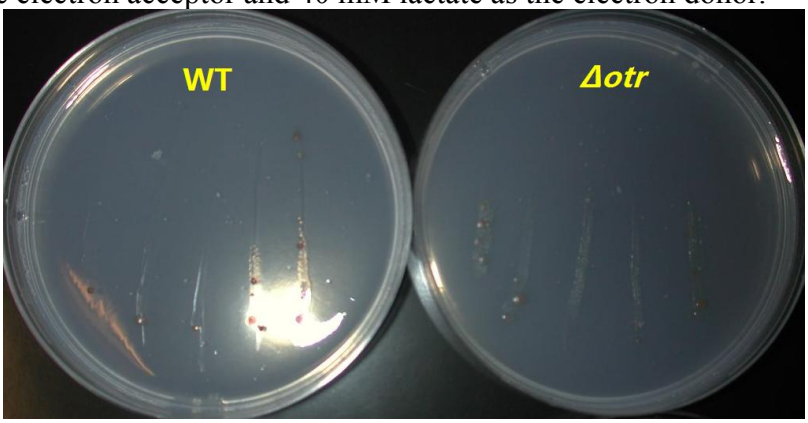

Appendices-4.3 Anaerobic growth (3 weeks) of wild-type *Shewanella oneidensis* MR-1 and its Δ*otr* strain on minimal media plates with 20 mM thiosulfate as the sole electron acceptor and 40 mM lactate as the electron donor.

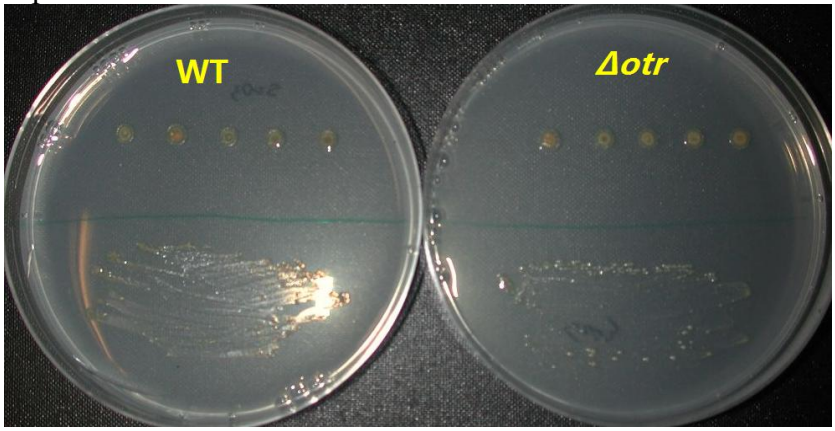

Appendices-4.4 Anaerobic growth (3 weeks) of wild-type *Shewanella oneidensis* MR-1 and its Δ*otr* strain on minimal media plates with 20 mM elemental sulphur as the sole electron acceptor and 40 mM lactate as the electron donor. The upper panel is the plate surface with cell colonies and the lower panel is the back of the media place showing dark area where the sulphur has been consumed.

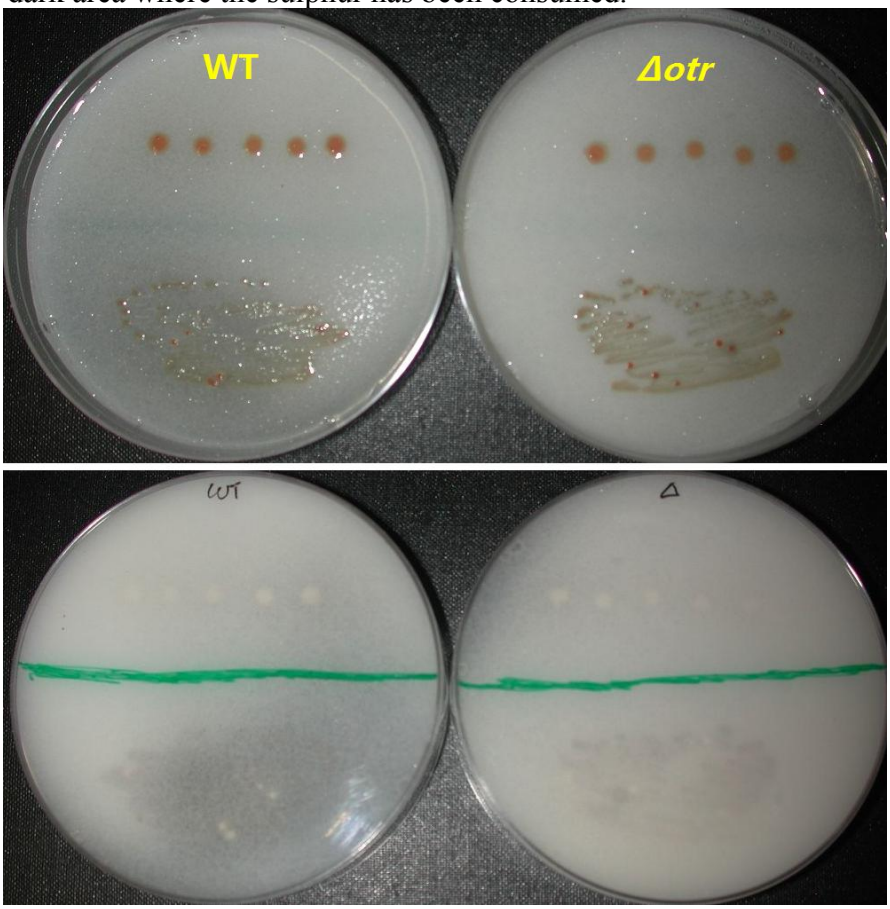

Appendices-4.5 Anaerobic growth (3 weeks) of wild-type *Shewanella oneidensis* MR-1 and its Δ*otr* strain on minimal media plates with 20 mM sulfite as the sole electron acceptor and 40 mM lactate as the electron donor.

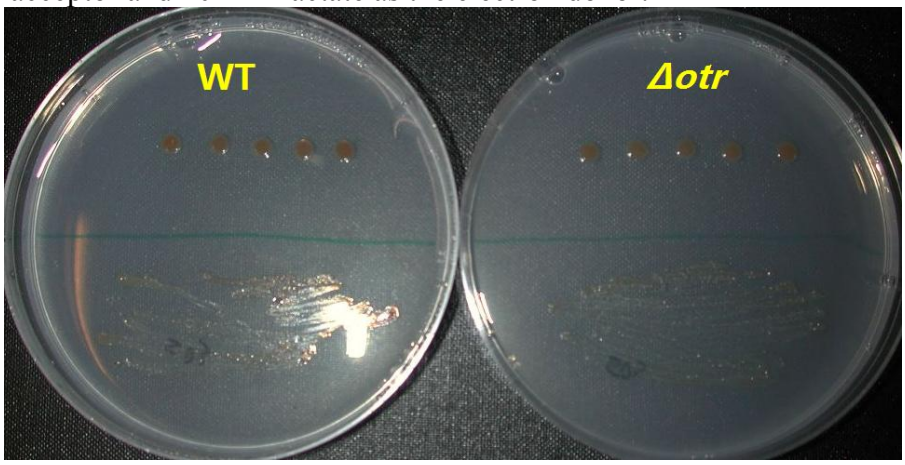

Appendices-4.6 Anaerobic growth (3 weeks) of wild-type *Shewanella oneidensis* MR-1 and its Δ*otr* strain on minimal media plates with 20 mM nitrate as the sole electron acceptor and 40 mM lactate as the electron donor.

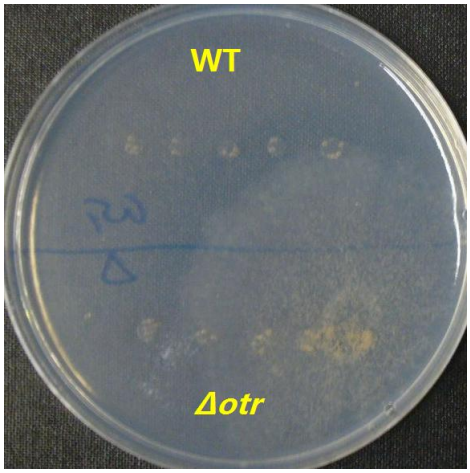

Appendices-4.7 Anaerobic growth (3 weeks) of wild-type *Shewanella oneidensis* MR-1 and its Δ*otr* strain on minimal media plates with 1 mM nitrite as the sole electron acceptor and 40 mM lactate as the electron donor.

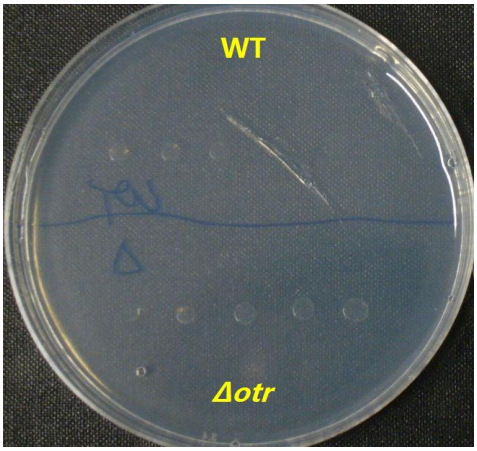

Appendices-4.8 Anaerobic growth (3 weeks) of wild-type *Shewanella oneidensis* MR-1 and its Δ*otr* strain on minimal media plates with 20 mM fumarate as the sole electron acceptor and 1.5 mM sulfide as the sole electron donor.

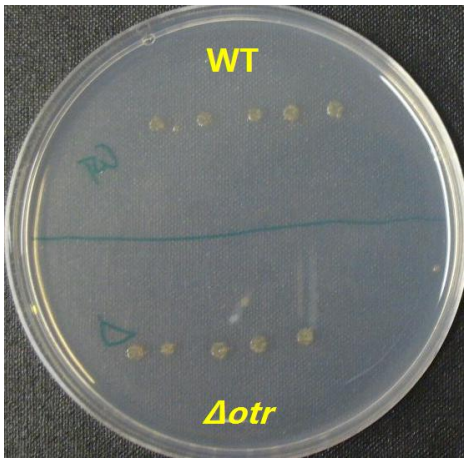

Part 5 - Mass spectroscopy data

Appendices-5.1 The peptide mass spectra of the trypsin-digested C64A, showing the Ala64-containing peptide (*m/z*=1733.3), the unknown species (*m/z*=1748.3) and the peptide attaching the heme II of OTR (*m/z*=1828.2).

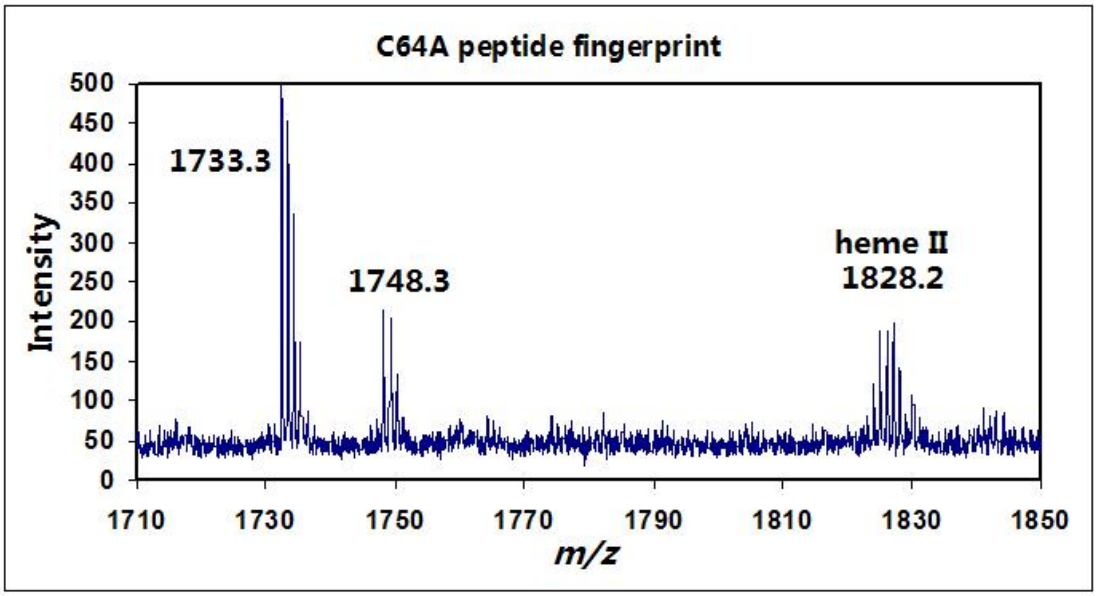

Appendices-5.2 The peptide mass spectra of the trypsin-digested wild-type OTR (the upper panel) and the "DTT+IAA"-treated sample (the lower panel), showing the heme-containing peptides that disappear in the lower panel.

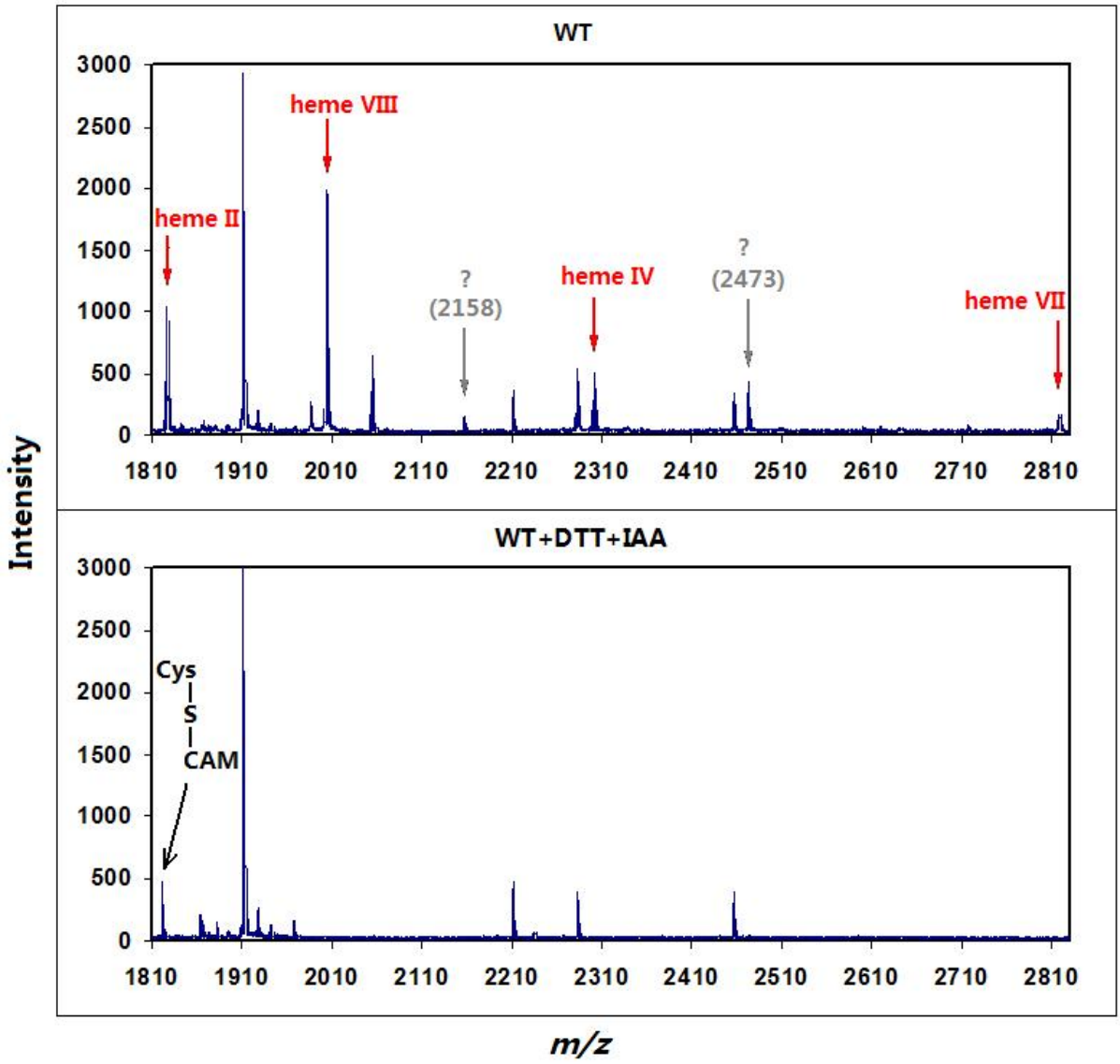

Appendices-5.3 The peptide mass spectra of the trypsin-digested wild-type OTR treated with DTT-only (the upper panel) and with IAA-only (the lower panel), showing the heme-containing peptides that are retained in both cases.

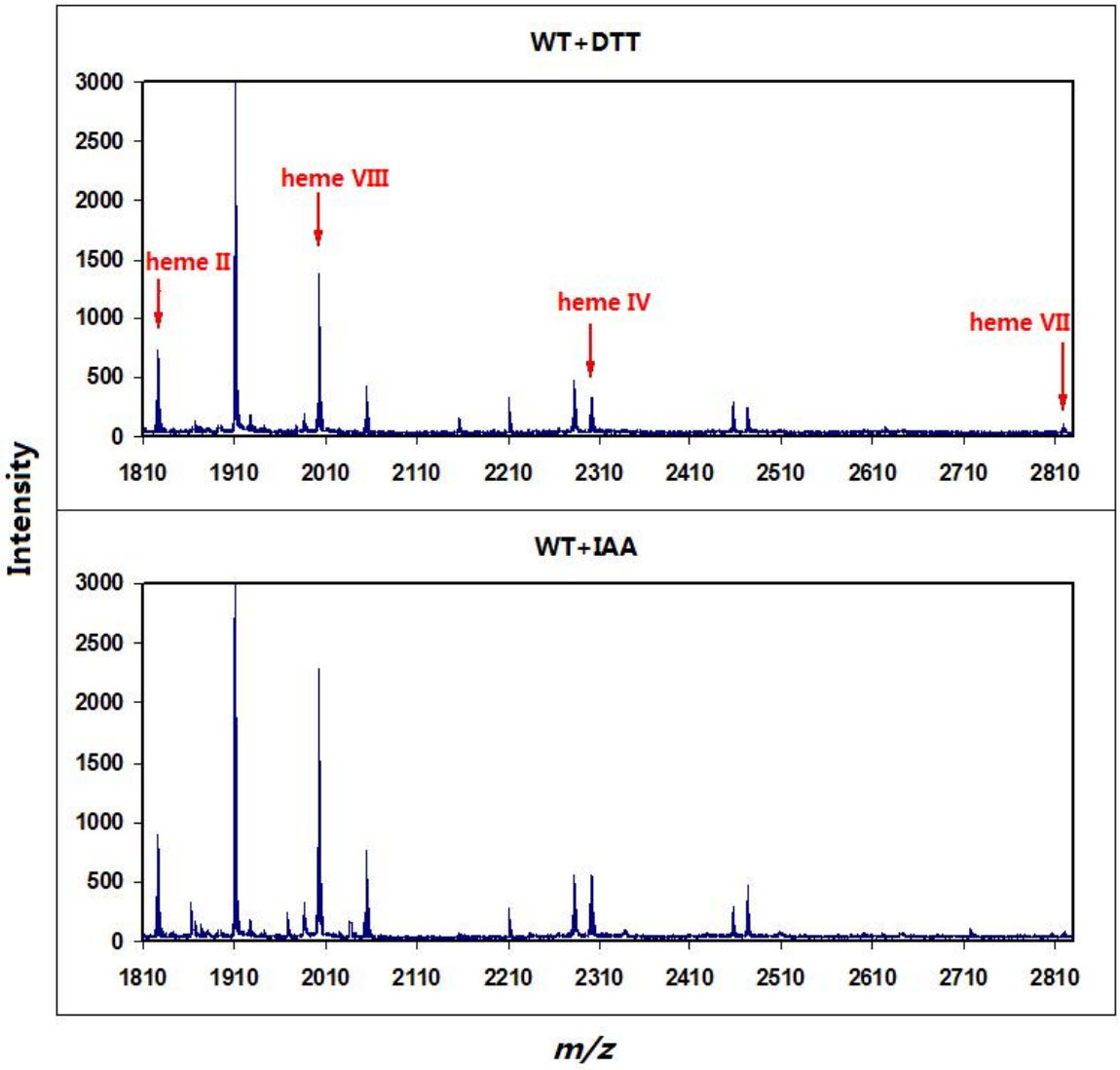

Appendices-5.4 Peptide mass spectra of trypsin-digested wild-type OTR, showing the identified typical methionine-containing peptide that has been partially oxidised.

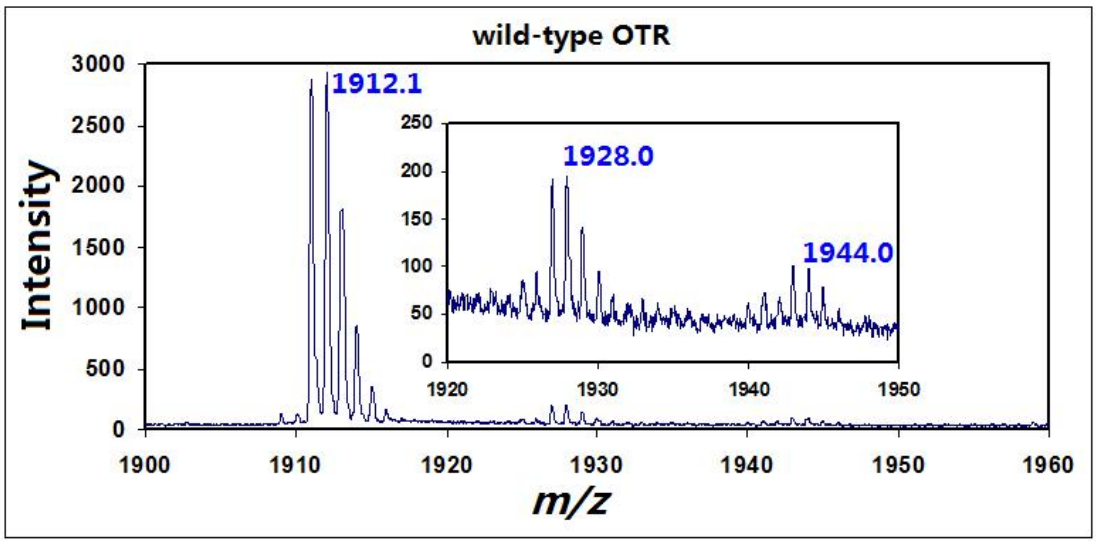

m/z	Peptide	Formula weight
1912.1	YSGEYDFAATEMWWR (383-397)	1911.8 Da
1928.0	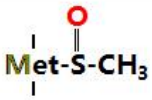	1927.8 Da
1944.0	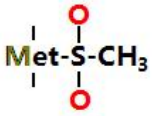	1933.8 Da

Part 6 – Crystals of OTR K56A

Appendices-6.1 Crystals of OTR K56A. The needle-shaped crystal clusters have been broken into pieces (Photographed by Ms. Laura Campbell).

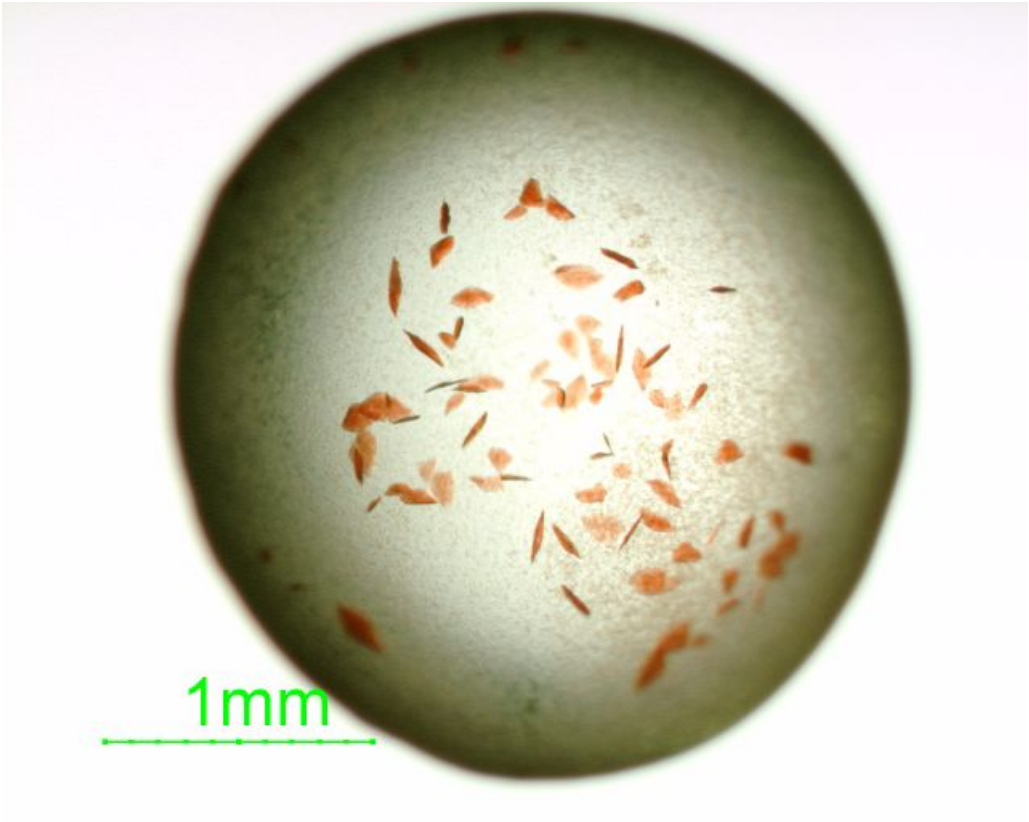

Part 7 – Multiple sequences alignment of OTR homologues

Appendices-7.1 Multiple sequences alignment of OTR homologues from 39 bacteria species by MAFFT FFT-NS-1 (v6.531b). Full names of these bacteria species can be found in Figure 4-7. Numbers labelled on the top of the alignment are the amino-acid sequence numbers of OTR from *S. oneidensis* MR-1.

```
SO4144           M-----------------------KQLLFI-ALAGM-------------------ALQA
Shewana3_3690    M-----------------------KKLIVI-ALAGM-------------------ALQA
Shewmr4_3513     M-----------------------KKLIVI-ALAGM-------------------ALQA
Shewmr7_0439     M-----------------------KKLIVI-ALAGM-------------------ALQA
Sbal223DRAFT_30  M-----------------------KRLLLI-ALAGM-------------------TLNT
Sbal195_0477     M-----------------------KRLLLI-ALAGM-------------------TLNT
Shew185_0458     M-----------------------RRLLLI-ALAGM-------------------TLNT
Ssed_4060        M-----------------------KHTLIP-FALALAGLSLLS------------SP-A
Shew_0514(S      M-----------------------KHTLSL-TAMFAAGVFGLA------------SLNA
swp_4579         M-----------------------KKIIVP-TLAFG---LLIS------------AQFA
Sfri_3556        M-----------------------K-------LLSALAVLLLL------------SSSA
Sama_3180        M-----------------------RTVFSQWALAPLSGVMLLG------------SGLA
Shal_0614        M-----------------------KTLPITLSLLTA----LLY------------CTSS
Cvib_0760        ME----------HEISVSIPNPSIMHKLMMARFIPVLLY-LFIT------------STVT
Plut_1197        M-------------------------------------LI-LFAS------------GPLS
Cpar_1055        M-----------------------KLSLIGRFVPVMITSLLFS------------TPLP
Cphamn1_2426     M-----------------------KKPLIAVLLPVISA-LFLC------------SSLH
Paes_2160(Prost  M-----------------------KKLFFVVFFLLVSP-SLYC------------SSLV
Ppha_1963        M-----------------------KKLILLRLVPVLVS-LFLF------------SLLF
Clim_2064        M-----------------------KKLLLTGTLLSGLL-FPLS------------EPLS
Cpha266_2104     M-----------------------KKLLLTGILLSGFL-FPLS------------KPLS
Dole_3005(Desul MLMWIMGFLSRKAINMEETMKHTFNGFCLVLACLMCISAAEWPA------------GAA-
Sfum_0090(Syntr MNAW------------------SVCGRWLAGAALAAVFFSSVPG------------WAQI
Dalk_1086        MY--------------------RKLGFFALAACLAIGLGLALSA------------SAAT
DVU_3144         MH------------NANASFPRRQ-----RLAVLALALTLLLPG------------ASAW
Dvul_0242        MH------------NANASFPRRQ-----RLAVLALALTLLLPG------------ASAW
DvMF_1694        MS------------SPHVSARRAHGGSPPTLLFLLLLLLLLLPGLAPLLAPAPPAHAAQL
Hhal_0149(Halor M---------------------IARRWLAGL-----LVLAVGVS------------SAAG
Maqu_0376(Marin M--------------------NNKRALRMLFSLKCLVLVASLV------------FAAN
Mmc1_0877(Magne M---------------------R----VPMHTGVWVLFFMAGLL------------LGST
Rfer_3635        M-----------------------RSRYLLVAALAALFFAVAAP------------AATK
Ctha_2243(Chlor M-----------------------RKILLALPAGALLAILFFA------------SFLT
GSU2201          M-----------------------KNTTFIATLMASVAVAALVQ----------------
Gmet_3088        M-----------------------IKILFTG-LVAGAVMASAAF----------------
Gbem_0758        M-----------------------KKTGMIAAVFGLALAATTAM----------------
Gura_3130        M-----------------------KLHGFVTTFMVACLASAPAM----------------
Adeh_0972        M-----------------------RRSAAVASALVALLQAPGAF----------------
AnaeK_1034       M-----------------------RRSAAVASALIALLQAPGAL----------------
Anae109_2593     M-----------------------SNM-IRSLALAAAILAGPAL----------------
                 *
```

```
                                          1       10        20        30
SO4144          -------------------------QAANPHKDVLKGPFTTGSEVTTQCLTCHEEQATDM
Shewana3_3690   -------------------------QAANPHKDVLKGPFATGSEVTTQCLTCHEEQATDM
Shewmr4_3513    -------------------------QAANPHKDVLKGPFATGSEVTTQCLTCHEEQATDM
Shewmr7_0439    -------------------------QAANPHKDVLKGPFATGSEVTTQCLTCHEEQATDM
Sbal223DRAFT_30 -------------------------YAANPHKEVLEGPFATGTQVTAQCLVCHEDQATDV
Sbal195_0477    -------------------------YAANPHKEVLEGPFATGTQVTAQCLMCHEDQATDV
Shew185_0458    -------------------------YAANPHKEVLEGPFATGTQVTAQCLVCHEDQATDV
Ssed_4060       -------------------------NAANQHKDYIEGPFTEGTQVTQQCIECHEDHAKDF
Shew_0514(S     -------------------------IAENPHKEAIQGPFTQGSQVTEQCIECHEDHAKDF
swp_4579        -------------------------MAANPHSEYVEGPFTQGSEVTTQCIECHEDHAKDF
Sfri_3556       -------------------------QAAFNHKEALKGPFANGPEVTTQCLTCHKEHAEEF
Sama_3180       -------------------------MADNPHKEAIEGPFASGTEVTQQCLACHEDEAHDF
Shal_0614       -------------------------WAAQDHSEFIEGPFSKGSDVTTQCIECHEDHAADF
Cvib_0760       AEVYHNPVDQLTKS-----------TADHTKFPQLKRNFKSGPEVTRACLECHTEASRQI
Plut_1197       GAVYHLPKDSLSVS-----------TADHSKFRQLQREFKSGPEVTKACLECHTEAAKQV
Cpar_1055       AVEFHQHLDSLSLS-----------TADHTKFKQLQKDFKSGPEVTKACLECHTEAAKQV
Cphamn1_2426    AETFHHRVDSLMIS-----------TADHTKFDELKKDFQSGPEVTAACLRCHTEASKQL
Paes_2160(Prost AKTFHPPVDSLMVS-----------TADHAKFDELKKDFKSGPEVTEACLRCHTEAAKQI
Ppha_1963       AKPFHQPVDPLIRS-----------TADHSKFQELKKEFKSGPEVTEACLKCYTEAAKQI
Clim_2064       AEPFHHKVDSLLIS-----------TTDHKKFKILQQDFKSGPEVTKACLTCHTEASKQL
Cpha266_2104    AEPFHHKVDSLLIS-----------TTDHKKFKILQQDFKSGPEVTKACLTCHTEASKQL
Dole_3005(Desul ---EPEKAPGIILADQAVKTKDLWITSDHSRHAILQKPFNSGPEVTAACLTCHNQAALQF
Sfum_0090(Syntr KVLDENQAPGRAMAQQATKGREIWITADHSLHPILKKEFKSGPEVTESCLSCHELAAGQF
Dalk_1086       GDGREGPKPPFGNPNSANN------TADHSKFEVLQKEFKSGPEVTKACLSCHNEAAEQF
DVU_3144        AAEVPPGATGLVGKLPEHH-----ITADHSKHPALQQPFASPQEVTKACLSCHNQAALQV
Dvul_0242       AAEVPPGATGLVGKLPEHH-----ITADHSKHPALQQPFASPQEVTKACLSCHNQAALQV
DvMF_1694       ATGVPAGATGAVKKPEAHA-----ITADHSRHPALQQPFATPQEVTKACLSCHNAAAQQV
Hhal_0149(Halor AEDVEPPIPGEEAAAEPGS------TADHSQFSILEGPFETGPEVTEACLQCHTEAAKQV
Maqu_0376(Marin GSASIAPVNGKST-----T------TADHSKFKALQGPFDRAEDVTAACLTCHTEAGEQI
Mmc1_0877(Magne TLHAEISTDGKTDSK---S------TANHSKFKQLEGPFNSGPEVTKACLGCHTEAAKQV
Rfer_3635       PAPAVAGTPAKLQT-----------TADHSKFKILDQDFASGPEVTKACLSCHTEAAKQI
Ctha_2243(Chlor TEHEESDLSLLKEKYSQKYTP----PVKHLEFEILQKPFASPQEVTAACISCHNLRHLEV
GSU2201         -------------------------AKDHPGKEYIQKNGYQGPAT---CEVCHPGAAKEF
Gmet_3088       -------------------------AKDHPGREYMEKNGYKGPET---CEVCHPGKAKEF
Gbem_0758       -------------------------A-EHPGKESIAKSGYKGPET---CEECHPGSAKGF
Gura_3130       -------------------------AKDHPGKEAIEKNGYKGPAT---CEECHPGTAKGF
Adeh_0972       -------------------------AAEHPGRSQIEKDGYKGPST---CEECHPGKAKEF
AnaeK_1034      -------------------------AAEHPGRSQIEKDGYEGPST---CEECHPGKAKEF
Anae109_2593    -------------------------AGEHPGNDVIREKGYQGPST---CEECHPGSAKAF
                                                :         .   *  *:      .
```

```
                     40            50          60                      70
SO4144          MKTSHWTWE-----LEQKLPDR-TVVRGKKNS-INNFC----------------VAISSN
Shewana3_3690   MKTSHWTWE-----LEQKLPDR-TVLRGKKNS-INNFC----------------VSISSN
Shewmr4_3513    MKTSHWTWE-----LEQKLPDR-TVLRGKKNS-INNFC----------------VSISSN
Shewmr7_0439    MKTSHWTWE-----LEQKLPDR-TVLRGKKNS-INNFC----------------VSISSN
Sbal223DRAFT_30 MKTSHWTWE-----LEQKLPDR-TVLRGKKNS-INNFC----------------TSISGN
Sbal195_0477    MKTSHWTWE-----LEQKLPDR-TVLRGKKNS-INNFC----------------TSISGN
Shew185_0458    MKTSHWTWE-----LEQKLPDR-TVLRGKKNS-INNFC----------------TSISGN
Ssed_4060       MKSSHWTWE-----LEQELPGR-TVKRGKKNS-INNFC----------------VAISGN
Shew_0514(S     MKSSHWTWE-----LEQKLPGR-TVKRGKKNA-INNFC----------------TSIAGN
swp_4579        MKSSHWTWE-----LEQKLPGR-TVKRGKKDA-INNFC----------------TSISGN
Sfri_3556       MKSSHWTWE-----LEQKLPDR-TVMRGKKNS-INNFC----------------VSISGN
Sama_3180       MKTSHWSWS-----LTQELPGR-TVERGKKNA-INNFC----------------TSIAGN
Shal_0614       MKSSHWTWE-----LEQTLSGR-TVKRGKKNT-INNFC----------------VAISSN
Cvib_0760       HRTKHWTWE-----VPM-KDGK-ML--GKQHV-VNNFC----------------ISVEGN
Plut_1197       HRTKHWTWE-----VPM-KDGK-ML--GKKNV-VNNFC----------------ISVESN
Cpar_1055       HRTKHWTWE-----VPM-KDGK-ML--GKRHV-VNNFC----------------ISVEGN
Cphamn1_2426    HRTKHWTWE-----VPM-KDGK-ML--GKRNV-VNNFC----------------ISVESN
Paes_2160(Prost HRTKHWTWE-----VPM-KDGK-ML--GKQHV-VNNFC----------------ISVEGN
Ppha_1963       HRTKHWTWE-----VPM-TDGK-ML--GKQHV-VNNFC----------------ISVGGN
Clim_2064       HRTRHWTWD-----VPM-KKGE-RL--GKKNV-VNNFC----------------ISVEGN
Cpha266_2104    HRTRHWTWD-----VPM-KKGE-RL--GKKNV-VNNFC----------------ISVEGN
Dole_3005(Desul HETIHWTWI-----DPATADTL-RF--GKAGMSVNNFC----------------LTILSN
Sfum_0090(Syntr QKTIHWTWL-----DPNVDPKL-RV--GKGGLSMNNFC----------------INIQSN
Dalk_1086       QKTIHWKWL-----CPAAKPEA-KL--GKAGYVVNNFC----------------ININSN
DVU_3144        HKTIHWTWL-----DPA-DPTR-KM--GKGGITFNNFC----------------IAVPSN
Dvul_0242       HKTIHWTWL-----DPA-DPTR-KM--GKGGITFNNFC----------------IAVPSN
DvMF_1694       HKTIHWTWL-----DPA-DPER-KM--GKGGITFNNFC----------------IAIPSN
Hhal_0149(Halor HSSIHWTWT-----YEQPETEQ-TL--GKRYV-LNNLC----------------MGIAGS
Maqu_0376(Marin RQTTHWTWL-----YEHDETGQ-TL--GKSKV-INSFC----------------GMTITN
Mmc1_0877(Magne MKTKHWTWE-----SKQADTGQ-ML--GKKHV-VNSFC----------------GTPKSN
Rfer_3635       HQTQHWKWE-----FINPDTKQ-VL--GKKHV-VNNFC----------------TSVRSN
Ctha_2243(Chlor MKSNHWNWE-----REEYIQGRGVVYIGKHNV-LNNFC----------------IGVRGN
GSU2201         LNSVHWKHASKVDNVENIDPKQ-EY--GMKNR-IYTMCNGNDIVNNLKEIPPSPETGKTK
Gmet_3088       LSTVHWTHASKVDNVENTDPTR-EY--GMKNR-IYTMCNGNDIVNNLKEIPKIPDAKGPK
Gbem_0758       MDTVHWKHASKVTNVDGLDPKK-EY--GMKNR-IYVMCNGNDIVNNLKEIPKSPVTGKSK
Gura_3130       LDSVHWKHASKVSNVEGLDPKK-EY--GMKNR-IYTMCNGNDIVNNLKEIPKSPETGKTK
Adeh_0972       LGTVHWKHASKVDNVDNLDPKQ-EY--GMKNR-IYTMCNGNDIVNNLKEIPKNAD-GKSK
AnaeK_1034      LGTVHWKHASKVDNVENLDPKQ-EY--GMKNR-IYTMCNGNDIVNNLKEIPKNAD-GKSK
Anae109_2593    LATVHWKHASKVTNVDNLDPRQ-EY--GMKNR-IYTFCNGNDIVNDLKEIPQN-ELGKTK
                  : **.                   *     .  :*                    .
```

```
                        80         90        100       110
SO4144           EPRCTSCHAGYGWKD-NTFDFKDKTKVDCLICHDTTGTYVKDPAGAGEPM----------
Shewana3_3690    EPRCTSCHAGYGWKD-SNFDFKDKTKVDCLVCHDTTGTYVKDPAGAGEPM----------
Shewmr4_3513     EPRCTSCHAGYGWKD-SNFDFKDKTKVDCLVCHDTTGTYVKDPAGAGEPM----------
Shewmr7_0439     EPRCTSCHAGYGWKD-SNFDFKDKTKVDCLVCHDTTGTYVKDPAGAGEPM----------
Sbal223DRAFT_30 EPRCTSCHAGYGWKD-NDYDFKDKTKVDCLVCHDTTGTYVKDPAGAGEPM----------
Sbal195_0477     EPRCTSCHAGYGWKD-NDFDFKDKTKVDCLVCHDTTGTYVKDPAGAGEPM----------
Shew185_0458     EPRCTSCHAGYGWKD-NDFDFKDKTKVDCLVCHDTTGTYVKDPAGAGEPM----------
Ssed_4060        EPRCTGCHAGYGWKD-NNFDFTDMTKVDCLVCHDTTGTYVKDPLRAGEVF----------
Shew_0514(S      EPRCTSCHAGYGWKD-NNFDFSDMTKVDCLVCHDTTGTYVKDPAGAGEAL----------
swp_4579         EPRCTSCHAGYGWKD-NNFDFTDMTKVDCLVCHDTTGTYVKDPAGAGEVL----------
Sfri_3556        EPRCTSCHAGYGWKD-STFDFKDMTKVDCLVCHDTTGTYIKDPAGAGEAL----------
Sama_3180        EPRCTSCHAGYGWKD-SSFDFADASKVDCLVCHDTTGTYIKDPAGAGEPL----------
Shal_0614        EPRCTSCHAGYGWKD-NNFDFSDMTKVDCLICHDTTGTYVKDPAGAGEVS----------
Cvib_0760        EPRCTSCHIGYGWKD-KKFDFASQLNVDCLICHDGTGTYQKLPAGAGHPA-YQTTVQ-E-
Plut_1197        EARCTSCHVGYGWKD-KQFDFRSEQNVDCLICHDGTGTYQKLPAGAGHPA-YEATVQ-E-
Cpar_1055        EPRCTSCHVGYGWKD-NSFDFASQEQVDCLVCHDGTATYKKLPPGAGHPA-YKETKV-E-
Cphamn1_2426     EARCTSCHIGYGWKD-RNFDFTSEKNVDCLVCHDATGTYKKYPSGAGHPS-IIDTVF-S-
Paes_2160(Prost EARCTSCHIGYGWKD-QKFDFASERNVDCLVCHDGTGTYKKYPSGAGHPA-YVDTVF-G-
Ppha_1963        EPRCTSCHIGYNWKD-KQFDFTSEKNVDCIVCHDGTGTYKKLPAGAGHPA-YTSTTF-E-
Clim_2064        EPRCTSCHIGYDWKD-KNFNFKSEENVDCLACHDMTGTYKKLPAGAGHPA-YQTTVF-E-
Cpha266_2104     EPRCTSCHIGYDWKD-KNFNFKSEENVDCLACHDMTGTYKKLPAGAGHPA-YFDTVF-E-
Dole_3005(Desul EPRCTSCHAGYGWKD-KNFDFSSQVNVDCLVCHEQTGTYEKFPAGSGHPA-AKETFF-AG
Sfum_0090(Syntr EPRCTSCHAGYGWKD-KTFDFSNAHSVDCLACHEQTGTYHKFPTGAGNPV-SEPTVF-KE
Dalk_1086        EPRCTSCHAGYGYKD-KNFDFSVQENVDCLVCHEQTGTYKKFPPGAGYVV-KEPTMF-G-
DVU_3144         EPRCTSCHAGYGWKD-KNFDFSAQENVDCLVCHDRTGTYKKFPTMAGMPV-SEPTKF-G-
Dvul_0242        EPRCTSCHAGYGWKD-KNFDFSAQENVDCLVCHDRTGTYKKFPTMAGMPV-SEPTKF-G-
DvMF_1694        EPRCTSCHAGFGWKN-AQFDFSSQENVDCMVCHDHTGTYKKFPTMAGLPV-SEPTEF-E-
Hhal_0149(Halor YERCSSCHVGYGWED-RDFDFTAEEKVDCLVCHDTTGDYVKFPTAAGHPP-YEDTEF---
Maqu_0376(Marin EPRCTSCHVGYGWNDMREPPPQAENAVDCLVCHDTTGEYWKFPTLAGHPT-YIPREWPKG
Mmc1_0877(Magne WAACTACHAGYGWQD-NDFDFTKQENVDCLVCHDHSGQYEKSVGGAGHPKGFESPEHKKY
Rfer_3635        EAACNSCHIGYGWKD-AKFDFTVEENVDCLACHDHTGKYTKPSGFAGNPV-ARDTEFPAG
Ctha_2243(Chlor EPKCAKCHIGYGSTT-DGLAIESAKNVDCLVCHDNTETYVKADEQGGAPE----------
GSU2201          YSGCNSCHPGNHIQDVGSTGPEAEAAVDCLVCHSSTYDHSKRKPFKDEKG----------
Gmet_3088        FSGCNTCHPGNHVSDVGSTGPEAEAAIDCLLCHSREYDYSKRKPFKDDQG----------
Gbem_0758        FTGCNTCHPGNHLSDVGSTGPEAEAAVDCLVCHSTDYDFRQRKASKNEKG----------
Gura_3130        FTGCNTCHPGNHLSDVGSTGEAAENAIDCLVCHSTDYDFRKRKPYKDEKG----------
Adeh_0972        FTGCNTCHPGNHLNDVGSTGPEAEAAVDCLVCHSTEYDFRQRKPYRDEQG----------
AnaeK_1034       FTGCNTCHPGNHLNDVGSTGPEAEAAVDCLVCHSTEYDFRQRKPYKDEQG----------
Anae109_2593     LTGCNSCHPGNHLSDVGSTGPDAEAAIDCLVCHSSKYDYSKRKPFKTADG----------
                    *  ** *               :**: **.    . :
```

```
                120               130       140       150       160       170
SO4144           -AKL--------DLAKIAQNVGAPVRDNCGSCHFYGGGGDAVKHGDLDSSMAYPDKATDV
Shewana3_3690    -AKL--------DLAKIAQNVGEPVRDNCGSCHFYGGGGDAVKHGDLDSSMAYPDKATDV
Shewmr4_3513     -AKL--------DLAKIAQNVGDPVRDNCGSCHFYGGGGDAVKHGDLDSSMAYPDKATDV
Shewmr7_0439     -AKL--------DLAKIAQNVGEPVRDNCGSCHFYGGGGDAVKHGDLDSSMAYPDKATDV
Sbal223DRAFT_30 -AKL--------DLAKIAQNVGKPVRDNCGSCHFYGGGGDAVKHGDLDSSMSYPDKATDV
Sbal195_0477     -AKL--------DLAKIAQNVGKPVRDNCGSCHFYGGGGDAVKHGDLDSSMSYPDKATDV
Shew185_0458     -AKL--------DLAKIAQNVGKPVRDNCGSCHFYGGGGDAVKHGDLDSSMSYPDKATDV
Ssed_4060        -ASV--------NLEKVAQNVGAPVRDNCGSCHFYGGGGDGVKHGDLDSSMSYPDKATDV
Shew_0514(S      -AKV--------NLERVAQNVGMPVRDNCGSCHFYGGGGDAVKHGDLDSSMAYPDKATDV
swp_4579         -AKV--------NLERVAKNVGAPVRDNCGTCHFFGGGGDAVKHGDLDSSMSYPDKATDV
Sfri_3556        -ARV--------NLANVAQNVGAPVRDNCGSCHFYGGGGDAVKHGDLDSSMSYPDKATDV
Sama_3180        -AKV--------DLEKVAKNVGKPVRDNCGSCHFYGGGGDAVKHGDLDSSMAYPDKATDV
Shal_0614        -SKV--------NLERVAKNVGTPVRDNCGTCHFYGGGGDGVKHGDLDSSMAYPDKRTDV
Cvib_0760        -KKTYKKV----NLSNIARHVQNPDRHNCGTCHFEGGGADAVKHGDLDNSLLKPDRSLDI
Plut_1197        -KKKYPKV----NLSYVARNVQNPDRQNCGICHFEGGGADAVKHGDLDGSLIKGPRSLDV
Cpar_1055        -GKVWPKV----DLAYVAQHIQNPDRHNCGQCHFEGGGADAVKHGDLDNSMVHPSESLDV
Cphamn1_2426     -GKPFPKS----DLTYIAQHVGNPERHNCGICHFEGGGADAVKHGDLDNSLIDPSESIDV
Paes_2160(Prost -KTPYPKV----DLAYVAQNVANPNRHNCGICHFEGGGADAVKHGDLDNSLIEPAPHVDV
Ppha_1963        -NKLYPKV----DLSHIAQHVQNPDRHNCGVCHFEGGGADAVKHGDLDNSLIKPDKSVDV
Clim_2064        -KKTFPKV----DLSFVAQRVGHPDRHNCGICHFEGGGADAVKHGDLDNSLLKPDRELDV
Cpha266_2104     -KKLYPKV----NLSYVAQRVGQPDRHNCGICHFEGGGADAVKHGDLDNSLLKPDRELDV
Dole_3005(Desul EGKTYYPP----DWNIVAQSVGRPTRENCGVCHFYGGGGDGVKHGDLDSSMTFPNKALDV
Sfum_0090(Syntr DGKTYMPP----EWNKVAQSVGRPTRQNCGTCHFFGGGGDGVKHGDMDSSLMKPNKELDV
Dalk_1086        -GKEWLPP----DFAKVAQSVALPTRKNCGTCHFYGGGGEGVKHGDLDASLYKPKWDLDV
DVU_3144         -EEQFDPP----DYNAVAAAVGRPTRDNCGNCHFYGGGGDAVKHGDLDSSLHTPKREIDV
Dvul_0242        -EEQFDPP----DYNAVAAAVGRPTRDNCGNCHFYGGGGDAVKHGDLDSSLHTPKREIDV
DvMF_1694        -GKTFNPP----DYNTIAASVGRPTRDNCGTCHFYGGGGDAVKHGDLDSTMFKPSRELDV
Hhal_0149(Halor RGTLFEAP----DLAHVARNVGDTSRATCGSCHFEGGGGNAVKHGDLDSSLLDPPRSVDV
Maqu_0376(Marin SGKMVQPP----DLERIARNVGASGRANCGSCHFHGGGADGVKHGDLDTSLINPPKSLDV
Mmc1_0877(Magne LDDQAKAPRDAVDLVAAAQSVGRPSRRNCGSCHFVGGGDDGVKHGDMDTSLIEPDEFLDV
Rfer_3635        SGKIIKGI----NLKEIAQKVGPTTRNTCGACHFKGGGGDGVKHGDLDSSLENPDKALDV
Ctha_2243(Chlor -KSL--------NLNLIAQSVGRPTRANCGICHFYGGGGNNVKHGDLESALFEPTKALDV
GSU2201          -NVVLGQD----RSTDAALSIATPTVKNCMTCHEAAGGGVLVKRG------FAFNKEHDV
Gmet_3088        -RVVLGQD----RSVKAALAIAKPTVKNCMTCHEAAGGGVLVKRG------FAFTKENDV
Gbem_0758        -QVVMGQD----RSTKAALAIGKPTVKNCMVCHEAAGGGVIVKRG------FTFNKETDA
Gura_3130        -QIVMGQD----RSTKAALAISKPTVKNCMVCHEAAGGGVLVKRG------FAFTAETDA
Adeh_0972        -RVVMGQD----RSTKAALAIGKPTVKNCMTCHETAGGGVLVKRG------FSFTKDTDA
AnaeK_1034       -RVVMGQD----RSTKAALAIGKPTVKNCMTCHETAGGGVLVKRG------FSFTKDTDA
Anae109_2593     -KVAIGQD----RSKEAALAVGKPTVKACMTCHETAGGGQLIKRG------FAFDAEHDV
                                 *  :  .    *  **  .**   :*:*            *
```

```
                        180       190                   200       210
SO4144           HM--DSDGNNFQCQNCHTTEKHQISGNAM------------GVSPGGIDHIGCE--NCH
Shewana3_3690    HM--DSDGNNFQCQNCHTTEKHQISGNAM------------GVSPGGIDHIGCE--NCH
Shewmr4_3513     HM--DSDGNNFQCQNCHTTEKHQISGNAM------------GVSPGGIDHIGCE--NCH
Shewmr7_0439     HM--DSDGNNFQCQNCHTTEKHQISGNAM------------GVSPGGIDHIGCE--NCH
Sbal223DRAFT_30  HM--DSDGNDFQCQNCHTTEKHQISGNAM------------GVSPGGIDHIGCE--NCH
Sbal195_0477     HM--DSDGNDFQCQNCHTTEKHQISGNAM------------GVSPGGIDHIGCE--NCH
Shew185_0458     HM--DSDGNDFQCQNCHTTEKHQISGNAM------------GVSPGGIDHIGCE--NCH
Ssed_4060        HM--DTDGNDFQCQACHTTEQHQITGNAM------------GVSPGGIDHIGCE--NCH
Shew_0514(S      HM--DSDGNDFQCQTCHTTQQHQITGNAM------------GVSPGGENDIGCE--NCH
swp_4579         HM--DTDGNDFQCQTCHTTEAHQITGNAM------------GVSPGGQNPIGCV--NCH
Sfri_3556        HM--DTDGNDFQCQTCHVTENHQITGNSM------------GVSPGGENKIGCV--NCH
Sama_3180        HM--DADGNDFQCQACHTTESHAISGNAM------------GVSPGGIDHIGCE--NCH
Shal_0614        HM--DVDGNDFPCQECHTTKEHQITGNAM------------GVSPGGDNPIGCN--NCH
Cvib_0760        HMASGKGELNMTCTDCHKTEGHQVPGSRY-EPTAADKHGFDYPLPDD--FPTTCS--SCH
Plut_1197        HMATGKNELNMTCVDCHKTEGHQVPGSRY-TPMARDTHGFDYPLADD--FPTSCA--SCH
Cpar_1055        HMASGKDQLNMTCIDCHKTTGHQVPGSRY-TPHASDAHGFDYPLPDD--FPATCS--SCH
Cphamn1_2426     HMASGKDELNMTCIDCHKTEGHQVPGSRY-EPTARDVHGFDYPLPDD--YPTTCG--SCH
Paes_2160(Prost  HMAVGEDGLNMTCIDCHQTKGHQVPGSRY-EPTARDVHGFDYPMPDD--YPTTCS--SCH
Ppha_1963        HMATGKGELDMTCIDCHKTKGHQVPGSRY-EPTARDMHGFDYPLPDD--YPTTCI--SCH
Clim_2064        HMAIGKKELNMTCADCHKTEGHQVPGSRY-TPEAHDTHGFDYPLADN--NPATCS--SCH
Cpha266_2104     HMAIGKKDLNMTCADCHKTEGHQVPGSRY-TPEAHDTHGFDYPLTDN--NPATCS--SCH
Dole_3005(Desul  HM--GTDGQNFDCSRCHSTTLHNIAGRVYATPAAEDRKTL---IEDDLATKITCE--SCH
Sfum_0090(Syntr  HM--GTDGQNFDCVRCHTTRVHHIAGRIYSTPAAKGRKSL---IEDDLTPKIMCE--SCH
Dalk_1086        HM--NVDGENFTCTRCHTTVQHAVAGRCYKSTPLTDRRSL---LDSDLIHRITCY--SCH
DVU_3144         HM--DVKGANFTCQRCHTTDVHFIAGRTYKEPAFTERKSL---VQDDQVKRIACE--SCH
Dvul_0242        HM--DVKGANFTCQRCHTTDVHFIAGRTYKEPAFTERKSL---VQDDQVKRIACE--SCH
DvMF_1694        HM--DVKGANFTCQRCHTTEAHVIAGRTYKQPAFTERKSV---LDDDRVHRIACE--SCH
Hhal_0149(Halor  HM--TPDGADFSCSNCHEFTGHIQSGSRY-HLTMPDTDDAPVPARPQ--DKPACV--ACH
Maqu_0376(Marin  HM--SPEGLNFGCSDCHTTMGHAVSGSRY-QANARDTLGIDVPGHTDF-SRASCE--SCH
Mmc1_0877(Magne  HM--DVNGKNFSCTACHRTHGHVIPGSRY-KSTAKDTKGVETPSEAH--SRTSCE--SCH
Rfer_3635        HM--DTKGLNFSCATCHKTDDHKVSGSRY-APTAKDKAPAHMRGEADKTSPDTCQ--ACH
Ctha_2243(Chlor  HM--GTDGSNLSCVDCHTTKEHNISGKMY------------SLSSMNHNRVTCD--QCH
GSU2201          HA-----AKGMVCVDCHKTKNHKIPTGYDPNNWAHDG------------VRLSCT--DCH
Gmet_3088        HA-----AKGMVCVDCHKAKNHKIPTGFDPNNWAHDG------------VRVACT--DCH
Gbem_0758        HA-----AKGMVCVDCHKAKNHKMPTGHDPNNWANDN------------VFISCSDTSCH
Gura_3130        HA-----AKGMVCVDCHTAKNHKIPTGYDPNNWANDG------------VRISCADTACH
Adeh_0972        HA-----AKGMVCVDCHQAKDHRIPTGFDPNNWANDG------------LRLSCD--GCH
AnaeK_1034       HA-----AKGMVCVDCHQAKDHRIPTGFDPNNWANDG------------LRLSCD--GCH
Anae109_2593     HA-----AKGMTCADCHKAKDHKIPTGFDPNNWANDG------------VRIGCA--DCH
                 *        .: *  **    *  .                        *    **
```

```
                      220       230       240       250       260
SO4144           DSAPHS---NKKLNTHTATVACQTCHIPFFAK-NEPTKMQWDWSTAGDDKPE-----TVD
Shewana3_3690    DSAPHS---NKKLNTHTATVACQTCHIPFFAK-NEPTKMHWDWSTAGDDKPE-----TVD
Shewmr4_3513     ESAPHS---NKKLNTHTATVACQTCHIPFFAK-NEPTKMRWDWSTAGDDKPE-----TVD
Shewmr7_0439     ESAPHS---NKKLNTHTATVACQTCHIPFFAK-NEPTKMHWDWSTAGDDKPE-----TVD
Sbal223DRAFT_30 DSAPHS---NKKLNTHTATVACQTCHIPYFAK-NEPTKMRWDWSTAGEDKPE-----AVD
Sbal195_0477     DSAPHS---NKKLNTHTATVACQTCHIPYFAK-NEPTKMRWDWSTAGEDKPE-----AVD
Shew185_0458     DSAPHS---NKKLNTHTATVACQTCHIPYFAK-NEPTKMRWDWSTAGEDKPE-----VVD
Ssed_4060        DSAPHK---NKRLNTHTATVACQTCHIPFFAK-NEPTKVSWDWSTAGQDKKG-----TVD
Shew_0514(S      DSAPHA---NKRLNTHTASVACQTCHIPFFAR-NEPTKMSWDWSTAGSDQEE-----TVD
swp_4579         YATPHK---NKKLNTHSASVACQTCHIPFFAR-NEATKMSWDWSTAGSDLEE-----TKD
Sfri_3556        DAAPHK---NKKLNTHTATVACQTCHIPSFAK-NEPTKMHWDWSQAGQDLPE-----TTD
Sama_3180        EGAPHK---NKKINEHTATVACQTCHIPFFAR-NEATKMSWDWSTAGQDREE-----TLD
Shal_0614        DSAPHE---KQKLNDHGQAIACQTCHIPEFAK-NEPTKMNWDWSTAGSSREQ-----TVD
Cvib_0760        GNTPHTT--NKKLNDHIDKVACQTCHIPQIAK-ERATKMWWDWSKAGKFDEKGKMIVKKD
Plut_1197        SLEPHRK--NKKLNDHIDKVACQTCHIPHIAK-ERPTKMWWDWSKAGKFDEKGKMITKKD
Cpar_1055        GLEPHKK--NKKLNDHIARVACQTCHIPYIAK-ERATKMWWDWSKAGIKDKEGKEITKKD
Cphamn1_2426     GLKPHEK--FKKLDDHIDKVACQTCHIPVMAK-ERATKMWWDWSKAGQFDDKGKEITRKD
Paes_2160(Prost GLKPHKQ--YSKLNDHVDKLACQTCHIPVMAK-ERPTKMWWDWSKAGKLNSKGGEITRKD
Ppha_1963        GLKPHKK--LKKLNDHIDKVACQTCHIPTIAK-KRATKMWWDWSQAGKFDKEGKEITRVD
Clim_2064        GLKPHKK--LKKLNDHVARVACQTCHIPFIAK-ERPTKMWWDWSKAGKFDKNGKEITIKD
Cpha266_2104     GLKPHKK--LKKLNDHVARVACQTCHIPFIAK-QRPTKMWWDWSKAGKFDKNGKEITIKD
Dole_3005(Desul SSRPHKA--GTKPNDHADKVACQSCHIPTFAR-VNPTKTWWDWSKAGTKK-DGKPYKEVD
Sfum_0090(Syntr SRTPHKP--GVKANAHTDKVACQSCHISTYAR-VNPTTMWWDWSKAGQMK-EGKPYKELD
Dalk_1086        SEKPHKT--DAKLNDHTDKVSCQACHIPEFAR-EHSTKMSWDWSTAGKKNAKGKPLV-IE
DVU_3144         TATPHKA--GHKANDHTDKVACQTCHIPAYAR-AIPTKMWWDWSTAGKKK-DGKNYKEKG
Dvul_0242        TATPHKA--GHKANDHTDKVACQTCHIPAYAR-AIPTKMWWDWSTAGKKK-DGKNYKEKG
DvMF_1694        TATPHRA--GHKANDHTDKLACQTCHIPAFAR-EMATKMWWDWSTAGKKK-DGKPFAEKG
Hhal_0149(Halor GSEPHEGRIHDKLNAHGEFIACQTCHVPEIARGGYPTKTLWDWSEAGRLDDDGQPIVEKD
Maqu_0376(Marin GLAPHD---KPKLNDHVDKLACQTCHIPAFARGGVPTKTWWDWSTAGRLDENGQPIKQLD
Mmc1_0877(Magne GSEVKKH--SAKLNDHVDKVACQTCHIPKIARGGVKTKMVWDWSTAGKLDENGKPISERN
Rfer_3635        GQAPHQ---IVRLNEHTAKIACQTCHIPAFARGGVPTKMSWDWSTAGKLDKDGKFQTIRD
Ctha_2243(Chlor GETPHD---KDILNEHTLKVACQTCHIPIYAK-EHATKIYWDWSTAGKLK-NGEPYEEED
GSU2201          TAKPHK---DEDYNRHTARIACQTCHIP---------------RTGGAFAKDFTKWEQ-L
Gmet_3088        TETPHK---DAEYNRHTARIACQTCHVT---------------RTGGAFAKDFTKWEK-L
Gbem_0758        GAKPHK---DADLNRHSAKIACQTCHIP---------------RTGGAFAKDFTVWEQ-T
Gura_3130        GNKPHK---DADLNRHTARIACQTCHIP---------------RTGGAFAKDFTKWEQ-S
Adeh_0972        GDKPHK---SADYNRHTARIACQTCHIP---------------RTGGAVAKDFTVWEK-G
AnaeK_1034       GEKPHK---SADYNRHTARIACQTCHIP---------------RTGGAVAKDFTVWEK-G
Anae109_2593     GAKPHK---DADYDAHTAKLACQTCHIP---------------TSGGAVAKDFTKWAKDE
                     :        : *   ::**:**:.                .*
```

```
                   270       280       290       300       310       320
SO4144           QYGKHTYQKKKGNFVWEKMVKPQYAWYNGTANAYMAGDKM-DSN-VVTKLTYPMGDINDA
Shewana3_3690    QYGKHTYQKKKGDFVWEKMVKPQYAWYNGTANAYMAGDKM-DPN-VVTKLTYPMGDINDA
Shewmr4_3513     QYGKHTYQKKKGDFVWEKMVKPQYAWYNGTANAYMAGDKM-DPN-VVTKLTYPMGDINDA
Shewmr7_0439     QYGKHTYQKKKGDFVWEKMVKPQYAWYNGTANAYMAGDKM-DPK-VVTKLTYPMGDINDA
Sbal223DRAFT_30 QYGKHTYQKKKGNFVWEKMVKPQYAWYNGTANAYMTGDKM-DPN-AITKLTYPIGDINDA
Sbal195_0477     QYGKHTYQKKKGNFVWEKMVKPQYAWYNGTANAYMTGDKM-DPN-AITKLTYPIGDINDA
Shew185_0458     QYGKHSYQKKKGNFVWEKMVKPQYAWYNGTANAYMTGDKM-DPN-AITKLTYPIGDINDA
Ssed_4060        ANGKHTYKKKKGSFVWEKMITPSYAWFNGKADAYMPGDKM-DPT-KVTKLAYPLGDIKDP
Shew_0514(S      EYGKHTFMKKKGSFVWGKMVKPEYAWYNGKADAYMVGDKM-DPS-KVTKLTAPLGDITDK
swp_4579         KYGKKSYQKKKGNFVWGKMVEPEYAWYNGNADAYMVGDKM-DPT-KVTKLTSPLGDINDS
Sfri_3556        QYGKHTFMKKKGSFIWQKDVKPQYAWFNGRADAYMAGDKM-DPT-KTVKLAYPLGDIRDP
Sama_3180        EYGRKTFQKKKGSFTWGKMVKPAYAWYNGKAGAYMAGDPI-KAD-EVTRLSYPLGDIQDA
Shal_0614        EYGKHSYMKKKGDFVWAKNVTPQYAWYNGKADAYMAGDKM-QAD-SVTKLTYPLGDINDL
Cvib_0760        STGLPTYITKKGEFRWEKNMEPEYRWFNGQMNYTTFLTTF-DDR-GIVQINHPDGKAGDT
Plut_1197        AAGMPTYVTKKGEFRWEKNARPEYRWFNGEMNYVTFHTTI-NDK-GVVSVNRPSGMTGDT
Cpar_1055        STGMPSYVTKKGEFKWAKNVAPEYRWFNGNMNQITFMNTI-DDK-KVVQINHPDGSCADS
Cphamn1_2426     STGLPVYMTKKGEFEWAKEVEPEYRWFKGEMNYVTFLSEI-DDS-GVVSINHPDGEPGDS
Paes_2160(Prost SSGLPLYMSKKGEFEWAKEVVPEYRWFNGEMNYVTFMTEI-NDS-GVVAINHPDGEPGDT
Ppha_1963        ASGIPLYISKKGEFKWSKNIEPEYRWFNGKMNYVTFLTKI-NDS-TVVAINHPDGHPGDT
Clim_2064        SSGCILYVSKKGEFRWAKNVAPEYSWFNGEMNYTTFKTII-DDR-KIVSVNHPDGAANDP
Cpha266_2104     SSGCVLYVSKKGAFRWAKNVAPEYRWFNGEMNYTTFNTQI-NDR-KVVSVNHPDGAANDT
Dole_3005(Desul ELGKPSYMTIKGEMRWEKNVKPEYFWYNGSMSYLTLEDTI-DPA-QPVWITKPAGSPNDP
Sfum_0090(Syntr EFGKPGYDTKKGEFKWARNVVPEYYWFNGSLTTLTARDTI-DPS-GVVAVGWPNGDKNDA
Dalk_1086        KDGRHSYNGMKGDFVWKKNVVPEYKWFNGKLTYLTLTDKI-DPAQQPIEINKAHGSYDDP
DVU_3144         PLGKPVYDTQKGDFRWEQNVVPEYKWYGGRMDYLLLTDKV-DPA-KPVEINRVIGSPDDP
Dvul_0242        PLGKPVYDTQKGDFRWEQNVVPEYKWYGGRMDYLLLTDKV-DPA-KPVEINRVIGSPDDP
DvMF_1694        PFGKPSYDSKKGDFRWEKDVTPEYHWSNGRMEFLLLTDKVDDTA-KPVEINRIDGDPADP
Hhal_0149(Halor DEGRVVYDGMKGVFEWDEDYPPDYRWFDGNMVYTLPDDTI-DPDD-EVPVNRPQGQPGEE
Maqu_0376(Marin DHGHPSYLSEKGDFRHGENVVPEYAWFDGTVKYTLAGDPL-DIENPPVAINRVEGSPDNG
Mmc1_0877(Magne SAGEITYSSKKGHFEWAEDVQPEYRWFDGQVRYTLFGDKV-DDSK-PVQINGIHGSYTDN
Rfer_3635        ENDYDTYMTIKGDFKWAENVTPEYVWFNGTNKYTLITDKI-EKGDKPVQINGFEGSATDG
Ctha_2243(Chlor SLGNHTYLSIKGSFVWQKNLQPEYFWFNGTASHYISGDVISDTS-KPVVLNELHGSYRDP
GSU2201          SNKFYEPTTLKKE---ANETAPVYAWYNLTVA-------------NRPDFIGPKGDRKDG
Gmet_3088        SSGYYEPTTLRKD---ANETVPVYAWYDKTVA-------------NRPDFIGPKGSRSDK
Gbem_0758        PDKFYEPTTLKKE---ANETTPVYAWYNGTVK-------------NTPHFIGPKGSRKDG
Gura_3130        PDKFYEPTTLKKE---ANETVPVYAWYNNTVK-------------NTPTFIGPKGNRKDK
Adeh_0972        GDGFYEPTTLKKD---ANETVPVYAWYDHTVR-------------NEPHFIGPKGSRKDA
AnaeK_1034       GDGFYEPTTLKKD---ANETVPVYAWYDRKVR-------------NEPHFIGPKGSRKDA
Anae109_2593     STGFYEPSTIRRD---PAGTKPVYAWFNGNVR-------------NEPHLIGPKGSRSDP
                           :          * * *                        .    *   :
```

```
                      330       340       350             360       370
SO4144           KAKIYPFKVHTGKQIYDKKLNIFITPKTY------GKGGYWSEFDWNLAAKLGMEANPTM
Shewana3_3690    KAKIYPFKVHTGKQIYDKKLNIFITPKTY------GKGGYWSEFDWNLAAKLGMEANPTM
Shewmr4_3513     KAKIYPFKVHTGKQIYDKKLNIFITPKTY------GKGGYWSEFDWNLAAKLGMEANTTM
Shewmr7_0439     KAKIYPFKVHTGKQIYDKKLNIFITPKTY------GKGGYWSEFDWNLAAKLGMEANTTM
Sbal223DRAFT_30 KAKIYPFKVHTGKQIYDKKLNIFVTAKVY------GKGGYWNDFDWNLAAKLGMEANPTM
Sbal195_0477     KAKIYPFKVHTGKQIYDKKLNVFVTAKVY------GKGGYWNDFDWNLAAKLGMEANPTM
Shew185_0458     KAKIYPFKVHTGKQIYDKKLNIFVTAKVY------GKGGYWSDFDWGLAAKLGMEANPTM
Ssed_4060        KAKIYPFKVHTGKQIYDKKLNIFISPKTF------GEGGYWSEFDWDLAAKLGMEANATM
Shew_0514(S      TAKIYPFKVHRGKQIYDKKQNIFVTAKVY------GKGGYWKEFDWDKAAKLGMEANQAL
swp_4579         TAKIYPFKVHRGKQIYDSKQNIFVTAKVY------GKGGYWKDYDWDKAAKLGMEANQVL
Sfri_3556        KAKIYPFKVHTGKQIYDAKLNILITPKTY------GEGGYWDKFDWDLAAKLGMEANPTM
Sama_3180        GAKIYPFKVHTGKQIYDKKHNILATAKTY------GAGGYWTEFDWDKAAKLGMEANPTL
Shal_0614        HAKITPFKVHTGKQIYDKKLNIFITPKVF------GKGGYWKTFDWDEAARLGMEQNPNM
Cvib_0760        LSRIWPFKVHRGKQPYDTQLKRFVKPKLY--GP-KGSGAYWSDFSWDKSISAGMTNA---
Plut_1197        LSRIWPFKVHRGLQPYDTELKHFVKPKLF--GP-KGSGAYWSDFDWKRSIEAGMRES---
Cpar_1055        RSRIWPFKVHRGKQPYDAELKRFVKPKLF--GP-KGSGAYWSDFDWGKSIEVGMKNA---
Cphamn1_2426     LSRIWPFKVHRGKQPYDAGLKRFVKPKLF--GP-KGSGAYWKDFDWDKSIKTGMEYA---
Paes_2160(Prost LSRIWPFKVHRGKQPYDRELKRFVKPKLF--GP-KGSGAYWKDFNWDKSIAEGMDYA---
Ppha_1963        LSRIWPFKVHRGKQPYDPVLKQFVKPLLY--GE-KGSGAYWSDFNWGTAIQKGMEYA---
Clim_2064        LSRIWPFKVHRGMQPYDPVLKRFVKPIVY--GP-KGSGAYWSDFNWDKSIRKGMENA---
Cpha266_2104     LSRIWPFKVHRGMQPYDPVLKRFVKPIVY--GP-KGSGAYWSDFNWDKSIRKGMENA---
Dole_3005(Desul KSRIFPFKIHAGKQPYDKISKRLVGIHLFPLGP-EDPAAYWKYFDWNKAIAYGMEYA---
Sfum_0090(Syntr NARIFPFKVHRGRQPYDKVNKTLVIPRLF--GK-EGTGAYWADYDWDKSAAAGMAYA---
Dalk_1086        DARIFPFKVHKGKQPFDKVNNTFVVPHLF---G-KDKNAYWKGYNWANAIQTGMDYT---
DVU_3144         NARIMPFKVHRGKQPFDPELKTFVVPHLF---G-KDDAAYWKTYDWAKAIEAGQKAV---
Dvul_0242        NARIMPFKVHRGKQPFDPELKTFVVPHLF---G-KDDAAYWKTYDWAKAIEAGQKAV---
DvMF_1694        RSRIMPFKAHRGRQPFDAGNRTFVAPHLF---G-KDDDAYWKTYDWMKAVEAGQKSL---
Hhal_0149(Halor GAKIWPFKIMYGQQLYDAEHHTLLVPQLF--GKEGDENAYWQNYDWDRAIEAGMEEARAV
Maqu_0376(Marin ESRIWPFKVMRGKQPFDTERQTLLATHVF--G--ADDTSLWSNFSWEKALQA------AS
Mmc1_0877(Magne QSRIWPFKIMKGKQVYDPVEKHLLVMHTY--G--DDDSSFWSNFDWKKSLEAGAKEPEAP
Rfer_3635        KSMIWPIKLFRGKQQYDPINKSLVITHLA----GNDDTAFWKNLDWVKAVTEGMAKG---
Ctha_2243(Chlor ASKIIPVKRHRALQPYDPVTKLLIQPKLF--STRKGDGAFWQEFDFQKAAAAGMKAL---
GSU2201          KSKIYPFKIFQGKAYFNKKDGQLL------------------SMDFAPPMATGDTLA---
Gmet_3088        ASRIYPFKVFQGKGFFDRKTGKLL------------------SMDFAPPMANGDTLA---
Gbem_0758        KSKISPFKIFQGKAFYNKQTGELL------------------SMDFAQPMSNGDTRA---
Gura_3130        TSKIYPFKIFQGKAFFDKKTGKLM------------------SMDFAPPMATGDTLA---
Adeh_0972        KSKIYPFKIYMGKAFYDAKTGKLL------------------SMDFAPPMATGDTRA---
AnaeK_1034       KSKIYPFKIYMGKAFYDAKSGKLL------------------SMDFAPPMANGDTRA---
Anae109_2593     KSKIFPFKIYEGRAYYDRRTGKLL------------------SMDFAQPTATGDTLA---
                  : * *.*   .   ::    :                    .:  .
```

```
                 380       390                   400       410       420
SO4144           LEKGIKYSGEYDFAAT------------EMWWRINHMVSPKEQALNCNDCH-NKGTRLD
Shewana3_3690    LEKGIKYSGEYDFAAT------------EMWWRINHMVSPKEQALNCNDCH-NKGTRLD
Shewmr4_3513     TEKGIKYSGEYGFAAT------------EMWWRINHMVSPKEQALNCNDCH-NKGTHLD
Shewmr7_0439     TEKGIKYSGEYGFAAT------------EMWWRINHMVSPKEQALNCNDCH-NKGTRLD
Sbal223DRAFT_30 VEKGLKYSGEYGFAET------------EMWWRINHMVSPKAQALNCNDCH-NKGSRLD
Sbal195_0477     VEKGLKYSGEYGFAET------------EMWWRINHMVSPKAQALNCNDCH-NKGSRLD
Shew185_0458     VEKGLKYSGEYGFAET------------EMWWRINHMVSPKAQALNCNDCH-NKGSRLD
Ssed_4060        VDKGLKYSGEHGFAAT------------EMWWRINHMVSPKEESLKCNDCH-KKGTRMN
Shew_0514(S      AQQGIKYSGEHGFAET------------EMWWRINHMVSPKDQALKCNDCH-NKGTRLD
swp_4579         AEKGITYSGEHGFAAT------------EMWWRINHMVSPKAAALKCGDCH-NKGTRMN
Sfri_3556        VEKGLKYSGQHGFVET------------EMWWRINHMVSPKDKALQCNDCH-NKGERLD
Sama_3180        KAKGIAYSGEYGFAPT------------EMWWRINHMVSKKEEALKCNACH-NGGDRLD
Shal_0614        VDKGIKYSGEYGFAAT------------EMWWPINHMVSPKEDALKCKDCH-SQQGRLD
Cvib_0760        ---GLKYSGKYDFIET------------EMYWPISHMVSPKEDAMGCVECH-AHGGRLE
Plut_1197        ---GLKYSGSYGFVET------------EMFWPISHMVSPKEDALGCVECH-ARGGRLE
Cpar_1055        ---GMDYSGKYGFVET------------EMYWPINHMVAPKEDALACAECH-ARHGRLD
Cphamn1_2426     ---GLKYSGNYGFVET------------EMYWPISHMVSQKEDALGCVDCH-ARGGRLE
Paes_2160(Prost ---GMQYSGKYGFVET------------EMYWPISHMVSPKDEALSCVECH-SRNGRLQ
Ppha_1963        ---NLKYSGTYGFVET------------EMSWPISHMVSPKEDAMSCAECH-SRNGRLE
Clim_2064        ---GLEYSGKYAFVET------------EMYWPISHMVSPKEKSLSCRECH-SRSGRLQ
Cpha266_2104     ---GLEYSGKYAFVET------------EMYWPISHMVSPKEKSLSCKECH-SRNGRLQ
Dole_3005(Desul ---GLPYSGEFDFVET------------KYLYPITHMVAPKDNVVTCIECHTAQESRMA
Sfum_0090(Syntr ---GLPFSGELGFVDS------------TYVFPITHMVAPKDKAVQCQECH-SKNGRLR
Dalk_1086        ---GLPYSGEFDFIST------------EYMYQTTHMVAPKEKALSCDACH-APQGRLA
DVU_3144         ---GLPWSGKYTFVET------------AYHYPITHMVAPKEKALQCADCHSPAG-RLA
Dvul_0242        ---GLPWSGKYTFVET------------AYHYPITHMVAPKEKALQCADCHSPAG-RLA
DvMF_1694        ---NLPFSGKLEFVDT------------VYYYPITHQVAPKERSVACGECHKPAGSRLA
Hhal_0149(Halor GQTEMVYSGEYGFVET------------RMYWPVNHMVAPAEESVACVDCH-SRDGRMA
Maqu_0376(Marin DLSGMPYSGEFSFIET------------TMHWPITHMVAPAEQAVKCGSCH-KAESRLA
Mmc1_0877(Magne -----PFNGQYAFVNT------------EMYWPITHMVAPASDALKCKACH-VQEGRLA
Rfer_3635        ---GVKFSGKVDFIET------------ESMWAINHMVAPKEKALGCVACH-AKVGRLD
Ctha_2243(Chlor ---NLPFSGTVSFIHT------------DMYWPINHMVSSKEESVTCKECHTRKNGRLA
GSU2201          ---GVASAAKILGIKD-----YEPVPGWQTIYFGSNHQVAPKEKALTCYNCH-APNGILN
Gmet_3088        ---GVASAAKILGIKQ-----YDPVPGWQTIMFGSNHLVT-KKNALTCNNCH-APNGVLR
Gbem_0758        ---GVLSAAKTLGMKNPEKVAKEAVAGWQTIYFGSNHLVT-KSKALFCANCH-APNGVLN
Gura_3130        ---GVASAAKTLGIKN-----YTPVPGWQTIYFGSNHLVT-KSKAFSCANCH-APNGVLN
Adeh_0972        ---GVESAARTLGMKDPAAVAKAAVPGWQTIYFGSNHLVT-RSKALNCVNCH-GVNGVLD
AnaeK_1034       ---GVESAARTLGMKDPAAVAKAAVPGWQTIYFGSNHLVT-RSKALNCVNCH-GVNGVLN
Anae109_2593     ---GVASAAKTLGLKK-----VDPVPGWQTIYFSNSHLVT-KTKALSCDRCH-TANGQLD
                        .                     :  .* *:     . *  **      :
```

```
                          430                                 440
SO4144           ----WQALG--YQGDPM--KNKQG----------------------PKHKQ-----------
Shewana3_3690    ----WQALG--YQGDPM--KNKQG----------------------PKHKQ----------P-
Shewmr4_3513     ----WQALG--YQGDPM--KNKQG----------------------PKHKQ----------P-
Shewmr7_0439     ----WQALG--YQGDPM--KNKQG----------------------PKHKQ----------P-
Sbal223DRAFT_30 ----WQALG--YQGDPM--KTKQG----------------------PKHKQ----------P-
Sbal195_0477     ----WQALG--YQGDPM--KTKQG----------------------PKHKQ----------P-
Shew185_0458     ----WQALG--YQGDPM--KNKQG----------------------PKHKQ----------P-
Ssed_4060        ----WQALG--YEGDPM--KNKKG----------------------EKHAK-----------
Shew_0514(S      ----WQALG--YEGDPM--KNKKG----------------------AKHAK-----------
swp_4579         ----WNALG--YDGDPM--KNKDG----------------------KRHAK-----------
Sfri_3556        ----WKALG--YDGDPM--KNRKG----------------------IKHTK----------AD
Sama_3180        ----WKALG--YEGDPM--KNKQG----------------------PRHNQ----------SK
Shal_0614        ----WQALG--YDGDPM--KVKGG----------------------QKHTK-----------
Cvib_0760        SLGGFYLPG--RDMNPL--VEIIGFLVTIGSLIGIIVHSIMRYTTQKKMK-RED------AA
Plut_1197        NLSGFYLPG--RDVNLF--VEIIGLLVTVGSLGGVIIHSIVRYYTTKKHKEREE------RA
Cpar_1055        QLCGIYMPG--RDANPV--VEIIGLIVIVGSVVGVSVHSVMRYISNRNIG-KGG------HE
Cphamn1_2426     NLGGFYLPG--RDASPF--VEIVGLLVIVGSLVGIIAHGIMRYIAHKNMK-QDG------EV
Paes_2160(Prost NLSGFYLPG--RDTDRY--LELFGLLVIVGSLAGVVVHGILRFASNKKRM-QDG------DA
Ppha_1963        KLGGFYLPG--RDASPF--VEIAGFVTIAGSLIGVLIHAFMRYFSHKKTK-SEG------AS
Clim_2064        NLSGFYLMG--RDTNPF--VEYFGLLAISGSLIGVIIHSIIRYFTVKKLK-KAG------GK
Cpha266_2104     NLSGFYLMG--RDTNPF--VEYFGLLAISGSLIGVIIHSIIRYFTVKKLK-KAG------GL
Dole_3005(Desul GLAGFYMPG--RDSFRF--LDAVGWFAVLASLVGVLLHGLGRIVSQKN---RRE---------
Sfum_0090(Syntr NLGGFYMPG--RDVNKP--IQVMGWILVLGSLAGVFFHGLGRMVARGK---KED---------
Dalk_1086        KLTGFYLPG--RDANGF--ADYVGWLIVVASLLGVLFHGLVRIASTGNG--KEE---------
DVU_3144         GVGGVWMPG--RDASSA--ADTLGWIAVIGSLCAVTVHGILRLNARKRN---DG---------
Dvul_0242        GVGGVWMPG--RDASSA--ADTLGWIAVIGSLCAVTVHGILRLNARKRN---DG---------
DvMF_1694        AVGGVWMPG--RDRNAG--VDAAGWIAVAGSVLAVGVHGFLRLAARGRNNRKED---------
Hhal_0149(Halor GLDGVYVPG--QDRHPR--IEAVGWTAVWLTLFAVLGHGGVRYYLYRRERLGNRHGEEGSSS
Maqu_0376(Marin GLGGIYMPG--HNGSVW--LDRIGWLLVAATLFGVLVHAMARVVFSGRK-----------DQ
Mmc1_0877(Magne ALTDFYMPG--RDRQPV--LDGIGWFAVLMTSVGVVGHGSLRVYWHYRRRRREKR-QNGEAQ
Rfer_3635        KIDGVYMPGRSRDHARW--LEIGGWLLAALTLLGVLGHGLVRIIVNKRNS------------
Ctha_2243(Chlor ALTDFYMPG--RDYSKV--VDFGGSSLLLLTLLGVLAHGSLRIISAFRNR-----------K
GSU2201          ----FRELG--YSSDEV--KKLTSPELYFEKIA------------EKM--REEW--------
Gmet_3088        ----FKELG--YSDDEV--KRLTSPELYLQKMA------------EKQ--REEW--------
Gbem_0758        ----FKDLG--YSDKEI--VRLTSPELFMKKLA------------EKQ--KEEW--------
Gura_3130        ----FKDLG--YSEKEI--LRLTSPAIYMESMV------------KKQ--KEEW--------
Adeh_0972        ----FRDLG--YSAAEV--KKLTNPELYFKQLI------------EKQ--KEEW--------
AnaeK_1034       ----FRELG--YAPAEV--KKLTNPELYFKQLV------------EKQ--KEEW--------
Anae109_2593     ----FEALG--YSKGEIARRKLKSAALWFDRLH------------EKERKKEEW--------
                             *                .
```

Part 8 – Calculation for the initial electron transfer rate in the pre-steady-state reaction between ferrous OTR and one of its *in vitro* substrates

Appendices-8.1

The reaction rate (V_{ini}) for the first-electron oxidation of ferrous OTR ($8Fe^{2+} \rightarrow 7Fe^{2+} + e + Fe^{3+}$), which was defined as the initial stage in this work, was given by the equation $V_{ini}=[OTR]/\Delta t=A_{ini}/(\varepsilon*\Delta t)$, where A_{ini} is the initial absorbance of ferrous OTR at 420 nm, ε is the extinction coefficient of ferrous OTR (1.2266 $\mu M^{-1}\cdot cm^{-1}$), and Δt is the timescale of the initial stage. Δt can be obtained according to the absorbance change (ΔA) that corresponds to the first-electron oxidation of ferrous OTR. The value of $\Delta A/A_{ini}$ should be constant for ferrous OTR at various concentrations in the same buffer and at the same temperature, which could be calculated from the standard titration curve (Figure 2-2, Page 47) to be $\Delta A/A_{ini}$ = (1.154-1.104)/1.154*(0.94μM/1μM) = 4.1%. Therefore $V_{ini} = A_{ini}/(\varepsilon*\Delta t)$ = $(\Delta A/4.1\%)/(\varepsilon*\Delta t) = 20*\Delta A/\Delta t$, where $\Delta A/\Delta t$ is the slope of the fitted straight line to the initial-stage data points in the stopped-flow curve (Figure 3-7, Page 65).